1972

Modal truncation of substructures used in vibration analysis

Suresh Kumar Tolani

Department: Mechanical and Aerospace Engineering

MODAL TRUNCATION OF SUBSTRUCTURES USED IN VIBRATION ANALYSIS

by

SURESH KUMAR TOLANI, 1946-

A DISSERTATION

Presented to the Faculty of the Graduate School of the

UNIVERSITY OF MISSOURI-ROLLA

In Partial Fulfillment of the Requirements for the Degree

DOCTOR OF PHILOSOPHY

IN

MECHANICAL ENGINEERING

1972

Jerry F. Lehnhoff
Advisor

Floyd M. Cunningham

R. J. Perrico

ABSTRACT

The objective of this study is to describe in a unified manner a group of structural dynamics analyses using the substructures technique. An additional effort is to provide a consistent basis for the selection of substructure principal modes as required by this method. Substructure principal mode frequency roots and strain energy are two criteria evaluated for the selection of substructure principal modes. System eigenvalues and system strain energy are investigated for the comparison of results in the principal modes. System strain energy should provide more rational results since it is proportional to the stress times the strain in the system and summed over the entire system. Expressions for estimating errors in system eigenvalues and strain energy in the principal modes due to omission of certain substructure principal modes are derived. To complete the solution to the free undamped vibrations problem, the substructures method is extended to include solution with initial conditions. A simple example of a cantilever beam is presented. It is noted through this example that the criterion based on substructure normal mode strain energy for retaining substructure principal modes provides slightly better results in terms of system eigenvalues and strain energy in the principal modes. Estimation of errors in system strain energy in the principal modes due to modal truncation is better in comparison to the estimate of errors in system eigenvalues. The substructures method is also applied to complex structures under forced excitation. Since the classical direct approach results in large order complete structure

matrices, computer storage may exceed that which is available on most digital machines. Partitioning of matrices, via the substructures method, is one of the important features of this study and helps keep the computer storage and cost to a minimum. Matrix partitioning is utilized to its fullest extent in deriving equations of motion and in providing their solutions. Several practical excitations are considered through a simple example of a cantilever beam. Approximate solutions for transverse displacements and system strain energy are evaluated for the purpose of comparisons with the 'exact' case when no modal truncation is used. Results show the applicability of the substructures method to systems under forced excitation.

ACKNOWLEDGEMENTS

The author desires to gratefully acknowledge the guidance and encouragement given by his former advisor Dr. Richard D. Rocke during his graduate work.

The author is especially grateful to Dr. Terry F. Lehnhoff, his present advisor, for the guidance, encouragement and valuable suggestions provided during the last phase of this work and the preparation of this manuscript.

Thanks are also extended to Mrs. Marlys Head for typing this manuscript.

TABLE OF CONTENTS

Table of Contents (continued)

LIST OF FIGURES

List of Figures (continued)

List of Figures (continued)

LIST OF TABLES

NOMENCLATURE

$\{a\}$	Vector of constants
A_0	peak transverse base acceleration
A	Area of cross section
$\{A\}$	Amplitude vector
$[A]$	Coefficient matrix defining structure equilibrium position due to a given base motion
$\{b\}$	Vector of constants
$[C]_i$	Compatibility matrix for the ith substructure
$[C]$	Total structure compatibility matrix
$[D]$	Matrix of direction cosines
e_x	Unit vector along x-axis
e_y	Unit vector along y-axis
e_z	Unit vector along z-axis
E	Modulus of elasticity
$f(t)$	Time-varying forcing function
$\{f_f\}$	Force vector applied at f points in the structure
$\{f(t)\}$	Time-varying forcing vector
$\{g\}$	Impulsive loading vector
G	Modulus of rigidity
I_p	Polar moment of inertia
I_{yy}	Second moment of area about y-axis
I_{zz}	Second moment of area about z-axis
$[I]$	Identity matrix
J_x	Mass moment of inertia about x-axis
J_y	Mass moment of inertia about y-axis

J_z	Mass moment of inertia about z-axis
$[k']$	Element stiffness matrix in local coordinates
$[k]$	Element stiffness matrix in global coordinates
$[K]_i$	Stiffness matrix for the ith substructure
$[\overline{K}]$	Structure stiffness matrix in the unconnected form
$[K]$	Transformed structure stiffness matrix
ℓ	Element Length
$[\ m'\ ]$	Element mass matrix in local coordinates
$[\ m\ ]$	Diagonal mass matrix
$[m]_i$	Mass matrix for the ith substructure
$[\overline{M}]$	Structure mass matrix in the unconnected form
$[M]$	Transformed structure mass matrix
N	Number of substructures
$\{p\}$	Principal coordinate vector
$\{p_0\}$	$\{p(t_0)\}$
$\{\dot{p}_0\}$	$\{\frac{dp}{dt}\ (t = t_0)\}$
P_i	System strain energy in the ith principal mode obtained through substructure untruncated solution
$\overline{P}_i$	System strain energy in the ith principal mode through substructure truncated solution
$\{q\}$	Reduced coordinate vector
$\{q_0\}$	$\{q(t_0)\}$
$\{\dot{q}_0\}$	$\{\frac{dp}{dt}\ (t = t_0)\}$
$[\overline{q}]$	Modal matrix in the reduced coordinates
$\{r\}$	Reduced coordinates in the unconnected form
$[R]$	Rotation matrix
$[\ S.E.\ ]_i$	Fixed constraint normal mode strain energy for the ith substructure

t	time
$[T]_i$	Transformation matrix for the ith substructure
$[T]$	Structure transformation matrix
πt_1	Half-sine pulse duration time
U_i	System strain energy in the ith principal mode obtained through direct solution
$\{U_B(t)\}$	Time-varying base displacement vector
$\{\ddot{U}_B(t)\}$	Time-varying base acceleration vector
w	Weight density
W	Weight of the plate element
$\{x_f\}$	Forced displacement vector
$\{x_s\}$	Displacement vector for s points in the structure
$\{x_f\}_i$	Forced displacement vector for the ith substructure
$\{x\}_i$	Discrete coordinate vector for the ith substructure
$\{\tilde{x}\}$	Relative coordinate vector
$\{x\}$	System eigenvector
$\{X\}$	Amplitude vector
$\{y_d\}$	Deleted coordinate vector
$\{y_r\}$	Retained coordinate vector
$\{y\}$	Amplitude vector
α_a	Angle of rotation
$\{\delta_E(t)\}$	Structure equilibrium position vector
$\delta\overline{P}_i$	Error estimation of system strain energy in the ith principal mode
δP_i	Exact error in system strain energy in the ith principal mode
$\delta\{y_r\}$	Small perturbation in the retained coordinates $\{y_r\}$

$\overline{\delta\lambda_i}$	Eigenvalue error estimate in the ith principal mode
$\delta\lambda_i$	Exact system eigenvalue error in the ith principal mode
ε	Impulse loading time
θ_0	Peak base rotation
λ_i	Substructure fixed constraint eigenvalue in the ith principal mode
ρ	Mass density per unit length
τ	Time
$[\phi]_i$	Substructure modes for the ith substructure
$[\phi_c]_i$	Constraint modes for the ith substructure
$[\phi_n]_i$	Normal modes for the ith substructure
$[\phi]$	Structure transformation matrix
ψ_i	Phase angle for the ith harmonic force
ω_i	System circular frequency root in the ith principal mode
$[\widetilde{\omega_i}]$	Matrix of system frequency roots
Ω_i	Forcing frequency for the ith harmonic force

CHAPTER I

INTRODUCTION

A general theory for solving vibration problems through the method of superposition of principal modes has been in existence for many years. In this method, termed as the normal mode method, equations of motion are derived through finite element or continuous techniques and are uncoupled through the normal modes of the structure. In the case of a complex structure, a finite element model is, in general, necessary in order to have a system with a finite number of degrees of freedom upon which matrix algebra operations can be performed. However, the number of equations of motion to be solved for complex structures is usually large. An eigensolution, which is the most important part of a dynamic analysis by the normal mode method, becomes uneconomical due to the large number of equations of motion and may require computer facilities of greater capacity than those that are available.

In the design of a complex structure, its major components, or substructures, are often designed by different engineering groups or at different times. The general normal mode method does not take this fact into account and treats the structure as a whole. As a result any modifications in any substructure design would require a complete re-evaluation of the structure's normal modes. This suggests that for ease of modification a complex structure should be considered as consisting of a number of distinct regions which will be referred to as 'substructures', where analyses may be applied separately.

In the substructures method, the total system principal modes or

response is obtained by parts rather than as a whole. It replaces the one eigenvalue problem relating to one large matrix by several preliminary eigenvalue problems relating to small matrices and also one final eigenvalue problem, again of smaller order. The method is based upon a transformation of coordinates to yield a smaller set of equations and transforms the equations in such a way that accurate solutions can be obtained very efficiently over a limited range of the frequency spectrum.

The columns of the transformation matrix are made up of substructure principal modes which are computed by utilizing the discrete-element analytical model available for each substructure. It is noted that the method of substructures does not necessarily require a finite element model of substructures. If a particular substructure can be represented by continuous elements, such as a beam, its principal modes may be obtained by continuous solutions. When all, or too many substructure principal modes are retained, then computational economy, which is one of the inviting features of the method, is not achieved. Retention of only a few of the available modes results in a smaller eigenvalue problem and hence the desired computational economy.

A. Literature Review

The substructures method has been in use for some time. The application of the method was first presented by Hunn(1,2)* for the free vibration analysis of an aircraft structure. Studies by Turner, Martin and Weikel (3) consider the analysis of complex structures by

*Numbers in parenthesis refer to the list of references.

stiffness or displacement methods in which major components are treated separately as free bodies. In the work by Argyris (4) primary emphasis is placed on force methods and the problem of dealing with indeterminate connection systems among the substructures is treated by considering the equilibrium of interaction redundant force systems. However, displacement methods are also considered by Argyris and in these it is suggested that the interconnection problem may be resolved by matching boundary displacements. Gladwell (5) developed a method which proceeds by dividing the complete problem into two stages. In the first, certain sets of constraints are imposed on the system and certain of the principal modes of the constrained system are found. In the second stage, these modes are used in a Rayleigh-Ritz analysis of the whole system. Przemieniecki (6) has developed a static method which falls into the category of displacement methods. In this method each substructure is first analyzed separately; assuming that all common boundaries with the adjacent substructures are completely fixed, these boundaries are then relaxed simultaneously and the actual boundary displacements are determined from the equations of equilibrium of forces at boundary joints. Hurty (7,8) has presented a method in which the displacement behavior of each substructure is described by a set of generalized coordinates generated in three categories: rigid body, constraint, and normal modes. Craig and Bampton (9) simplify Hurty's method by employing two forms of generalized coordinates: constraint modes and substructure normal modes, together with conditions of geometrical compatability along substructure boundaries. Hurty (10) is

also credited with the development of an error algorithm to determine the eigenvalue error introduced due to omission of given substructure principal modes. Bajan and Feng (11) and Bajan, Feng and Jaszlics (12) have presented a modal substitution technique in which approximate system principal modes, in conjunction with a selected set of previously unused substructure normal modes, are used in successive modal substitution cycles to improve approximate system principal modes utilized as well as their corresponding eigenvalues.

Collins (13) describes mathematically the effect of randomness in structural element properties on eigenvalues and eigenvectors of large structures. At the time of completion of this study, Hasselman and Hart (14) presented a method for assessing and improving upon the convergence of structural modes, based on minimization of the Rayleigh quotient in a coordinate space, expanded from that of the initial solution, by the inclusion of additional component mode functions. In the present investigation the substructures method introduced by Craig and Bampton, and Bajan and Feng is presented in a more systematic and elucidating manner. Partitioning of large order matrices is actually utilized in deriving equations of motion. A criterion based on substructure normal mode strain energy is used for the selection of substructure principal modes. This semi-empirical criterion retains those lower order substructure principal modes with strain energy levels below a specified value and attempts to optimize the formulation of system equations. For the purpose of comparison the criterion of substructure frequency roots suggested by Bajan and Feng is also included. Two bases of comparisons are used to evaluate system behavior

due to partial retaining of substructure principal modes. The first one, which has been used in the past by others, is based on system eigenvalues, while the second basis uses system strain energy in the principal modes. Strain energy is proportional to the stress times the strain in the system and summed over the entire system. Hence, it should be indicative of displacements and stresses in the system, independent of their position within the system. Furthermore, the system strain energy should be a better measure of total system distortion than any other particular parameter, e.g., displacement or stress.

In the survey of the literature it was found that little work has been done on the solution of systems under forced excitation through the use of the substructures method. Pakstys (15) has shown the applicability of this method to shock analysis of complex structures. Saczalski and Huang (16) present a unified formulation of hybrid elastodynamic equations to describe the deterministic and non-deterministic response characteristics of coupled spatial vibratory systems, consisting of continuous elements, point masses and rigid bodies.

In this study equations of motion are derived for systems under forced excitation through the use of the substructures method. It is assumed that the given structure is linear and that damping is negligible. Four different types of excitations are studied: General time-varying displacement excitation, harmonic force excitation, base acceleration excitation, and general time-varying force excitation. System displacement response and system strain energy are used as the two bases of comparison of results.

B. Contents of Thesis

Chapter II outlines the analysis of a typical substructure to obtain its constraint and principal modes. A compatability matrix to solve the problem of substructure interconnection at the boundary is derived by matching boundary displacements. Two criteria for retention of substructure principal modes are included.

Chapter III describes the assemblage of substructure characteristic behavior to yield a much smaller set of equations of motion for the total system. The number of equations in this set can be controlled by varying the size of the transformation matrix. An eigensolution of the reduced set of equations gives approximate system eigenvalues and eigenvectors. An expression for obtaining system strain energy in the principal modes is presented. A detailed error analysis of system eigenvalues and strain energy in the principal modes due to omission of certain substructure principal modes is carried out.

The study of the free vibrations solution in the presence of initial conditions and impulsive loadings is also treated.

Chapter IV discusses the application of the substructures method to systems under forced excitation. The use of partitioning of matrices is utilized to keep computer time and storage to a minimum. Equations of motion are solved to yield system displacement response.

In Chapter V comparison of results in free vibrations is presented on the basis of system eigenvalues and strain energy in the principal modes. Under forced excitations the system displacements and system strain energy are used as the basis of comparisons. Use of an IBM-360-50 computer has been made to establish all numerical results using

an example of a cantilever beam. A flow chart of the computer program developed for the substructures method is included in Appendix A.

The substructures method is verified by comparing solutions obtained by retaining all substructure principal modes against the corresponding solutions obtained by the usual direct approach. Solutions obtained through modal truncation are superimposed on exact solutions for a direct comparison.

CHAPTER II

FREE VIBRATION SUBSTRUCTURE ANALYSIS

In the study which follows a free undamped vibration solution of a complex structure is derived. The given structure is divided into several small structures, called "substructures". In the substructure method, unlike the usual direct method, the complete solution is obtained by parts rather than directly as a whole. It is a technique based on utilizing characteristic behavior of individual substructures for formulating the differential equations of motion which govern the complete structure.

Individual treatment of the substructures yields a transformation matrix [T] for the total structure, where [T], in general, is not a square matrix. Matrix [T] is of the order r x c, where r > c. A reduced set of equations of motion are then solved for system eigenvalues, eigenvectors and strain energy in the principal modes. The size of matrix [T] can be controlled by varying the number of substructure fixed constraint normal modes retained. A comparison of system eigenvalues and strain energy in the principal modes is made in Chapter V with the number of reduced equations of motion solved.

A. Substructure Analysis

A finite element mathematical model of the given structure is drawn up first to closely represent the behavior of the actual structure. The structure model is then partitioned into several component substructures whose boundaries may be specified arbitrarily. However, care should be taken to ensure that the substructure boundaries are

selected in the most economical way since this affects the subsequent matrix operations.

A substructure contains a set of movable constraints at connections or boundaries where it joins neighboring substructures. All joints inside the substructure are called interior joints. An individual substructure may also contain any original external constraints applied to the total structure.

In the discussion which follows a typical substructure is analyzed to obtain its constraint modes and fixed constraint normal modes which are then used to form the transformation matrix [T]. A compatibility matrix to ensure compatible displacements at the substructure boundaries is derived.

Consider the ith substructure from the finite element model of the given structure. The mass and stiffness matrices for the ith substructure would depend upon the types of finite elements or lumped parameter models used to describe the structure. A discussion on types of finite elements and their mass and stiffness matrices is included in Appendix B. For this study, it is assumed that the mass and stiffness matrices for the ith substructure are known. Furthermore, damping is assumed to be negligible. The differential equations of motion in matrix notation for free undamped vibrations of the ith substructure are:

$$[m]_i \{\ddot{x}\}_i + [K]_i \{x\}_i = \{0\}, \qquad (1)$$

where: $[m]_i$ = mass matrix for the ith substructure

$[K]_i$ = stiffness matrix for the ith substructure

$\{x\}_i$ = displacements at the discrete coordinates in the ith substructure.

Letting:

$$\{x\}_i = [\phi]_i \{r\}_i, \tag{2}$$

gives:

$$\{\ddot{x}\}_i = [\phi]_i \{\ddot{r}\}_i, \tag{3}$$

where the columns of matrix $[\phi]_i$ are the ith substructure constraint modes and fixed constraint normal modes, grouped together. Thus,

$$[\phi]_i = [\phi_c \mid \phi_n]_i, \tag{4}$$

where $[\phi_c]_i$ and $[\phi_n]_i$ are the constraint modes and the fixed constraint normal modes for the ith substructure, respectively. It is now shown how matrices $[\phi_c]_i$ and $[\phi_n]_i$ are obtained for the ith substructure.

1. Constraint Modes of a Substructure

The displacement configuration in the substructure due to a unit displacement at a single connection constraint, with all other boundary constraints being fixed, is termed a 'constraint mode'. The connection or boundary constraints are constraints at the connecting points of neighboring substructures. The connection constraints are usually located at mass points. These points, one at a time, are given a unit displacement in the direction of each degree of freedom considered, resulting in the deflection of the substructure. These deflected configurations of the substructure are the constraint modes

for that substructure. The number of linearly independent substructure constraint modes equals the number of substructure connection constraints. In order to compute these modes, let the unit displacements at the connecting constraints of the ith substructure be given by:

$$[T_c]_i = [\urcorner I \llcorner]_i , \tag{5}$$

where $[\urcorner I \llcorner]$ is an identity matrix and c denotes constraint modes.

The displacements at the interior or the unconstrained coordinates may be represented by $[T_u]_i$ for the ith substructure. By definition of the stiffness matrix, the external static forces, at connection constraints in the ith substructure, required to produce the constraint modes $[\phi_c]_i$ are given by:

$$[F]_i = [K]_i \, [\phi_c]_i , \tag{6}$$

where $[\phi_c]_i$ is given by:

$$[\phi_c]_i = \begin{bmatrix} T_c \\ \hline T_u \end{bmatrix}_i = \begin{bmatrix} \urcorner I \llcorner \\ \hline T_u \end{bmatrix}_i . \tag{7}$$

In Eq. (6), each column of $[F]_i$ corresponds to a particular constraint mode. To compute $[T_u]_i$, Eq. (6) is partitioned as follows:

$$\begin{bmatrix} F_c \\ \hline F_u \end{bmatrix}_i = \left[\begin{array}{c|c} K_{cc} & K_{cu} \\ \hline K_{uc} & K_{uu} \end{array}\right]_i [\phi_c]_i , \quad \text{or}$$

$$\begin{bmatrix} F_c \\ \hline F_u \end{bmatrix}_i = \left[\begin{array}{c|c} K_{cc} & K_{cu} \\ \hline K_{uc} & K_{uu} \end{array}\right] \begin{bmatrix} \urcorner I \llcorner \\ \hline T_u \end{bmatrix}_i , \tag{8}$$

where c and u represent constraint and unconstrained coordinates respectively.

Expanding Eq. (8) gives:

$$[F_c]_i = [K_{cc}]_i [I]_i + [K_{cu}]_i [T_u]_i, \text{ and} \tag{9}$$

$$[F_u]_i = [K_{uc}]_i [I]_i + [K_{uu}]_i [T_u]_i . \tag{10}$$

Since there are no external forces at the unconstrained coordinates in a constraint mode,

$$[F_u]_i \equiv [0]_i . \tag{11}$$

In view of Eq. (11), Eq. (10) gives:

$$[T_u]_i = - [K_{uu}]_i^{-1} [K_{uc}]_i . \tag{12}$$

Thus from Eq. (7), $[\phi_c]_i$ becomes:

$$[\phi_c]_i = \begin{bmatrix} I \\ \hline - K_{uu}^{-1} K_{uc} \end{bmatrix}_i , \tag{13}$$

in which matrices $[K_{uu}]_i$ and $[K_{uc}]_i$ are obtained from Eq. (8).

2. Fixed Constraint Normal Modes of a Substructure

Constraint modes are obtained through a static analysis. Fixed constraint normal modes are obtained through a free vibration analysis of the substructure. These modes represent substructure displacements relative to the connection constraints and can be computed by performing an eigenvalue analysis of the substructure with connection

constraints held fixed. Fixed constraint normal modes for those substructures that may be represented by continuous elements may be obtained by continuous solutions. The number of linearly independent fixed constraint normal modes equals the number of unconstrained or interior coordinates of the substructure. To compute the fixed constraint normal modes for the ith substructure, partition Eq. (1) to obtain:

$$\left[\begin{array}{c|c} m_{cc} & m_{cu} \\ \hline m_{uc} & m_{uu} \end{array}\right]_i \left\{\begin{array}{c} \ddot{x}_c \\ \hline \ddot{x}_u \end{array}\right\}_i + \left[\begin{array}{c|c} K_{cc} & K_{cu} \\ \hline K_{uc} & K_{uu} \end{array}\right]_i \left\{\begin{array}{c} x_c \\ \hline x_u \end{array}\right\}_i = \left\{\begin{array}{c} 0 \\ \hline 0 \end{array}\right\}. \quad (14)$$

Since connection constraints are fixed for a normal mode analysis,

$$\{x_c\}_i = \{0\}, \text{ and} \quad (15)$$

$$\{\ddot{x}_c\}_i = \{0\}. \quad (16)$$

Expanding Eq. (14) and using Eqs. (15) and (16) gives:

$$[m_{cu}]_i \{\ddot{x}_u\}_i + [K_{cu}]_i \{x_u\}_i = \{0\}, \text{ and} \quad (17)$$

$$[m_{uu}]_i \{\ddot{x}_u\}_i + [K_{uu}]_i \{x_u\}_i = \{0\}. \quad (18)$$

Equation (18) is in terms of unconstrained coordinates only and is solved for eigenvalues and eigenvectors. Let the eigenvalues be denoted by $[\lambda_j]_i$ and the eigenvectors by $[\phi_{nu}]_i$, in which subscript n indicates noraml modes. The modal matrix $[\phi_{nu}]_i$ of Eq. (18) is normalized so that it satisfies the following orthogonality properties:

$$[\phi_{nu}]_i^T [m_{uu}]_i [\phi_{nu}]_i = [I]_i, \text{ and} \tag{19}$$

$$[\phi_{nu}]_i^T [K_{uu}]_i [\phi_{nu}]_i = [\lambda_j]_i. \tag{20}$$

Thus the fixed constraint normal modes $[\phi_n]_i$ are given by:

$$[\phi_n]_i = \left[\begin{array}{c} \phi_{nc} \\ \hline \phi_{nu} \end{array}\right]_i, \tag{21}$$

where $[\phi_{nc}]_i$ represents displacement at the connection constraints.

Since connection constraints are held fixed in a normal mode analysis,

$$[\phi_{nc}]_i = [0]. \tag{22}$$

Having obtained the substructure constraint and fixed constraint normal modes, the transformation matrix $[\phi]_i$ is given by Eq. (4), i.e.,

$$[\phi]_i = [\phi_c \vdots \phi_n]_i. \tag{23}$$

Substituting for $[\phi_c]_i$ and $[\phi_n]_i$ from Eqs. (13) and (23), respectively, yields:

$$[\phi]_i = \left[\begin{array}{c:c} I & 0 \\ \hline -K_{uu}^{-1} K_{uc} & \phi_{nu} \end{array}\right]_i. \tag{24}$$

At this point, if the equations of motion for all the substructures are assembled to obtain the equations of motion for the total structure, they would be in the unconnected form. Therefore, it must first be

shown how a "connection" or a "compatibility" matrix is formed. This matrix is then used in defining a transformation [T] given by:

$$[T] = [\phi][C], \tag{25}$$

where:

$$[\phi] = \begin{bmatrix} \phi_1 & & 0 \\ & \ddots\ \phi_i & \\ 0 & & \ddots\ \phi_N \end{bmatrix},$$

in which $[\phi]_{i,\ i=1,N}$ are given by Eq. (24), and matrix [C] represents the compatibility matrix for the entire structure.

B. Compatibility Matrix

The matrix which ensures the compatibility of displacements at the connections of adjacent substructures is called the "compatibility matrix". This matrix relates reduced coordinates {r}, which are in the unconnected form, to the compatibly reduced set of coordinates {q} through the relations:

$$\{r\} = [C]\{q\}. \tag{26}$$

Consider two substructures i and j at a common connection s. It will now be shown how the compatibility matrix for these two substructures can be formed. Rewriting Eq. (2) in terms of constraint and unconstrained coordinates, i.e., for the ith substructure:

$$\left\{\begin{matrix} x_c \\ \hline x_u \end{matrix}\right\}_i = \left[\begin{array}{c|c} I & 0 \\ \hline T_u & \phi_{nu} \end{array}\right]_i \left\{\begin{matrix} r_c \\ \hline r_u \end{matrix}\right\}_i, \tag{27}$$

and likewise for the jth substructure:

$$\left\{\begin{array}{c} x_c \\ \hline x_u \end{array}\right\}_j = \left[\begin{array}{c|c} I & 0 \\ \hline T_u & \phi_{nu} \end{array}\right]_j \left\{\begin{array}{c} r_c \\ \hline r_u \end{array}\right\}_j . \tag{28}$$

At the common connection, s, the above equations yield:

$$\{x_c\}_i^s = \{r_c\}_i^s, \text{ and} \tag{29}$$

$$\{x_c\}_j^s = \{r_c\}_j^s \tag{30}$$

where the superscript s refers to the common connection s.

It must be noted that the coordinate vectors $\{x_c\}_i^s$ and $\{x_c\}_j^s$ are expressed in the coordinate frames of their respective substructures. Hence, before establishing compatible displacement relations, these must be expressed in a common reference frame. Let the common coordinate system be represented by $\{q\}^s$. Then the constraint mode displacements of connection s in the ith substructure are $\{q_c\}_i^s$ and those in the jth substructure are $\{q_c\}_j^s$. Let the rotation matrix which transforms local coordinates to global coordinates at connection s be given by $[R]_i^s$ for the ith substructure and by $[R]_j^s$ for the jth substructure. In general for a three dimensional problem, i.e., six degrees of freedom at any coordinate point, the rotation matrix is given by:

$$[R]_i^s = \left[\begin{array}{cc} a & 0 \\ 0 & a \end{array}\right]_i^s , \tag{31}$$

where:

$$[a]_i^s = \begin{bmatrix} a_{11} & a_{12} & a_{13} \\ a_{21} & a_{22} & a_{23} \\ a_{31} & a_{32} & a_{33} \end{bmatrix}_i^s , \tag{32}$$

in which a_{uv} are the direction cosines from the global axis v to the substructure axis u.

Thus,

$$\{r_c\}^s_i = [R]^s_i \{q_c\}^s_i, \text{ and} \tag{33}$$

$$\{r_c\}^s_j = [R]^s_j \{q_c\}^s_j . \tag{34}$$

In the substructure normal mode analysis, the fixed constraint normal modes are not affected by the local coordinates for the ith and jth substructures, since connection s is fixed for these modes. Hence,

$$\{r_n\}_i = [I]\{q_n\}_i, \text{ or}$$

$$\{r_n\}_i = \{q_n\}_i, \tag{35}$$

and similarly,

$$\{r_n\}_j = \{q_n\}_j . \tag{36}$$

The necessary and sufficient condition for compatible displacements at connection s is given by:

$$\{q_c\}^s_i = \{q_c\}^s_j = \{q_c\}^s . \tag{37}$$

A matrix equation which satisifes equations (33-36) becomes:

$$\begin{Bmatrix} r_c^s \\ r_{ni} \\ r_c^s \\ r_{nj} \end{Bmatrix} = \left[\begin{array}{c|c|c} R_i^s & 0 & 0 \\ \hline 0 & I & 0 \\ \hline R_j^s & 0 & 0 \\ \hline 0 & 0 & I \end{array}\right] \begin{Bmatrix} q_c^s \\ q_{ni} \\ q_{nj} \end{Bmatrix} . \tag{37}$$

The first matrix on the right hand side of Eq. (37) is the compatibility or the connection matrix for the substructures i and j at a common connection s.

Further, it can be shown through the above procedure, that if substructure j is connected to substructure ℓ at a connection u, the compatibility matrix is given by:

$$\begin{Bmatrix} r_c^s \\ \hline r_{ni} \\ \hline r_c^s \\ \hline r_c^u \\ \hline r_{nj} \\ \hline r_c^u \\ \hline r_{n\ell} \end{Bmatrix} = \left[\begin{array}{c|c|c|c|c} R_i^s & 0 & 0 & 0 & 0 \\ \hline 0 & 0 & I & 0 & 0 \\ \hline R_j^s & 0 & 0 & 0 & 0 \\ \hline 0 & R_j^u & 0 & 0 & 0 \\ \hline 0 & 0 & 0 & I & 0 \\ \hline 0 & R_\ell^u & 0 & 0 & 0 \\ \hline 0 & 0 & 0 & 0 & I \end{array}\right] \begin{Bmatrix} q_c^s \\ \hline q_c^u \\ \hline q_{ni} \\ \hline q_{nj} \\ \hline q_{n\ell} \end{Bmatrix} . \tag{38}$$

In general,

$$\{r\} = [C]\{q\}, \tag{39}$$

in which the compatibility matrix [C] may be partitioned as:

$$[C] = \begin{bmatrix} C_1 \\ \vdots \\ C_i \\ \vdots \\ C_N \end{bmatrix} , \tag{40}$$

where $[C]_i$ represents the partitioned compatibility matrix for the ith substructure. Having formed the compatibility matrix for each substructure, the transformation matrix [T] may now be obtained.

C. Transformation Matrix [T]

Matrix [T] transforms the total set of substructure coordinates {x} into the reduced coordinates {q} through the relation:

$$\{x\} = [T]\{q\}. \tag{41}$$

From Eq. (2),

$$\{x\} = [\phi]\{r\} , \quad \text{and}$$

from Eq. (39)

$$\{r\} = [C]\{q\}.$$

Thus matrix [T] is given by:

$$[T] = [\phi][C], \tag{25}$$

where:

$$[\phi] = \begin{bmatrix} \phi_1 & & 0 \\ & \ddots \phi_i \ddots & \\ 0 & & \phi_N \end{bmatrix} , \text{ and}$$

$$[C] = \begin{bmatrix} C_1 \\ \vdots \\ C_i \\ \vdots \\ C_N \end{bmatrix} .$$

Using partitioned forms of matrices $[\phi]$ and $[C]$, matrix $[T]$ becomes:

$$[T] = \begin{bmatrix} \phi_1 C_1 \\ \vdots \\ \phi_i C_i \\ \vdots \\ \phi_N C_N \end{bmatrix} , \text{ or} \qquad (42)$$

$$[T] = \begin{bmatrix} T_1 \\ \vdots \\ T_i \\ \vdots \\ T_N \end{bmatrix} ,$$

in which for the ith substructure:

$$[T]_i = [\phi]_i [C]_i . \qquad (43)$$

Columns of matrix $[T]$ contain constraint modes of the entire structure and fixed constraint normal modes of individual substructures, i.e.,

matrix [T] may be partitioned as follows:

$$[T] = [T_c \vdots T_n], \tag{44}$$

where subscripts c and n represent constraint and fixed constraint normal modes.

It is from transformation matrix [T] that certain fixed constraint normal modes are retained and the rest are deleted. The constraint modes cannot be eliminated since these describe the overall system motion. The omission of certain fixed constraint normal modes gives the desired reduction in the number of system differential equations of motion to be solved.

D. Criteria for Selection of Substructure Fixed Constraint Normal Modes

For problems which are carefully formulated it has been found in general that the system lower modes determined by the substructures approach are very accurate and that unacceptably large errors may be found in the higher order modes. Furthermore, these errors depend primarily on the unused substructure fixed constraint normal modes. The selection of a minimum number of substructure fixed constraint normal modes is based on two criteria which are discussed in the next two sections.

1. The first criterion, referred to as a frequency root criterion, is based on substructure fixed constraint frequency roots (11) obtained in the fixed constraint normal mode analysis. Usually the number of differential equations of motion which can be solved by numerical

computation is known from the limited core storage available in a digital computer. This means, that the maximum total number of fixed constraint normal modes which can be retained from all substructures is usually known.

In the frequency root criterion, some upper limit is set on the total structure frequency roots and only those substructure lower order normal modes are retained which have modal frequencies below the set level. This upper limit can usually be predicted depending upon the structure application, for example, flutter frequency for an aircraft. By varying the number of modes retained, a study of eigenvalues and principal mode accuracies can be made for the total structure.

2. The second criterion, referred to as strain energy criterion, is based on substructure fixed constraint strain energy in the normal modes. In this case an upper limit is set on the total structure principal mode strain energy and the lower order fixed constraint normal modes retained from all substructures have strain energies below the above set level. This substructure strain energy may be computed as follows.

Consider the ith substructure whose fixed constraint normal modes are given by $[\phi_{nu}]_i$. Strain energy in these modes is given by:

$$[\text{S.E.}]_i = \frac{1}{2} [\phi_{nu}]_i^T [K_{uu}]_i [\phi_{nu}]_i , \tag{45}$$

in which $[K_{uu}]_i$ is obtained from Eq. (8).

Again, the total number of differential equations of motion for the entire structure can be controlled by varying the maximum number of fixed constraint normal modes retained. A study of system

eigenvalues and strain energy in the principal modes, against the number of equations of motion solved, can be made.

A comparison of the above two criteria for the selection of substructure fixed constraint normal modes can be made by comparing the system eigenvalues and strain energy in the principal modes.

Once the number of fixed constraint normal modes retained is decided, matrix [T] can be formed. The size of matrix [T] determines the number of equations of motion in the reduced set of coordinates {q}. It will now be shown, how the total structure equations of motion are put together and transformed into a much smaller set. This will be discussed in Chapter III.

CHAPTER III

FREE VIBRATION SYSTEM ANALYSIS

It is sometimes seen in structural dynamics that the most convenient set of coordinates in which a problem is formulated turns out not to be the most suitable for solution. Although finite element techniques model a structure in a simple manner, the number of finite elements required to describe accurately the many interfaces and connection points that exist in a structure is large. This results in equations of motion numbering in thousands. It is, therefore, practically unreasonable to solve these equations directly, the approach being uneconomical. Dividing the structure into substructures results in a transformation which relates the discrete coordinates to a much smaller set, eigensolution of which is economical and accurate.

It is shown in Chapter II how the transformation matrix [T] can be obtained. Through the use of either of the two criteria for the selection of substructure fixed constraint normal modes, certain columns of matrix [T] can be omitted, resulting in a much smaller size of matrix [T]. This transformation is similar to the normal mode transformation given by:

$$\{\eta\} = [\mu]\{\zeta\},$$

where a partial expansion in terms of normal coordinates $\{\zeta\}$ requires only a few modal columns, $\{\mu\}_i$, to obtain accurate estimates of discrete coordinates $\{\eta\}$.

This chapter will be partially concerned with the system equations of motion and their reduction to a smaller set. Eigensolution of this smaller set of equations results directly in system eigenvalues, while eigenvectors need to be transformed to the original set of coordinates through the transformation matrix [T]. Partitioning of matrices is utilized wherever possible to derive the equations of motion in the reduced set of coordinates. This helps in keeping the computer operations most economical.

After establishing equations of motion in reduced coordinates {q}, and the system eigenvalues and eigenvectors, the method of substructures can also be applied to include a free vibration solution with known initial conditions. An advantage in applying the substructures approach is that only smaller sized matrices are treated in the digital computation resulting in a saving of storage. A special solution for impulsive loading which results in initial velocities with zero initial displacements is also presented in this chapter.

Finally, expressions for an error estimate to the system eigenvalues and strain energy in the principal modes caused by the omission of certain substructure fixed constraint normal modes, are presented. A comparison of these estimates of errors in system eigenvalues and strain energy in the principal modes is made in Chapter V against the number of reduced equations of motion solved.

A. General Differential Equations of Motion

The equations of motion for the total structure for free undamped

vibrations in the unconnected form are obtained by grouping together the equations of motion for all N substructures as they would be described in matrix form separately, i.e.,

$$\begin{bmatrix} m_1 & & & 0 \\ & \ddots & & \\ & & m_i & \\ & & & \ddots \\ 0 & & & m_N \end{bmatrix} \begin{Bmatrix} \ddot{x}_1 \\ \vdots \\ \ddot{x}_i \\ \vdots \\ \ddot{x}_N \end{Bmatrix} + \begin{bmatrix} K_1 & & & 0 \\ & \ddots & & \\ & & K_i & \\ & & & \ddots \\ 0 & & & K_N \end{bmatrix} \begin{Bmatrix} x_1 \\ \vdots \\ x_i \\ \vdots \\ x_N \end{Bmatrix} = \begin{Bmatrix} 0 \\ \vdots \\ 0 \\ \vdots \\ 0 \end{Bmatrix}, \text{ or} \quad (46)$$

in general matrix notation,

$$[\overline{M}]\{\ddot{x}\} + [\overline{K}]\{x\} = \{0\}, \quad (47)$$

where:

$$[\overline{M}] = \begin{bmatrix} m_1 & & & 0 \\ & \ddots & & \\ & & m_i & \\ & & & \ddots \\ 0 & & & m_N \end{bmatrix} \quad (48)$$

$$[\overline{K}] = \begin{bmatrix} K_1 & & & 0 \\ & \ddots & & \\ & & K_i & \\ & & & \ddots \\ 0 & & & K_N \end{bmatrix} \quad (49)$$

$$\{x\} = \begin{Bmatrix} x_1 \\ \vdots \\ x_i \\ \vdots \\ x_N \end{Bmatrix}, \text{ and}$$

$$\{\ddot{x}\} = \begin{Bmatrix} \ddot{x}_1 \\ \vdots \\ \ddot{x}_i \\ \vdots \\ \ddot{x}_N \end{Bmatrix}.$$

It may be noted that any boundary conditions applied to the total structure are directly reflected in substructure discrete coordinates $\{x\}_i$. The transformation

$$\{x\} = [T]\{q\}, \tag{41}$$

gives:

$$\{\ddot{x}\} = [T]\{\ddot{q}\}. \tag{50}$$

Substituting Eqs. (41) and (50) into Eq. (47) yields:

$$[\overline{M}][T]\{\ddot{q}\} + [\overline{K}][T]\{q\} = \{0\}. \tag{51}$$

Premultiplying Eq. (51) by $[T]^T$ gives:

$$[T]^T[\overline{M}][T]\{\ddot{q}\} + [T]^T[\overline{K}][T]\{q\} = \{0\}, \text{ or} \tag{52}$$

$$[M]\{\ddot{q}\} + [K]\{q\} = \{0\}, \tag{53}$$

where, [M] and [K] are transformed symmetric system mass and stiffness matrices given by:

$$[M] = [T]^T[\overline{M}][T], \tag{54}$$

$$[K] = [T]^T[\overline{K}][T]. \tag{55}$$

As in Eq. (42), partitioning of the [T] matrix gives:

$$[T] = \begin{bmatrix} T_1 \\ \vdots \\ T_i \\ \vdots \\ T_N \end{bmatrix}, \tag{56}$$

where for the ith substructure,

$$[T]_i = [\phi]_i\ [C]_i. \tag{57}$$

Substituting Eq. (56) into Eq. (54) gives:

$$[M] = [T_1^T \mid \cdots \mid T_i^T \mid \cdots \mid T_N^T] \begin{bmatrix} m_1 & & & 0 \\ & \ddots & & \\ & & m_i & \\ & & & \ddots \\ 0 & & & m_N \end{bmatrix} \begin{bmatrix} T_1 \\ \vdots \\ T_i \\ \vdots \\ T_N \end{bmatrix}, \text{ or}$$

$$[M] = [T_1^T m_1 T_1 + \cdots + T_i^T m_i T_i + \cdots + T_N^T m_N T_N], \text{ or}$$

$$[M] = [\sum_{i=1,N} T_i^T m_i T_i]. \tag{58}$$

Similarly using Eqs. (55) and (56) gives:

$$[K] = [T_1^T K_1 T_1 + \cdots + T_i^T K_i T_i + \cdots T_N^T K_N T_N], \text{ or}$$

$$[K] = [\sum_{i=1,N} T_i^T K_i T_i]. \tag{59}$$

The contributions from the ith substructure to the coefficients of $\{\ddot{q}\}$ and $\{q\}$ in Eq. (53) are given by:

$$[T]_i^T [m]_i [T]_i, \text{ and} \tag{60}$$

$$[T]_i^T [K]_i [T]_i. \tag{61}$$

Taking Eq. (60) and expanding using Eq. (42) gives:

$$[T]_i^T[m]_i[T]_i = [C]_i^T[\phi]_i^T[m]_i[\phi]_i[C]_i, \text{ or} \tag{62}$$

$$= [C]_i^T[\phi_c \vdots \phi_n]_i^T[m]_i[\phi_c \vdots \phi_n]_i[C]_i, \text{ or}$$

$$= [C]_i^T \left[\begin{array}{c:c} \phi_c^T m \phi_c & \phi_c^T m \phi_n \\ \hdashline \phi_n^T m \phi_c & \phi_n^T m \phi_n \end{array}\right]_i [C]_i, \text{ or}$$

$$= [C]_i^T \left[\begin{array}{c:c} m_{cc} & m_{cn} \\ \hdashline m_{nc} & m_{nn} \end{array}\right]_i [C]_i, \tag{63}$$

where:

$$[m_{nn}]_i = [\phi_n]_i^T[m]_i[\phi_n]_i, \text{ or}$$

$$[m_{nn}]_i = [I], \text{ and} \tag{64}$$

$$[m_{cc}]_i = [\phi_c]_i^T[m]_i[\phi_c]_i \tag{65}$$

$$[m_{cn}]_i = [\phi_c]_i^T[m]_i[\phi_n]_i \tag{66}$$

$$[m_{nc}]_i = [\phi_n]_i^T[m]_i[\phi_c]_i. \tag{67}$$

Hence, the result for the ith substructure form is:

$$[T]_i^T[m]_i[T]_i = [C]_i^T \left[\begin{array}{c:c} m_{cc} & m_{cn} \\ \hdashline m_{nc} & I \end{array}\right]_i [C]_i. \tag{68}$$

In the above equation matrix $[C]_i$, which is the partitioned compatability matrix for the ith substructure, connects the ith substructure with its neighboring substructures. Furthermore, it

places the contribution of the ith substructure in proper slots of the total structure mass matrix in the reduced set of coordinates {q}, i.e., Eq. (68) becomes:

$$[T]_i^T[m]_i[T]_i = \left[\begin{array}{c|c|c|c|c} 0 & 0 & 0 & 0 & 0 \\ \hline 0 & m_{cc_i} & 0 & m_{cn_i} & 0 \\ \hline 0 & 0 & 0 & 0 & 0 \\ \hline 0 & m_{nc_i} & 0 & I & 0 \\ \hline 0 & 0 & 0 & 0 & 0 \end{array}\right] . \qquad (69)$$

Similarly it can be shown that Eq. (61) in general form becomes:

$$[T]_i^T[K]_i[T]_i = \left[\begin{array}{c|c|c|c|c} 0 & 0 & 0 & 0 & 0 \\ \hline 0 & K_{cc_i} & 0 & K_{cn_i} & 0 \\ \hline 0 & 0 & 0 & 0 & 0 \\ \hline 0 & K_{nc_i} & 0 & K_{nn_i} & 0 \\ \hline 0 & 0 & 0 & 0 & 0 \end{array}\right] , \qquad (70)$$

in which:

$$[K_{cc}]_i = [\phi_c]_i^T[K]_i[\phi_c]_i , \text{ and} \qquad (71)$$

$$[K_{nn}]_i = [\phi_n]_i^T[K]_i[\phi_n]_i , \text{ or}$$

$$= [\lambda_i] , \qquad (72)$$

where λ_i are eigenvalues of the ith substructure obtained in the principal mode analysis of the region with the interconnecting boundary coordinates fixed or constrained.

The submatrices $[K_{cn}]_i$ and $[K_{nc}]_i$ in Eq. (70) are null matrices because of the orthogonality property of the columns of the modal matrix $[\phi]_i$. Hence,

$$[\phi_c]_i^T [K]_i [\phi_n]_i = [0], \text{ and} \tag{73}$$

$$[\phi_n]_i^T [K]_i [\phi_c]_i = [0]. \tag{74}$$

Using Eqs. (73) and (74) with Eq. (70) yields:

$$[T]_i^T [K]_i [T]_i = \begin{bmatrix} 0 & 0 & 0 & 0 & 0 \\ 0 & K_{cc_i} & 0 & 0 & 0 \\ 0 & 0 & 0 & 0 & 0 \\ 0 & 0 & 0 & \lambda_i & 0 \\ 0 & 0 & 0 & 0 & 0 \end{bmatrix} . \tag{75}$$

Using Eqs. (69) and (75) and retaining all principal modes from the respective substructure eigensolutions, Eq. (53) becomes:

$$\begin{bmatrix} M_{cc} & M_{cnr} & M_{cnd} \\ M_{nrc} & M_{nrnr} & M_{nrnd} \\ M_{ndc} & M_{ndnr} & M_{ndnd} \end{bmatrix} \begin{Bmatrix} \ddot{q}_c \\ \ddot{q}_{nr} \\ \ddot{q}_{nd} \end{Bmatrix} + \begin{bmatrix} K_{cc} & K_{cnr} & K_{cnd} \\ K_{nrc} & K_{nrnr} & K_{nrnd} \\ K_{ndc} & K_{ndnr} & K_{ndnd} \end{bmatrix} \begin{Bmatrix} q_c \\ q_{nr} \\ q_{nd} \end{Bmatrix} = \{0\}, \tag{76}$$

and further reduction gives:

$$\begin{bmatrix} M_{cc} & M_{cnr} & M_{cnd} \\ M_{nrc} & I & 0 \\ M_{ndc} & 0 & I \end{bmatrix} \begin{Bmatrix} \ddot{q}_c \\ \ddot{q}_{nr} \\ \ddot{q}_{nd} \end{Bmatrix} + \begin{bmatrix} K_{cc} & 0 & 0 \\ 0 & \lambda_r & 0 \\ 0 & 0 & \lambda_d \end{bmatrix} \begin{Bmatrix} q_c \\ q_{nr} \\ q_{nd} \end{Bmatrix} = \{0\}, \tag{77}$$

where nr indicates normal modes retained and nd normal modes deleted. λ_r and λ_d are substructure fixed constraint normal mode eigenvalues for retained and deleted modes, respectively. Since $\{q_{nd}\}$ are deleted coordinates these do not appear in the final equations of motion for the total structure. The reduced equations of motion for the total structure in matrix notation, thus, become:

$$\begin{bmatrix} M_{cc} & M_{cnr} \\ M_{nrc} & I \end{bmatrix} \begin{Bmatrix} \ddot{q}_c \\ \ddot{q}_{nr} \end{Bmatrix} + \begin{bmatrix} K_{cc} & 0 \\ 0 & \lambda_r \end{bmatrix} \begin{Bmatrix} q_c \\ q_{nr} \end{Bmatrix} = \{0\}. \qquad (78)$$

Equation (78) governs the motion of the total structure and is expressed in the reduced set of coordinate {q}. An eigensolution of Eq. (78) would yield approximate system eigenvalues and approximate system eigenvectors can be obtained in the original system coordinates through Eq. (41).

B. General Solution with Initial Conditions

Free vibrations of a structure are usually the result of some known initial conditions. Initial conditions define the position and velocity of the structure in space at a known time $t = t_0$. The equations of motion for a conservative elastic structure undergoing free vibrations are given by:

$$\begin{bmatrix} m_1 & & & 0 \\ & \ddots & & \\ & & m_i & \\ & & & \ddots \\ 0 & & & m_N \end{bmatrix} \begin{Bmatrix} \ddot{x}_1 \\ \vdots \\ \ddot{x}_i \\ \vdots \\ \ddot{x}_N \end{Bmatrix} + \begin{bmatrix} K_1 & & & 0 \\ & \ddots & & \\ & & K_i & \\ & & & \ddots \\ 0 & & & K_N \end{bmatrix} \begin{Bmatrix} x_1 \\ \vdots \\ x_i \\ \vdots \\ x_N \end{Bmatrix} = \begin{Bmatrix} 0 \\ \vdots \\ 0 \\ \vdots \\ 0 \end{Bmatrix}, \qquad (79)$$

in which it is assumed that the structure is divided into N substructures and that $[m]_i$ and $[K]_i$ are the mass and stiffness matrices for the ith substructure.

It is noted that Eq. (79) is in the unconnected form. Let the initial displacements at time $t = t_0$ be represented by $\{x_0\}$ and the initial velocities by $\{\dot{x}_0\}$. Vectors $\{x_0\}$ and $\{\dot{x}_0\}$ are also given in the unconnected form and can be partitioned for each substructure as follows:

$$\{x_0\} = \begin{Bmatrix} x_1(t_0) \\ \hline \vdots \\ \hline x_i(t_0) \\ \hline \vdots \\ \hline x_N(t_0) \end{Bmatrix} \tag{80}$$

$$\{\dot{x}_0\} = \begin{Bmatrix} \dot{x}_1(t_0) \\ \hline \vdots \\ \hline \dot{x}_i(t_0) \\ \hline \vdots \\ \hline \dot{x}_N(t_0) \end{Bmatrix} . \tag{81}$$

Using the transformation,

$$\{x\} = [T]\{q\}$$

in Eq. (79) and premultiplying the result by $[T]^T$ yields:

$$[T]^T \begin{bmatrix} m_1 & & & 0 \\ & \ddots & & \\ & & m_i & \\ & & & \ddots \\ 0 & & & m_N \end{bmatrix} [T]\{\ddot{q}\} + [T]^T \begin{bmatrix} K_1 & & & 0 \\ & \ddots & & \\ & & K_i & \\ & & & \ddots \\ 0 & & & K_N \end{bmatrix} [T]\{q\} = \{0\}, \text{ or} \tag{82}$$

$$[M]\{\ddot{q}\} + [K]\{q\} = \{0\}, \tag{83}$$

where:

$$[M] = [T]^T \begin{bmatrix} m_1 & & & 0 \\ & \ddots & & \\ & & m_i & \\ & & & \ddots \\ 0 & & & m_N \end{bmatrix} [T], \text{ and}$$

$$[K] = [T]^T \begin{bmatrix} K_1 & & & 0 \\ & \ddots & & \\ & & K_i & \\ & & & \ddots \\ 0 & & & K_N \end{bmatrix} [T].$$

Equation (83) contains a much smaller set of equations of motion in the reduced coordinates $\{q\}$, since not all substructure normal modes are retained. This reduced equation is solved for its eigenvalues and eigenvectors. The modal matrix $[\bar{q}]$ of Eq. (83) is obtained by putting together the eigenvector columns in the ascending order of eigenvalues, i.e.,

$$[q] = [q_1 \; q_2 \; \cdots \; q_i \; \cdots \; q_n]. \tag{84}$$

Assuming the standard superposition of normal mode solution,

$$\{q\} = [\bar{q}]\{p\}, \tag{85}$$

gives from Eq. (83):

$$[M][\bar{q}]\{\ddot{p}\} + [K][\bar{q}]\{p\} = \{0\}. \tag{86}$$

Premultiplication of Eq. (86) by $[\bar{q}]^T$ yields:

$$[\bar{q}]^T[M][\bar{q}]\{\ddot{p}\} + [\bar{q}]^T[K][\bar{q}]\{p\} = \{0\}. \tag{87}$$

The orthogonality relations of modal matrix $[\bar{q}]$ are given by:

$$[\bar{q}]^T[M][\bar{q}] = [\,I\,], \text{ and} \tag{88}$$

$$[\bar{q}]^T[K][\bar{q}] = [\,\omega_i^2\,], \tag{89}$$

where $[\,I\,]$ is an identity matrix and $[\,\omega_i^2\,]$ is a matrix of system eigenvalues.

Using equations (88) and (89) in Eq. (87) gives:

$$\{\ddot{p}\} + [\,\omega_i^2\,]\{p\} = \{0\}. \tag{90}$$

Eq. (90) contains the uncoupled equations of motion which can be readily solved. It may be noted here that the number of uncoupled equations in Eq. (90) is much reduced since not all substructure normal modes are retained in the transformation,

$$\{x\} = [T]\{q\}.$$

The total solution of Eq. (90) is found by superposition of all solutions of Eq. (90), i.e.,

$$\{p\} = [\,\cos\,\omega_i(t-t_0)\,]\{a\} + [\,\sin\,\omega_i(t-t_0)\,]\{b\}, \tag{91}$$

where {a} and {b} are vectors of constants to be evaluated from the initial conditions.

At time $t = t_0$,

$$\{p_0\} = \{a\}, \text{ and} \tag{92}$$

$$\{\dot{p}_0\} = [\tilde{\omega}_i]\{b\}, \text{ or}$$

$$\{b\} = [\tilde{\omega}_i]^{-1}\{\dot{p}_0\}. \tag{93}$$

From Eq. (41), at time $t = t_0$

$$\{x_0\} = [T]\{q_0\}, \text{ and} \tag{94}$$

$$\{\dot{x}_0\} = [T]\{\dot{q}_0\}. \tag{95}$$

Premultiplying Eq. (94) by

$$[T]^T \begin{bmatrix} m_1 & & 0 \\ & \ddots & \\ & & m_N \end{bmatrix}$$

yields:

$$[T]^T \begin{bmatrix} m_1 & & 0 \\ & \ddots & \\ & & m_N \end{bmatrix} \{x_0\} = [T]^T \begin{bmatrix} m_1 & & 0 \\ & \ddots & \\ & & m_N \end{bmatrix} [T]\{q_0\}, \text{ or}$$

$$[T]^T \begin{bmatrix} m_1 & & 0 \\ & \ddots & \\ & & m_N \end{bmatrix} \{x_0\} = [M]\{q_0\}, \tag{96}$$

since:

$$[M] = [T]^T \begin{bmatrix} m_1 & & & 0 \\ & \ddots & & \\ & & m_i & \\ & & & \ddots \\ 0 & & & m_N \end{bmatrix} [T]$$

as defined earlier in Eq. (54).

Again, using Eq. (85) at time $t = t_0$, gives:

$$\{q_0\} = [\bar{q}]\{p_0\}. \tag{97}$$

Substituting Eq. (97) into Eq. (96) and premultiplying the result by $[\bar{q}]^T$ gives:

$$[\bar{q}]^T[T]^T \begin{bmatrix} m_1 & & & 0 \\ & \ddots & & \\ & & m_i & \\ & & & \ddots \\ 0 & & & m_N \end{bmatrix} \{x_0\} = [\bar{q}]^T[M][\bar{q}]\{p_0\}. \tag{98}$$

The orthogonality relations of $[\bar{q}]$ defined in Eq. (88) simplify Eq. (98) to give:

$$[\bar{q}]^T[T]^T \begin{bmatrix} m_1 & & & 0 \\ & \ddots & & \\ & & m_i & \\ & & & \ddots \\ 0 & & & m_N \end{bmatrix} \{x_0\} = \{p_0\}. \tag{99}$$

Thus from Eq. (92),

$$\{a\} = \{p_0\}, \text{ or}$$

$$\{a\} = [\bar{q}]^T[T]^T \begin{bmatrix} m_1 & & & 0 \\ & \ddots & & \\ & & m_i & \\ & & & \ddots \\ 0 & & & m_N \end{bmatrix} \{x_0\}. \tag{100}$$

Similarly, it can be shown that vector {b} is given by:

$$\{b\} = [\tilde{\omega}_i]^{-1}[\bar{q}]^T[T]^T \begin{bmatrix} m_1 & & 0 \\ & \ddots & \\ & & m_N \end{bmatrix} \{\dot{x}_0\}. \qquad (101)$$

The transformation matrix may be partitioned for each substructure to give:

$$[T] = \begin{bmatrix} T_1 \\ \vdots \\ T_i \\ \vdots \\ T_N \end{bmatrix},$$

where $[T]_i$ is the transformation matrix for the ith substructure. The above partitioning of matrix [T] simplifies the product

$$[T]^T \begin{bmatrix} m_1 & & 0 \\ & \ddots & \\ & & m_N \end{bmatrix} \{x_0\},$$

in Eq. (100) to yield:

$$[T]^T \begin{bmatrix} m_1 & & 0 \\ & \ddots & \\ & & m_N \end{bmatrix} \{x_0\} = [T_1^T \,|\, \cdots \,|\, T_i^T \,|\, \cdots \,|\, T_N^T] \begin{bmatrix} m_1 & & 0 \\ & \ddots & \\ & & m_N \end{bmatrix} \begin{Bmatrix} x_1(t_0) \\ \vdots \\ x_i(t_0) \\ \vdots \\ x_N(t_0) \end{Bmatrix}, \text{ or}$$

$$= [T_1^T m_1 x_1(t_0) + \cdots + T_i^T m_i x_i(t_0) + \cdots + T_N^T m_N x_N(t_0)], \text{ or}$$

$$= [\sum_{i=1,N} T_i^T m_i x_i(t_0)]. \tag{102}$$

Similarly,

$$[T]^T \begin{bmatrix} m_1 & & & 0 \\ & \ddots & & \\ & & m_i & \\ & & & \ddots \\ 0 & & & m_N \end{bmatrix} \{\dot{x}_0\} = [\sum_{i=1,N} T_i^T m_i \dot{x}_i(t_0)]. \tag{103}$$

Substituting for vectors {a} and {b} from Eqs. (100) and (101) into Eq. (91) gives:

$$\{p\} = \begin{bmatrix} \cos \omega_i(t-t_0) \end{bmatrix} [\bar{q}]^T [T]^T \begin{bmatrix} m_1 & & & 0 \\ & \ddots & & \\ & & m_i & \\ & & & \ddots \\ 0 & & & m_N \end{bmatrix} \{x_0\}$$

$$+ \begin{bmatrix} \sin \omega_i(t-t_0) \end{bmatrix} \begin{bmatrix} \omega_i \end{bmatrix}^{-1} [\bar{q}]^T [T]^T \begin{bmatrix} m_1 & & & 0 \\ & \ddots & & \\ & & m_i & \\ & & & \ddots \\ 0 & & & m_N \end{bmatrix} \{\dot{x}_0\}. \tag{104}$$

The total system solution, {x}, is given by:

$$\{x\} = [T]\{q\}, \text{ or}$$

$$\{x\} = [T][\bar{q}]\{p\}, \text{ or}$$

$$\{x\} = [T][\bar{q}] \left(\left[\cos \omega_i (t-t_0) \right] [\bar{q}]^T [T]^T \begin{bmatrix} \bar{m}_1 & & & 0 \\ & \ddots & & \\ & & m_i & \\ & & & \ddots \\ 0 & & & m_N \end{bmatrix} \{x_0\} \right.$$

$$\left. + \left[\sin \omega_i (t-t_0) \right] [\omega_i]^{-1} [\bar{q}]^T [T]^T \begin{bmatrix} \bar{m}_1 & & & 0 \\ & \ddots & & \\ & & m_i & \\ & & & \ddots \\ 0 & & & m_N \end{bmatrix} \{\dot{x}_0\} \right) . \quad (105)$$

Equation (105) gives approximately the structure response for all time $t \geq t_0$ due to the given initial conditions $\{x_0\}$ and $\{\dot{x}_0\}$.

The objective of the above analysis has been to show the applicability of substructures method to obtain solutions to initial conditions problems. It may be noted that at time $t = t_0$, Eq. (105) does not reduce to the given initial displacements, $\{x_0\}$, and the initial velocities, $\{\dot{x}_0\}$, because of the modal truncation allowed in the substructures technique. This suggests that the number of substructure normal modes retained, may have to be large to obtain system response within the limits of engineering accuracy.

C. Solution with Initial Conditions Applied to Impulsive Loadings

In many instances, structures are subjected to impulsive type of loading. The result of such a loading is that points in the structure develop initial velocities. The loading time, ε, needs to be small such that displacements are zero while initial velocities are achieved. The initial velocities of the structure can be determined as follows:

Consider a structure subjected to a set of impulses at time $t = t_0$

which are represented by vector $\{g\}$. The change in momentum, at time $t = t_0$, must equal the impulsive loading, i.e.,

$$[m]\{\dot{x}(t_0)\} = \{g\}, \tag{106}$$

where $[m]$ is the structure mass matrix in the connected form and can be obtained by treating the structure as a whole. Premultiplying Eq. (106) by $[m]^{-1}$ gives:

$$\{\dot{x}(t_0)\} = [m]^{-1}\{g\}. \tag{107}$$

The initial velocities $\{\dot{x}_0\}$ in the unconnected form can now be obtained from Eq. (107) by considering each substructure separately.

Since initial displacements of the structure at time $t = t_0$ are zero,

$$\{x_0\} = \{0\}. \tag{108}$$

The total solution is available from the free vibration solution with initial conditions, i.e.,

$$\{x(t)\} = [T][\bar{q}]\left[\sin \omega_i(t-t_0)\right]\left[\omega_i\right]^{-1}[\bar{q}]^T[T]^T \begin{bmatrix} \bar{m}_1 & & & 0 \\ & \ddots & & \\ & & m_i & \\ & & & \ddots \\ 0 & & & m_N \end{bmatrix} \{\dot{x}_0\}. \tag{109}$$

Equation (109) gives the structure response due to impulsive loading for all time $t \geq t_0$. The advantage of the substructures approach, utilized to obtain solutions to impulsive loadings, lies in the fact that smaller order matrices are treated in the computations.

This gives the necessary saving in storage required for problems involving large structures.

D. Principal Mode Error Analysis

Any discrete analysis of a continuous system results in an approximate solution. If the number of coordinates used are enough and proper, the solution may be considered to be accurate or for all practical purposes "exact". A substructure type analysis which gives the total solution in parts would result in an "exact" solution if the transformation from the discrete coordinates $\{x\}$ to the set of coordinates $\{q\}$ were one to one or, in other words, if all of the substructure fixed constraint normal modes were retained. Since the purpose of this analysis is to obtain a much smaller set of equations of motion to be solved through modal truncation, only approximate system eigenvalues and eigenvectors are obtained.

Hurty (10) has derived a method for approximating the eigenvalue error based on a linear perturbation of system eigenvalues and eigenvectors. The basic assumption is that the eigenvalue error is small so that higher order terms in the perturbation are negligible. The technique is applied to substructures analysis and yields a criterion that indicates which system modes are accurate and which system modes are inaccurate.

A similar error analysis is presented by Bajan and Feng (11) and as an extension they provide a method to improve upon system eigenvalues and eigenvectors. The approximate error derived in this way provides a good estimate of the error as long as the error remains small. In

the present study an approximate eigenvalue error analysis presented by Bajan and Feng is repeated only for the purpose of illustration.

System strain energy in the principal modes is in error since system eigenvectors obtained through modal truncation are approximate. An expression for an error estimate to the system strain energy in the principal modes caused by the omission of certain substructure modes is derived. Strain energy errors give an indication of the errors involved in the system eigenvectors without actual calculation of such eigenvector errors. Strain energy errors, like eigenvalue errors, involve only one-number comparisons. This motivates their comparison with the eigenvalue error from the reduced number of equations of motion. This comparison will be discussed in Chapter V.

1. Estimation of System Eigenvalue Error

The system eigenvalue problem obtained by eliminating the deleted coordinates is compared, using a linear perturbation technique, with the one obtained by omitting substructure fixed constraint normal modes. This yields the desired expression for estimating the system eigenvalue error.

Rewriting Eq. (77) gives:

$$\begin{bmatrix} M_r & M_{rd} \\ M_{dr} & I \end{bmatrix} \begin{Bmatrix} \ddot{q}_r \\ \ddot{q}_d \end{Bmatrix} + \begin{bmatrix} K_r & 0 \\ 0 & \lambda_j \end{bmatrix} \begin{Bmatrix} q_r \\ q_d \end{Bmatrix} = \begin{Bmatrix} 0 \\ 0 \end{Bmatrix} , \qquad (110)$$

in which r refers to retained coordinates while d incidates deleted coordinates.

Assuming or taking a principal mode,

$$\{q\} = \{y\}e^{i\omega t},$$

Eq. (79) becomes:

$$\left(-\omega^2 \left[\begin{array}{c|c} M_r & M_{rd} \\ \hline M_{dr} & I \end{array}\right] + \left[\begin{array}{c|c} K_r & 0 \\ \hline 0 & \lambda_j \end{array}\right]\right) \left\{\begin{array}{c} y_r \\ \hline y_d \end{array}\right\} = \left\{\begin{array}{c} 0 \\ \hline 0 \end{array}\right\}, \qquad (111)$$

where ω^2 represents eigenvalues of the total structure.

In the above equation, since $\{y_d\}$ are not known, these are eliminated as follows:

Expanding Eq. (111) gives:

$$-\omega^2[M_r]\{y_r\} - \omega^2[M_{rd}]\{y_d\} + [K_r]\{y_r\} = \{0\}, \text{ and} \qquad (112)$$

$$-\omega^2[M_{dr}]\{y_r\} - \omega^2\{y_d\} + [\lambda_j]\{y_d\} = \{0\}. \qquad (113)$$

Equation (113) yields:

$$\{y_d\} = \frac{\omega^2[M_{dr}]\{y_r\}}{[\lambda_j] - \omega^2[I]}, \text{ or}$$

$$\{y_d\} = \left[\frac{\omega^2}{\lambda_j - \omega^2}\right][M_{dr}]\{y_r\}. \qquad (114)$$

Using Eq. (114) in Eq. (112) yields:

$$-\omega^2[M_r]\{y_r\} - \omega^2[M_{rd}]\left[\frac{\omega^2}{\lambda_j - \omega^2}\right][M_{dr}]\{y_r\} + [K_r]\{y_r\} = \{0\},$$

or

$$[K_r]\{y_r\} = \omega^2([M_r] + [M_{rdr}])\{y_r\}, \qquad (115)$$

where:

$$[M_{rdr}] = [M_{rd}] \left[\frac{\omega^2}{\lambda_j - \omega^2}\right][M_{dr}]. \tag{116}$$

Eq. (115) defines an eigenvalue problem with an effective mass matrix of,

$$[M_r] + [M_{rdr}],$$

in which $[M_{rdr}]$ is defined in Eq. (116).

This eigenvalue problem is the consequence of eliminating coordinates $\{y_d\}$. The eigenvalue problem obtained by the omission of coordinates $\{y_d\}$ may be defined by:

$$[K_r]\{\bar{y}_r\} = \bar{\omega}^2[M_r]\{\bar{y}_r\}, \tag{117}$$

in which $\{\bar{y}_r\}$ and $\bar{\omega}^2$ are approximate system eigenvectors and eigenvalues obtained through an eigensolution of Eq. (78).

An "exact" eigenvalue error may be defined as:

$$\delta\lambda = \bar{\omega}^2 - \omega^2. \tag{118}$$

In the ensuing paragraphs an estimate, $\delta\bar{\lambda}$, of the above exact error, $\delta\lambda$, will be obtained.

Assuming a linear perturbation of the system eigenvector, i.e.,

$$\{y_r\} = \{\bar{y}_r\} + \delta\{y_r\}, \tag{119}$$

and substituting in Eq. (117) along with Eq. (118) gives:

$$[K_r]\{\bar{y}_r\} + [K_r]\delta\{y_r\} = (\bar{\omega}^2 - \delta\lambda)([M_r] + [M_{rdr}])(\{\bar{y}_r\} + \delta\{y_r\}). \tag{120}$$

Subtracting Eq. (115) from Eq. (120) and disregarding higher order terms yields:

$$[K_r]\delta\{y_r\} = \bar{\omega}^2[M_{rdr}]\{\bar{y}_r\} + \bar{\omega}^2[M_{rdr}]\delta\{y_r\} + \bar{\omega}^2[M_r]\delta\{y_r\}$$

$$- \delta\lambda([M_r] + [M_{rdr}])\{\bar{y}_r\}. \tag{121}$$

In Eq. (115), approximating ω^2 by $\bar{\omega}^2$ and replacing $\{y_r\}$ by $\delta\{y_r\}$ gives:

$$[K_r]\delta\{y_r\} \simeq \bar{\omega}^2([M_r] + [M_{rdr}])\delta\{y_r\}. \tag{122}$$

In view of Eq. (122), Eq. (121) becomes:

$$0 \simeq \bar{\omega}^2[M_{rdr}]\{\bar{y}_r\} - \delta\bar{\lambda}([M_r] + [M_{rdr}])\{\bar{y}_r\}, \tag{123}$$

in which $\delta\lambda$ has been replaced by $\delta\bar{\lambda}$, since Eq. (122), used in Eq. (121), is only an approximate result.

Premultiplying Eq. (123) by $\{\bar{y}_r\}^T$ gives:

$$\delta\bar{\lambda}\{\bar{y}_r\}^T([M_r] + [M_{rdr}])\{\bar{y}_r\} \simeq \bar{\omega}^2\{\bar{y}_r\}^T[M_{rdr}]\{\bar{y}_r\}. \tag{124}$$

The orthogonality relation of $\{\bar{y}_r\}$ with respect to $[M_r]$ is given by:

$$\{\bar{y}_r\}^T[M_r]\{\bar{y}_r\} = 1. \tag{125}$$

Using Eq. (125) in Eq. (124) yields:

$$\delta\bar{\lambda} \simeq \bar{\omega}^2\{\bar{y}_r\}^T[M_{rdr}]\{\bar{y}_r\}, \tag{126}$$

in which the term $\delta\bar{\lambda}[M_{rdr}]$ has been neglected since,

$$\delta\bar{\lambda}\left[\frac{\omega^2}{\lambda_j - \omega^2}\right] << 1.$$

This restriction on Eq. (126) is justified since substructure eigenvalues, λ_j, are much greater than system eigenvalues ω^2.

Rewriting Eq. (126) in terms of original nomenclature gives:

$$\delta\bar{\lambda} \simeq \bar{\omega}^2 \begin{Bmatrix} \bar{y}_c \\ \hline \bar{y}_{nr} \end{Bmatrix}^T \begin{bmatrix} M_{cnd} \\ \hline 0 \end{bmatrix} \left[\frac{\omega^2}{\lambda_j - \omega^2}\right] [M_{ndc} \mid 0] \begin{Bmatrix} \bar{y}_c \\ \hline \bar{y}_{nr} \end{Bmatrix}, \text{ or}$$

$$\delta\bar{\lambda} \simeq \bar{\omega}^2 \{\bar{y}_c\}^T [M_{cnd}] \left[\frac{\bar{\omega}^2}{\lambda_j - \bar{\omega}^2}\right] [M_{ndc}]\{\bar{y}_c\}, \qquad (127)$$

in which ω^2 is approximated by $\bar{\omega}^2$ to give an estimate, $\delta\bar{\lambda}$, of the "exact" eigenvalue error, $\delta\lambda$, which is introduced because of the omission of higher frequency substructure fixed constraint principal modes.

2. Error Estimation of System Principal Mode Strain Energy

An estimate of the difference between "exact" and approximate system strain energy in principal modes is obtained as an indicator of the errors involved in the system eigenvectors. If $\{x^i\}$ is a system eigenvector in the ith principal mode, strain energy in this mode is given by:

$$U^i = \frac{1}{2}\{x^i\}^T [\bar{K}]\{x^i\}, \qquad (128)$$

where U^i represents system strain energy in the ith principal mode and $[\bar{K}]$ is given by Eq. (49).

Through the coordinate transformation,

$$\{x^i\} = [T]\{q^i\},$$

Eq. (128) becomes:

$$U^i = \frac{1}{2}\{q^i\}^T [T]^T [\bar{K}][T]\{q^i\}. \tag{129}$$

Use of Eq. (55) in Eq. (129) yields:

$$U^i = \frac{1}{2}\{q^i\}^T [K]\{q^i\}. \tag{130}$$

System strain energy in the ith principal mode for the "exact" case is obtained by premultiplying the left hand side of Eq. (115) by $\frac{1}{2}\{y_r^i\}^T$, i.e.,

$$U^i = \frac{1}{2}\{y_r^i\}^T [K_r]\{y_r^i\}$$

$$= \frac{1}{2}\omega^{i^2}\{y_r^i\}^T ([M_r] + [M_{rdr}])\{y_r^i\}, \tag{131}$$

where $\{y_r^i\}$ represents the "exact" ith mode eigenvector obtained by eliminating coordinates $\{y_d\}$.

Omission of coordinates $\{y_d\}$ gives an approximate solution defined by Eq. (117). Premultiplying the left hand side of Eq. (117) by $\frac{1}{2}\{\bar{y}_r^i\}^T$ yields the approximate system strain energy in the ith

principal mode, i.e.,

$$\bar{U}^i = \frac{1}{2} \{\bar{y}_r^i\}^T [K_r] \{\bar{y}_r^i\}, \text{ or}$$

$$= \frac{1}{2} \bar{\omega}^{i2} \{\bar{y}_r^i\}^T [M_r] \{\bar{y}_r^i\}, \tag{132}$$

where $\{\bar{y}_r^i\}$ represents "approximate" ith mode system eigenvector and $\bar{\omega}^{i2}$ gives the corresponding eigenvalue. Subtracting Eq. (132) from Eq. (131) gives the required system strain energy error in the ith principal mode, i.e.,

$$\delta U^i = U^i - \bar{U}^i, \text{ or}$$

$$= \frac{1}{2} \omega^{i2} \{y_r^i\}^T ([M_r] + [M_{rdr}]) \{y_r^i\} - \frac{1}{2} \bar{\omega}^{i2} \{\bar{y}_r^i\}^T [K_r] \{\bar{y}_r^i\}. \tag{133}$$

Approximating ω^{i2} by $\bar{\omega}^{i2}$ and $\{y_r^i\}$ by $\{\bar{y}_r^i\}$on the right hand side of Eq. (133) gives an expression for estimating the system strain energy in the ith principal mode, i.e.,

$$\overline{\delta U}^i = \frac{1}{2} \bar{\omega}^{i2} \{\bar{y}_r^i\}^T [M_{rdr}] \{\bar{y}_r^i\}, \text{ or} \tag{134}$$

$$\overline{\delta U}^i \simeq \frac{1}{2} \overline{\delta\lambda}^i, \tag{135}$$

where $\overline{\delta\lambda}^i$ approximates the system eigenvalue error in the ith principal mode and is given by Eq. (127) with $\{\bar{y}_c^i\}$ replacing $\{\bar{y}_c\}$ and $\bar{\omega}^i$ replacing $\bar{\omega}$.

Having obtained system eigenvalues and strain energy in the principal modes and estimates of various error indicators, the substructures

technique will now be applied to systems under forced excitation. This will be discussed in Chapter IV.

CHAPTER IV

FORCED UNDAMPED VIBRATIONS OF SYSTEMS

In Chapters II and III a free vibration solution of systems has been obtained in terms of principal modes. To continue the application of the substructures approach the response of systems under forced excitation is obtained. It is assumed that damping is small and can be neglected. The solution of the forced vibration depends intimately on the results of the free vibration by virtue of the fact that the normal modes established for the system lead to the possibility of expanding arbitrary forcing functions. Also, the orthogonality relations of these normal modes help in uncoupling the equations of motion.

In the present chapter systems under forced excitation are analyzed for system response, incorporating the substructures method of analysis. A survey of the literature on substructures analysis shows little has been done to obtain solutions of the forced vibration problem through the method of substructures. This approach results in a transformation which can be used to yield a much smaller set of approximate equations to be solved. It transforms the equations in such a way that accurate solutions can be obtained more efficiently. The approach also allows direct use of modal test data and economizes on computer time and storage since the problem size to be solved is much smaller.

System response solutions for the following types of forced excitation are derived:

(i) General Time-Varying Displacement Excitation

(ii) Harmonic Force Excitation

(iii) Base Acceleration type of Excitation

(iv) General Time-Varying Force Excitation.

A. General Time-Varying Displacement Excitation

In some cases the excitation may be given as a prescribed motion at a prescribed location on the system. Some examples, which are typical of this type of excitation, are motion of automobiles on roads, machinery where cams give definite displacements, etc. In the finite element model of the given system, nodes on which displacements are specified are eliminated and motion of the rest of the structure studied. Since the substructure boundary nodes yield constraint modes which cannot be eliminated, care should be taken that the substructure boundary nodes do not coincide with those at which motion is prescribed.

The given structure is divided into several substructure regions in exactly the same way as described for the free vibration solution, so that the transformation matrices developed for the free vibration solution can be directly utilized in the forced excitation solution. The differential equations of motion for the total structure in the unconnected form are given by:

$$\begin{bmatrix} m_1 & & 0 \\ & \ddots & \\ & & m_i \\ & & & \ddots \\ 0 & & & & m_N \end{bmatrix} \begin{Bmatrix} \ddot{x}_1 \\ \vdots \\ \ddot{x}_i \\ \vdots \\ \ddot{x}_N \end{Bmatrix} + \begin{bmatrix} K_1 & & 0 \\ & \ddots & \\ & & K_i \\ & & & \ddots \\ 0 & & & & K_N \end{bmatrix} \begin{Bmatrix} x_1 \\ \vdots \\ x_i \\ \vdots \\ x_N \end{Bmatrix} = \{f(t)\}. \qquad (136)$$

Eq. (136) is partitioned to group the specified displacement together, i.e.,

$$\left[\begin{array}{c|c} \begin{matrix} m_1 & & 0 \\ & m_i & \\ 0 & & m_N \end{matrix} & \begin{matrix} m_{sf} \end{matrix} \\ \hline \begin{matrix} m_{fs} \end{matrix} & \begin{matrix} m_{ff} \end{matrix} \end{array}\right] \left\{\begin{matrix} \ddot{x}_1 \\ \vdots \\ \ddot{x}_i \\ \vdots \\ \ddot{x}_n \\ \hline \ddot{x}_f \end{matrix}\right\} + \left[\begin{array}{c|c} \begin{matrix} K_1 & & 0 \\ & K_i & \\ 0 & & K_N \end{matrix} & \begin{matrix} K_{sf} \end{matrix} \\ \hline \begin{matrix} K_{fs} \end{matrix} & \begin{matrix} K_{ff} \end{matrix} \end{array}\right] \left\{\begin{matrix} x_1 \\ \vdots \\ x_i \\ \vdots \\ x_N \\ \hline x_f \end{matrix}\right\} = \left\{\begin{matrix} 0 \\ \vdots \\ 0 \\ \vdots \\ 0 \\ \hline f_f \end{matrix}\right\}, \tag{137}$$

where $[m]_i$ and $[K]_i$ are modified mass and stiffness matrices of the ith substructure obtained by fixing those coordinates of the ith substructure on which displacements are specified; $\{f_f\}$ are the unknown forces required to produce the known displacements $\{x_f\}$.

Rewriting Eq. (137) with condensed notation gives:

$$\left[\begin{array}{c|c} m_{ss} & m_{sf} \\ \hline m_{fs} & m_{ff} \end{array}\right] \left\{\begin{matrix} \ddot{x}_s \\ \hline \ddot{x}_f \end{matrix}\right\} + \left[\begin{array}{c|c} K_{ss} & K_{sf} \\ \hline K_{fs} & K_{ff} \end{array}\right] \left\{\begin{matrix} x_s \\ \hline x_f \end{matrix}\right\} = \left\{\begin{matrix} 0 \\ \hline f_f \end{matrix}\right\}, \tag{138}$$

in which,

$$[m_{ss}] = \begin{bmatrix} m_1 & & 0 \\ & m_i & \\ 0 & & m_N \end{bmatrix}, \text{ and}$$

$$[K_{ss}] = \begin{bmatrix} K_1 & & 0 \\ & K_i & \\ 0 & & K_N \end{bmatrix}.$$

Expanding Eq. (138) yields:

$$[m_{ss}]\{\ddot{x}_s\} + [m_{sf}]\{\ddot{x}_f\} + [K_{ss}]\{x_s\} + [K_{sf}]\{x_f\} = \{0\}, \text{ and} \quad (139)$$

$$[m_{fs}]\{\ddot{x}_s\} + [m_{ff}]\{\ddot{x}_f\} + [K_{fs}]\{x_s\} + [K_{ff}]\{x_f\} = \{f_f\}. \quad (140)$$

Since $\{x_f\}$ are specified, Eq. (139) is rearranged and solved for displacement $\{x_s\}$, i.e., the system response due to the prescribed motion $\{x_f\}$.

Rearranging Eq. (139) gives:

$$[m_{ss}]\{\ddot{x}_s\} + [K_{ss}]\{x_s\} = -([m_{sf}]\{\ddot{x}_f\} + [K_{sf}]\{x_f\}). \quad (141)$$

Equation (141) is a nonhomogeneous equation in which

$$-([m_{sf}]\{\ddot{x}_f\} + [K_{sf}]\{x_f\})$$

is the forcing term. Using the substructures approach, a principal mode analysis of each substructure by itself with coordinates on which displacements are specified as being fixed, yields a transformation matrix $[T_s]$. Matrix $[T_s]$, in general, is not a square matrix and its columns consist of substructure constraint modes and substructure fixed constraint normal modes. The higher modes of the substructure fixed constraint normal modes can be deleted since these contribute very little towards a free vibration solution or solution of systems under a low frequency excitation or other excitations where lower modes are shown to be most important. Using the transformation,

$$\{x_s\} = [T_s]\{q_s\}, \text{ gives:} \quad (142)$$

$$[m_{ss}][T_s]\{\ddot{q}_s\} + [K_{ss}][T_s]\{q_s\} = -[m_{sf}]\{\ddot{x}_f\} - [K_{sf}]\{x_f\}.$$

Premultiplication of the above equation by $[T_s]^T$ yields:

$$[T_s]^T[m_{ss}][T_s]\{\ddot{q}_s\} + [T_s]^T[K_{ss}][T_s]\{q_s\}$$

$$= - [T_s]^T[m_{sf}]\{\ddot{x}_f\} - [T_s]^T[K_{sf}]\{x_f\}, \text{ or} \qquad (143)$$

$$[M_s]\{\ddot{q}_s\} + [K_s]\{q_s\} = - ([T_s]^T[m_{sf}]\{\ddot{x}_f\} + [T_s]^T[K_{sf}]\{x_f\}). \qquad (144)$$

Equation (144) is the reduced set of equations of motion in which,

$$[M_s] = [T_s]^T[m_{ss}][T_s], \text{ and}$$

$$[K_s] = [T_s]^T[K_{ss}][T_s].$$

Matrices $[M_s]$ and $[K_s]$ are symmetric since $[M_s]^T = [M_s]$, and $[K_s]^T = [K_s]$.

A free vibration analysis of the homogeneous part of Eq. (144) yields its modal matrix $[\bar{q}_s]$. Equation (144) is uncoupled through the transformation:

$$\{q_s\} = [\bar{q}_s]\{p_s\}. \qquad (145)$$

Using Eq. (145) in Eq. (144) and premultiplying the results by $[\bar{q}_s]^T$ gives:

$$[\bar{q}_s]^T[M_s][\bar{q}_s]\{\ddot{p}_s\} + [\bar{q}_s]^T[K_s][\bar{q}_s]\{p_s\}$$

$$= - [\bar{q}_s]^T[T_s]^T[m_{sf}]\{\ddot{x}_f\} - [\bar{q}_s]^T[T_s]^T[K_{sf}]\{x_f\}. \qquad (146)$$

The orthogonal relations of $[\bar{q}_s]$ are given by:

$$[\bar{q}_s]^T[M_x][\bar{q}_s] = [\,I\,], \text{ and} \tag{147}$$

$$[\bar{q}_s]^T[K_s][\bar{q}_s] = [\,\omega_i^2\,], \tag{148}$$

where ω_i is the system circular frequency in the ith principal mode with the points of excitation taken to be actually fixed during the homogeneous part of the solution, i.e., with $\{x_f\} = \{0\}$.

In view of Eqs. (147) and (148), Eq. (146) becomes:

$$\{\ddot{p}_s\} + [\,\omega_i^2\,]\{p_s\} = -[\bar{q}_s]^T[T_s]^T[m_{sf}]\{x_f\} - [\bar{q}_s][T_s]^T[K_{sf}]\{x_f\}. \tag{149}$$

Equation (149) is of the form,

$$\{\ddot{p}_s\} + [\,\omega_i^2\,]\{p_s\} = \{F(t)\},$$

whose solution with zero initial conditions is given by Duhamel's integral as:

$$\{p_s\} = [\,\omega_i\,]^{-1} \int_0^t [\,\sin\,\omega_i(t-\tau)\,]\{F(\tau)\}d\tau. \tag{150}$$

Thus, solution of Eq. (149) with zero initial conditions is given by:

$$\{p_s\} = -[\,\omega_i\,]^{-1} \int_0^t [\,\sin\,\omega_i(t-\tau)\,]([\bar{q}_s]^T[T_s]^T[m_{sf}]\{\ddot{x}_f(\tau)\} +$$

$$[\bar{q}_s]^T[T_s]^T[K_{sf}]\{x_f(\tau)\})d\tau. \tag{151}$$

The total solution $\{x_s\}$ is obtained through the use of Eqs. (142), (145) and (151), i.e., with zero initial conditions:

$$\{x_s\} = -[T_s][\bar{q}_s][\omega_i]^{-1} \int_0^t [\sin \omega_i(t-\tau)]([\bar{q}_s]^T[T_s]^T[m_{sf}]\{\ddot{x}_f(\tau)\} +$$

$$[\bar{q}_s]^T[T_s]^T[K_{sf}]\{x_f(\tau)\})d\tau. \qquad (152)$$

Usually the size of matrix $[T_s]$ is large and its partitioning at the substructure's level helps reduce computer time. Matrix $[T_s]$ is partitioned as follows:

$$[T_s] = \begin{bmatrix} T_{s_1} \\ \vdots \\ T_{s_i} \\ \vdots \\ T_{s_N} \end{bmatrix},$$

where $[T_s]_i$ is the transformation matrix for the ith substructure.

The forms of matrices $[m_{sf}]$ and $[K_{sf}]$ are given by:

$$[K_{sf}] = \begin{bmatrix} K_{sf_1} & & 0 \\ & \ddots & \\ & & K_{sf_N} \\ 0 & & \end{bmatrix}, \quad [m_{sf}] = \begin{bmatrix} m_{sf_1} & & 0 \\ & \ddots & \\ & & m_{sf_N} \\ 0 & & \end{bmatrix}$$

and vectors $\{x_f\}$ and $\{\ddot{x}_f\}$ may be partitioned as:

$$\{x_f\} = \begin{Bmatrix} x_{f_1} \\ \vdots \\ x_{f_i} \\ \vdots \\ x_{f_N} \end{Bmatrix}, \quad \{\ddot{x}_f\} = \begin{Bmatrix} \ddot{x}_{f_1} \\ \vdots \\ \ddot{x}_{f_i} \\ \vdots \\ \ddot{x}_{f_N} \end{Bmatrix},$$

where $\{x_f\}_i$ are the specified displacements at the interior joints of the ith substructure. Thus the matrix product

$$[T_s]^T[m_{sf}]\{\ddot{x}_f\}$$

in Eq. (152) simplifies to:

$$[T_s]^T[m_{sf}]\{\ddot{x}_f\} = [T_1^T m_{sf_1} \ddot{x}_{f_1} + \cdots + T_i^T m_{sf_i} \ddot{x}_{f_i} +$$

$$\cdots + T_N^T m_{sf_N} \ddot{x}_{f_N}], \text{ or}$$

$$= [\sum_{i=1,N} T_i^T m_{sf_i} \ddot{x}_{f_i}]. \tag{153}$$

Similarly, the matrix product

$$[T_s]^T[K_{sf}]\{x_f\}$$

simplifies to:

$$[T_s]^T[K_{sf}]\{x_f\} = [\sum_{i=1,N} T_i^T K_{sf_i} x_{f_i}]. \tag{154}$$

Use of Eqs. (153) and (154) allows working with one substructure at a time and thus matrices of much smaller sizes are handled in the digital computer. This results in a saving of computer time and storage.

For completeness it may be noted that forces $\{f_f\}$ required to produce the displacement excitation $\{x_f\}$ can be obtained through Eq. (140) in which structure response $\{x_s\}$ is obtained by using Eq. (152).

B. Harmonic Force Excitation

Frequently vibrations of a structure are the result of harmonic forces acting at various points of that structure. An excitation which is sinusoidal in nature may be termed harmonic excitation, e.g.,

$$\{f(t)\} = \{f'\} \sin \Omega t, \text{ or}$$

$$\{f(t)\} = \{f'\} \cos \Omega t,$$

where $\{f'\}$ is a vector of constants and Ω is the forcing frequency, each forcing function having the same frequency. Phase angles may also be associated with this type of excitation, i.e.,

$$\{f(t)\} = \begin{Bmatrix} f'_1 \sin (\Omega t + \psi_1) \\ \vdots \\ f'_i \sin (\Omega t + \psi_i) \\ \vdots \\ f'_n \sin (\Omega t + \psi_n) \end{Bmatrix}, \text{ or}$$

$$\{f(t)\} = \begin{Bmatrix} f'_1 \cos (\Omega t + \psi_1) \\ \vdots \\ f'_i \cos (\Omega t + \psi_i) \\ \vdots \\ f'_n \cos (\Omega t + \psi_n) \end{Bmatrix}.$$

In addition harmonic forcing functions with different frequencies may be treated.

$$\{f(t)\} = \begin{Bmatrix} f_1' \sin(\Omega_1 t + \psi_1) \\ \vdots \\ f_i' \sin(\Omega_i t + \psi_i) \\ \vdots \\ f_n' \sin(\Omega_n t + \psi_n) \end{Bmatrix} , \text{ or}$$

$$\{f(t)\} = \begin{Bmatrix} f_1' \cos(\Omega_1 t + \psi_1) \\ \vdots \\ f_i' \cos(\Omega_i t + \psi_i) \\ \vdots \\ f_n' \cos(\Omega_n t + \psi_n) \end{Bmatrix} ,$$

where n represents the number of structure points excitated.

Since this study is restricted to linear systems, total structure motion due to harmonic excitations with different frequencies, as illustrated by the above equations, is obtained by superimposing the structure motion caused by each excitation separately. Furthermore excitations not in phase can be simplified to those in phase. Hence it is sufficient to present solutions to harmonic excitations with arbitrary phase relationships to complete the general case. Finally it is shown that a periodic excitation which repeats itself in equal intervals of time, can be represented by a Fourier Series. Thus solutions obtained for harmonic excitations can also be applied to yield system response to periodic excitations.

1. Harmonic Excitations of the Same Forcing Frequency

Excitations of this type are assumed to have a common forcing frequency and an arbitrary phase relationship. It will first be shown that this type of excitation reduces to simpler

forms of sine and cosine excitations. The given structure is again considered to be divided into several substructures to yield the necessary transformation matrix [T]. Forces located at the boundaries of substructures are shared equally among all substructures which meet at those given boundary points. Partitioning the forcing vector,

$$\{f(t)\} = \begin{Bmatrix} f_1(t) \\ \vdots \\ f_i(t) \\ \vdots \\ f_N(t) \end{Bmatrix} ,$$

where $\{f_i(t)\}$ represents harmonic forces acting on the ith substructure and can be written as:

$$\{f_i(t)\} = \begin{Bmatrix} a_1 \sin(\Omega t + \psi_1) \\ \vdots \\ a_j \sin(\Omega t + \psi_j) \\ \vdots \\ a_n \sin(\Omega t + \psi_n) \end{Bmatrix} . \qquad (155)$$

In Eq. (155), sine functions may be replaced by cosine functions, but no loss in generality is made if sine functions only are treated. Solutions for cosine functions will be given directly.

Considering the forcing vector of the ith substructure defined in Eq. (155) and expanding the sine functions gives:

$$\{f_i(t)\} = \begin{Bmatrix} \\ \vdots \\ (a_j \cos \psi_j) \\ \vdots \\ \end{Bmatrix} \sin \Omega t + \begin{Bmatrix} \\ \vdots \\ (a_j \sin \psi_j) \\ \vdots \\ \end{Bmatrix} \cos \Omega t, \text{ or}$$

$$= \{a'_j\} \sin \Omega t + \{a''_j\} \cos \Omega t, \tag{156}$$

where:

$$\{a'_j\} = \begin{Bmatrix} a_1 \cos \psi_1 \\ \vdots \\ a_j \cos \psi_j \\ \vdots \\ a_n \cos \psi_j \end{Bmatrix}, \text{ and}$$

$$\{a''_j\} = \begin{Bmatrix} a_1 \sin \psi_1 \\ \vdots \\ a_j \sin \psi_j \\ \vdots \\ a_n \sin \psi_n \end{Bmatrix}.$$

It is obvious that vectors $\{a'_j\}$ and $\{a''_j\}$ are constant vectors since $\sin \psi_i$ and $\cos \psi_i$ are constants. Equation (156) gives the simpler form of Eq. (155) and consists of sine and cosine forcing functions. To obtain solutions to excitations given by Eq. (155) for the ith sub-structure, superposition of solutions for excitations given by

$$\{a'_j\} \sin \Omega t, \text{ and} \tag{157}$$

$$\{a''_j\} \cos \Omega t \tag{158}$$

is required. Solution for excitation of the type given in Eq. (157) is now required.

The equations of motion in matrix notation for the total structure in the unconnected form are given by:

$$\begin{bmatrix} m_1 & & & 0 \\ & \ddots & & \\ & & m_i & \\ & & & \ddots \\ 0 & & & m_N \end{bmatrix} \begin{Bmatrix} \ddot{x}_1 \\ \vdots \\ \ddot{x}_i \\ \vdots \\ \ddot{x}_N \end{Bmatrix} + \begin{bmatrix} K_1 & & & 0 \\ & \ddots & & \\ & & K_i & \\ & & & \ddots \\ 0 & & & K_N \end{bmatrix} \begin{Bmatrix} x_1 \\ \vdots \\ x_i \\ \vdots \\ x_N \end{Bmatrix} = \begin{Bmatrix} f_1(t) \\ \vdots \\ f_i(t) \\ \vdots \\ f_N(t) \end{Bmatrix}, \tag{136}$$

in which the vector $\{f_i(t)\}$ gives the harmonic forces acting on the ith substructure. Using the coordinate transformation particular to the substructure approach, i.e.,

$$\{x\} = [T]\{q\},$$

gives:

$$[\bar{M}][T]\{\ddot{q}\} + [\bar{K}][T]\{q\} = \{f(t)\},$$

where $[\bar{M}]$ and $[\bar{K}]$ are given by Eqs. (48) and (49), respectively and

$$\{f(t)\} = \begin{Bmatrix} f_1(t) \\ \vdots \\ f_i(t) \\ \vdots \\ f_N(t) \end{Bmatrix}.$$

Premultiplying the above equation by $[T]^T$ and using Eqs. (54) and (55)

$$[M]\{\ddot{q}\} + [K]\{q\} = [T]^T\{f(t)\}. \tag{159}$$

Equation (159) gives the reduced equations of motion for the total structure under any general excitation $f(t)$. When no forces act on the structure, i.e., when

$$\{f(t)\} = \{0\},$$

Eq. (159) reduces to its homogeneous form as given by:

$$[M]\{\ddot{q}\} + [K]\{q\} = \{0\}, \tag{83}$$

which has been solved in Chapter III. Grouping together the eigenvectors of Eq. (83) in the ascending order of eigenvalues gives the modal matrix, $[\bar{q}]$, of Eq. (83), i.e.,

$$[\bar{q}] = [q_1\ q_2\ \ldots\ q_i\ \ldots\ q_m]. \tag{84}$$

Modal matrix $[\bar{q}]$ satisfies orthogonality relations given by:

$$[\bar{q}]^T[M][\bar{q}] = [\sim I \sim], \text{ and} \tag{88}$$

$$[\bar{q}]^T[K][\bar{q}] = [\sim \omega_i^2 \sim], \tag{89}$$

where ω_i is the system frequency root in the ith principal mode.

To uncouple the equations of motion of Eq. (159), a transformation of coordinates,

$$\{q\} = [\bar{q}]\{p\}, \tag{160}$$

which amounts to superposition of principal modes, is used in Eq. (159), i.e.,

$$[M][\bar{q}]\{\ddot{p}\} + [K][\bar{q}]\{p\} = [T]^T\{f(t)\}.$$

Premultiplying the above equation by $[\bar{q}]^T$ and using the orthogonality relationships of $[\bar{q}]$ yields the uncoupled equations of motion in $\{p\}$ coordinates,

$$\{\ddot{p}\} + [\sim \omega_i^2 \sim]\{p\} = [\bar{q}]^T[T]^T\{f(t)\}. \tag{161}$$

Equation (161) is valid for any general excitation, $\{f(t)\}$, and can be solved by the use of Duhamel's integral. This would be similar to the solution provided in section A when considering the displacement excitation. However, the case of harmonic excitations will be solved in a different manner. It has been shown that a solution to excitation of the type given in Eq. (155) can be obtained by adding solutions to excitations of Eqs. (157) and (158). In view of this, the form of $\{f(t)\}$ may be assumed to be:

$$\{f(t)\} = \{F\} \sin \Omega t, \tag{162}$$

where constant vector $\{F\}$ is given by:

$$\{F\} = \begin{Bmatrix} F_1 \\ \vdots \\ F_i \\ \vdots \\ F_N \end{Bmatrix}, \tag{163}$$

in which N represents the number of substructures.

Thus, Eq. (161) becomes:

$$\{\ddot{p}\} + [\omega_i^2]\{p\} = [\bar{q}]^T[T]^T\{F\} \sin \Omega t. \tag{164}$$

Assuming a steady state solution which follows from the classical solution of differential equations with constant coefficients, i.e.,

$$\{p\} = \{A\} \sin \Omega t, \tag{165}$$

gives:

$$\{\ddot{p}\} = -\Omega^2\{A\} \sin \Omega t. \tag{166}$$

Using the particular solution assumed and substituting back into the differential equation gives:

$$-\Omega^2\{A\} + [\omega_i^2]\{A\} = [\bar{q}]^T[T]^T\{F\}, \text{ or} \tag{167}$$

$$\{A\} = [\omega_i^2 - \Omega^2]^{-1}[\bar{q}]^T[T]^T\{F\}. \tag{168}$$

$$\therefore \{p\} = [\omega_i^2 - \Omega^2]^{-1}[\bar{q}]^T[T]^T\{F\} \sin \Omega t. \tag{169}$$

Use of Eqs. (41) and (160) thus gives displacements $\{x\}$, i.e.,

$$\{x\} = [T][\bar{q}][\omega_i^2 - \Omega^2]^{-1}[\bar{q}]^T[T]^T\{F\} \sin \Omega t. \tag{170}.$$

The product $[T]^T\{F\}$ in Eq. (170) can be simplified through partitioning of matrices as under:

$$[T]^T\{F\} = [T_1^T | \cdots | T_i^T | \cdots | T_N^T] \begin{Bmatrix} F_1 \\ \vdots \\ F_i \\ \vdots \\ F_N \end{Bmatrix}, \text{ or}$$

$$= [T_1^T F_1 + \cdots + T_i^T F_i + \cdots + T_N^T F_N], \text{ or}$$

$$= [\sum_{i=1,N} T_i^T F_N]. \tag{171}$$

Equation (170) gives the steady state solution for a harmonic excitation of the type given in Eq. (162). For a forcing function of the type,

$$\{f(t)\} = \{F\} \cos \Omega t, \tag{172}$$

the solution becomes:

$$\{x\} = [T][\bar{q}][\lceil\omega_i^2 - \Omega^2\rfloor]^{-1}[\bar{q}]^T[T]^T\{F\} \cos \Omega t. \qquad (173)$$

Superimposing solutions given by Eqs. (170) and (173) yields solutions for harmonic forcing functions with a common forcing frequency but having a phase difference between the point forces, i.e.,

$$\{x\} = [T][\bar{q}][\lceil\omega_i^2 - \Omega^2\rfloor]^{-1}[\bar{q}]^T[T]^T(\{a_i'\} \sin \Omega t + \{a_i''\} \cos \Omega t).$$

2. Harmonic Excitations with Different Forcing Frequencies

In the preceeding section harmonic forcing functions had a common frequency Ω. If the forcing frequencies are different, solution is obtained for each of the forces acting individually on the structure. Since the structure is linear, the total solution is formed by superimposing all individual solutions, i.e.,

$$\{x\} = \sum_{i=1,\ell} \{x\}_i, \text{ or} \qquad (174)$$

$$\{x\} = \sum_{i=1,\ell} [T][\bar{q}][\lceil\omega_j^2 - \Omega_i^2\rfloor]^{-1}[\bar{q}]^T[T]^T\{F\} \sin \Omega_i t, \qquad (175)$$

where Ω_i is forcing frequency for the ith harmonic force and ℓ is the total number of forces applied to the structure. For excitations given by Eq. (172), the above solution modifies to:

$$\{x\} = \sum_{i=1,\ell} [T][\bar{q}][\lceil\omega_j^2 - \Omega_i^2\rfloor]^{-1}[\bar{q}]^T[T]^T\{F\} \cos \Omega_i t. \qquad (176)$$

Having discussed solutions to harmonic excitations, it is now

shown that the above solutions can also be applied to periodic excitations.

3. Periodic Excitations

An exciting force which repeats itself in equal periods of time, τ, is referred to as a periodic force. A periodic exciting force has the property that

$$f(t) = f(t+\tau). \tag{177}$$

A periodic function can usually be represented by a Fourier Series having the form:

$$f(t) = \sum_{n=1}^{\infty} A_n \sin(n\Omega t) + B_0 + \sum_{n=1}^{\infty} B_n \cos(n\Omega t). \tag{178}$$

The frequency Ω is called the fundamental frequency, related to the period by $\Omega\tau = 2\pi$. It is customary to refer to the terms with n = 1 as the fundamental and the nth terms as the nth harmonic. Given a periodic function f(t), the evaluation of the constants A_n and B_n is simplified by the orthogonality of the functions of the series, i.e.,

$$\int_0^{\tau} \sin(n\Omega t)dt = 0 \tag{179}$$

$$\int_0^{\tau} \cos(n\Omega t)dt = 0 \tag{180}$$

$$\int_0^{\tau} \sin(m\Omega t)\cos(n\Omega t)dt = 0 \tag{181}$$

$$\int_0^{\tau} \sin(m\Omega t)\sin(n\Omega t)dt = 0, \; m\neq n \tag{182}$$

$$\int_0^{\tau} \cos(m\Omega t)\cos(n\Omega t)dt = 0, \; m\neq n\,. \tag{183}$$

In view of the above relations, the constants A_m, B_0, and B_m are given by:

$$A_m = \frac{2}{\tau} \int_0^{\tau} f(t) \sin(m\Omega t)dt \tag{184}$$

$$B_0 = \frac{1}{\tau} \int_0^{\tau} f(t)dt \tag{185}$$

$$B_m = \frac{2}{\tau} \int_0^{\tau} f(t) \cos(m\Omega t)dt. \tag{186}$$

The utility of a Fourier series representation rests on the convergence of the terms in the series. Very often the convergence is rapid and only a few terms are needed to represent adequately the function. Solution to each term in the series can easily be obtained by treating it as a harmonic excitation. Then the steady state response to the given periodic excitation is given by superposition of the separate responses.

C. Base Acceleration Excitation

Forced vibrations may also result from a motion of the constraints on the given structure. Structure motion resulting from motion of the supports or the base will be of prime interest in this study. This formulation is practical, for example, when calculating the response of a tall buildings to earthquake movement. Other cases, when the input excitations to structures can be easily measured by accelerometers, are directly amenable to this approach.

The equations of motion for the total structure in the unconnected

form are given by:

$$\begin{bmatrix} m_B & & & & 0 \\ & m_1 & & & \\ & & \ddots & & \\ & & & m_i & \\ & & & & \ddots \\ 0 & & & & m_N \end{bmatrix} \begin{Bmatrix} \ddot{U}_B \\ \ddot{x}_1 \\ \vdots \\ \ddot{x}_i \\ \vdots \\ \ddot{x}_N \end{Bmatrix} + \begin{bmatrix} K_B & & & & 0 \\ & K_1 & & & \\ & & \ddots & & \\ & & & K_i & \\ & & & & \ddots \\ 0 & & & & K_N \end{bmatrix} \begin{Bmatrix} U_B \\ x_1 \\ \vdots \\ x_i \\ \vdots \\ x_N \end{Bmatrix} = \begin{Bmatrix} f_B \\ 0 \\ \vdots \\ 0 \\ \vdots \\ 0 \end{Bmatrix} , \tag{187}$$

where $[m_B]$ and $[K_B]$ are the mass and stiffness matrices of the base, respectively, and are unknown quantities. $\{U_B(t)\}, \{\ddot{U}_B(t)\}$ are known base displacements and accelerations, respectively. For six degrees of freedom, $\{U_B(t)\}$ or $\{\ddot{U}_B(t)\}$ would be of 6 x 1 size. Vector $\{f_B\}$ represents forces applied at the base or supports to produce base displacements $\{U_B(t)\}$ or accelerations $\{\ddot{U}_B(t)\}$.

Due to the base displacements the structure equilibrium position experiences a time-varying rigid body motion. It is about this equilibrium position that the structure vibrates. The location of the time-varying equilibrium position at any time 't' may be given by

$$\{\delta_E(t)\} = [A]\{U_B(t)\}, \tag{188}$$

in which matrix [A] is the coefficient matrix defining motion of the structure equilibrium position due to unit base displacements in the direction of $\{U_B(t)\}$.

If the structure motion is measured relative to a frame of reference fixed to the base, the transformation between the absolute coordinates $\{x\}$ and the relative coordinates $\{\tilde{x}\}$ becomes:

$$\{x\} = \{\tilde{x}\} + [A]\{U_B(t)\}. \tag{189}$$

As shown in Appendix C, Eq. (187) is transformed by use of Eq. (189) to:

$$\begin{bmatrix} m_1 & & & 0 \\ & \ddots & & \\ & & m_i & \\ & & & \ddots \\ 0 & & & m_N \end{bmatrix} \begin{Bmatrix} \ddot{\tilde{x}}_1 \\ \vdots \\ \ddot{\tilde{x}}_i \\ \vdots \\ \ddot{\tilde{x}}_N \end{Bmatrix} + \begin{bmatrix} K_1 & & & 0 \\ & \ddots & & \\ & & K_i & \\ & & & \ddots \\ 0 & & & K_N \end{bmatrix} \begin{Bmatrix} \tilde{x}_1 \\ \vdots \\ \tilde{x}_i \\ \vdots \\ \tilde{x}_N \end{Bmatrix} = - \begin{bmatrix} m_1 & & & 0 \\ & \ddots & & \\ & & m_i & \\ & & & \ddots \\ 0 & & & m_N \end{bmatrix}$$

$$\times [A]\{\ddot{U}_B(t)\}, \text{ or} \tag{190}$$

in general matrix notation,

$$[\bar{M}]\{\ddot{\tilde{x}}\} + [\bar{K}]\{\tilde{x}\} = - [\bar{M}][A]\{\ddot{U}_B(t)\} \tag{191}$$

where $[\bar{M}]$ and $[\bar{K}]$ are the structure mass and stiffness matrices in the unconnected form with the structure base held fixed and are defined in Eqs. (48) and (49), respectively. Evidently the forced vibration problem with applied forces or with base motion are identical, if the forces applied at mass points are equal to the inertial forces created, due to the base acceleration $\{\ddot{U}_B(t)\}$.

Using the transformation

$$\{\tilde{x}\} = [T]\{\tilde{q}\}, \tag{192}$$

where matrix [T] is obtained as described in Chapter II, results in:

$$\{\ddot{\tilde{x}}\} = [T]\{\ddot{\tilde{q}}\}. \tag{193}$$

In view of Eqs. (192) and (193), Eq. (191) becomes:

$$[\bar{M}][T]\{\ddot{\tilde{q}}\} + [\bar{K}][T]\{\tilde{q}\} = - [\bar{M}][A]\{\ddot{U}_B(t)\}. \tag{194}$$

Premultiplication of Eq. (194) by $[T]^T$ and use of Eqs. (54) and (55) gives:

$$[M]\{\ddot{\tilde{q}}\} + [K]\{\tilde{q}\} = - [T]^T[\bar{M}][A]\{\ddot{U}_B(t)\}. \tag{195}$$

An eigensolution of the homogeneous part of Eq. (195) yields a modal matrix $[\bar{q}]$ and frequency roots $\tilde{\omega}_i$ of the total structure with its base held fixed. To uncouple the equations of motion given by Eq. (195), the following transformation of coordinates, based on superposition of principal modes, is defined:

$$\{\tilde{q}\} = [\bar{q}]\{\tilde{p}\}. \tag{196}$$

Using Eq. (196) in Eq. (195) and premultiplying the result by $[\bar{q}]^T$ yields

$$[\bar{q}]^T[M][\bar{q}]\{\ddot{\tilde{p}}\} + [\bar{q}]^T[K][\bar{q}]\{\tilde{p}\} = - [\bar{q}]^T[T]^T[\bar{M}][A]\{\ddot{U}_B(t)\}, \text{ or} \tag{197}$$

$$\{\ddot{\tilde{p}}\} + [\tilde{\omega}_i^2]\{\tilde{p}\} = - [\bar{q}]^T[T]^T[\bar{M}][A]\{\ddot{U}_B(t)\}, \tag{198}$$

since $[\bar{q}]$ satisfies the orthogonality conditions given by:

$$[\bar{q}]^T[M][\bar{q}] = [I], \text{ and} \tag{199}$$

$$[\bar{q}]^T[K][q] = [\tilde{\omega}_i^2]. \tag{200}$$

Eq. (198) gives the uncoupled equations of motion in matrix notation. The right hand side represents the forcing term. This equation with zero initial conditions can be solved through Duhamel's integral solution given by:

$$\{\tilde{p}\} = [\tilde{\omega}_i]^{-1} \int_0^t [\sin \tilde{\omega}_i(t-\tau)]\{f(\tau)\}d\tau, \qquad (201)$$

where:

$$\{f(t)\} = -[\bar{q}]^T[T]^T[\bar{M}][A]\{\ddot{U}_B(t)\}, \qquad (202)$$

and the initial conditions are assumed to be zero.

Thus Eq. (201) becomes:

$$\{\tilde{p}\} = -[\tilde{\omega}_i]^{-1} \int_0^t [\sin \tilde{\omega}_i(t-\tau)][\bar{q}]^T[T]^T[\bar{M}][A]\{\ddot{U}_B(\tau)\}d\tau. \qquad (203)$$

The total solution $\{x\}$ with zero initial conditions is given by:

$$\{\tilde{x}\} = -[T][\bar{q}][\tilde{\omega}_i]^{-1} \int_0^t [\sin \tilde{\omega}_i(t-\tau)][\bar{q}]^T[T]^T[\bar{M}][A]\{\ddot{U}_B(\tau)\}d\tau. \qquad (204)$$

If matrix [A] is partitioned at the substructure's level, i.e.,

$$[A] = \begin{bmatrix} A_1 \\ \vdots \\ A_i \\ \vdots \\ A_N \end{bmatrix}, \qquad (205)$$

the product $[T]^T[\bar{M}][A]$ in Eq. (204) simplifies to:

$$[T]^T[\bar{M}][A] = [T_1^T \vdots \cdots \vdots T_i^T \vdots \cdots \vdots T_N^T] \begin{bmatrix} m_1 & & & 0 \\ & \ddots & & \\ & & m_i & \\ & & & \ddots \\ 0 & & & m_N \end{bmatrix} \begin{bmatrix} A_1 \\ \vdots \\ A_i \\ \vdots \\ A_N \end{bmatrix}, \text{ or}$$

$$= [T_1^T m_1 A_1 + \cdots + T_i^T m_i A_i + \cdots + T_N^T m_N A_N], \text{ or}$$

$$= [\sum_{i=1,N} T_i^T m_i A_i]. \qquad (206)$$

Equation (204) gives the motion of the structure relative to its base. Use of Eq. (189) would yield absolute motion of the structure but the vibratory system strain energy is obtained through the use of structure motion relative to its base. Also to find stresses in the structure, it is the relative displacement which is of primary interest and not the absolute displacement.

D. General Time-Varying Force Excitation

Consider the system when subjected to time-varying forces $\{f(t)\}$. To complete the study of most structural dynamics problems, through the substructures approach, this general case is of interest. Equations of motion in the uncoupled form, as obtained in section B, are given by:

$$\{\ddot{p}\} + [\omega_i^2]\{p\} = [\bar{q}]^T[T]^T\{f(t)\}. \qquad (207)$$

Duhamel's integral solution, assuming zero initial conditions, gives:

$$\{p\} = [\omega_i]^{-1} \int_0^t [\sin \omega_i(t-\tau)][\bar{q}]^T[T]^T\{f(\tau)\}\, d\tau. \qquad (208)$$

The total structure solution in its unconnected form thus becomes:

$$\{x\} = [T][\bar{q}][\omega_i]^{-1} \int_0^t [\sin \omega_i(t-\tau)][\bar{q}]^T[T]^T\{f(\tau)\}d\tau. \tag{209}$$

If the duration of $\{f(t)\}$ is finite and given by t_0, solution for time t, $0 \leq t \leq t_0$ is given by Eq. (209). For time $t \geq t_0$ the above solution modifies to:

$$\{x\} = [T][\bar{q}][\omega_i]^{-1} \int_0^{t_0} [\sin \omega_i(t-\tau)][\bar{q}]^T[T]^T\{f(\tau)\}d\tau. \tag{210}$$

Solutions through the substructures method, to four different types of excitations have been obtained in this chapter. Numerical verification of these results with a comparison to the classical direct matrix approach is treated in Chapter V with several example problems.

CHAPTER V

COMPARISON OF RESULTS

Comparisons of results obtained through numerical computation of equations derived in Chapters II, III and IV are presented in this chapter. Numerical examples have been investigated to verify the theoretical derivations contained in this study and provide a basis for comparing the various error indicators.

For the purpose of comparison, solutions obtained through the substructures approach with no modal truncation are verified by the usual direct method. Appendix D gives equations of motion obtained directly for example problems worked in this study and presents their corresponding displacement solutions. Use of an IBM-360-50 computer has been made to establish all numerical work.

A. Free Vibrations Results

The objective of this investigation has been to obtain a consistent basis for truncation of substructure fixed constraint normal modes in the vibratory analysis of a complex structure when using the method of substructures. Retention of only certain of the substructure normal modes results in a much smaller set of equations of motion to be solved. Truncation of these modes is equivalent to imposing constraints on the motion of a structure thereby introducing a measure of error in the system eigenvalues and eigenvectors. Two bases of retaining these modes are discussed in Chapter II. One of the bases is founded on substructure fixed constraint normal mode frequency roots and under this criterion only a given number of principal modes below a frequency

limit are retained. The other criterion is based on the substructure fixed constraint normal mode strain energy. Modes associated with lower strain energy are retained under this criterion.

To evaluate the results of the above two criteria and to determine if levels can be found which tend to give valid trends, system eigenvalues and strain energy in the principal modes are computed. System eigenvalues are obtained by solving an eigen problem of the reduced equations of motion while system strain energy in the ith principal mode is given by:

$$U^i = \frac{1}{2} \{x^i\}^T [\bar{K}]\{x^i\}, \text{ or} \tag{97}$$

$$= \frac{1}{2} \{q^i\}^T [K]\{q^i\}. \tag{99}$$

Strain energy is indicative of displacements and stresses in the system, independent of their spatial dependence within the system. Furthermore, this basis of comparison of results should give a better measure of total system distortion than any one particular parameter, e.g., maximum displacement or maximum stress.

Estimates of errors in the system eigenvalues and strain energy in the principal modes as a function of the number of retained principal modes from the substructures can be obtained through Eqs. (127) and (135) derived in Chapter III. For the numerical evaluation of trends from the various criteria and error indicators contained in this study, an example is presented. Simplicity and generality are the foremost considerations in the formulation of this example.

Consider a uniform cantilever beam divided into two substructures

at boundary cc as shown in Fig. 1. The beam is subdivided into six finite elements. Substructure 1 is comprised of the first three identical elements while the remaining three identical elements constitute substructure 2. Properties of a typical element from each substructure are given.

Each modal point has two degrees of freedom, i.e., the transverse displacement and rotation in the plane. The complete structure has a total of twelve degrees of freedom. Two of these are associated with the common boundary cc of the substructures. Substructure 1 has four interior coordinates while substructure 2 has six of them. For simplicity, element mass matrices used are diagonal and are given in Appendix B.

Tables I and II give the substructure fixed constraint normal mode frequency roots and strain energy in the principal modes, respectively. Reduced sets of equations based on several combinations of substructure normal modes retained from the two substructures are solved on an IBM-360-50 digital computer. In each case, system eigenvalues and strain energy in the principal modes is obtained. Selection of lower order substructure normal modes is based on substructure frequency roots and substructure strain energy criteria. Table III gives the combinations of substructure normal modes, retained from each substructure, based on the substructure frequency roots criterion. Table IV gives the above combinations based on substructure strain energy in the normal modes. In addition to these normal modes, the two substructure constraint modes which describe the total structure motion must also be retained. Size of the reduced problem is obtained by

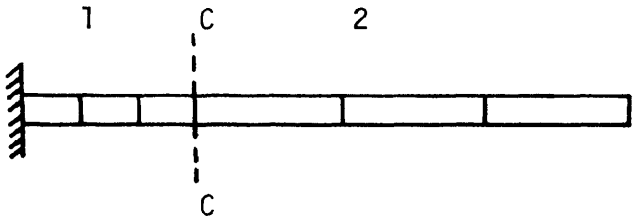

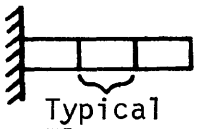

Substructure 1

Element Properties

ℓ = 14 in.

A = $\frac{1}{2}$ in. x 2 in.

E = 30 x 10^6 lb/in.^{2}

ω = 0.3 lb/in.^{3}

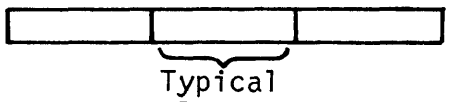

Substructure 2

Element Properties

ℓ = 36 in.

A = $\frac{1}{2}$ in. x 2 in.

E = 30 x 10^6 lb/in.^{2}

ω = 0.3 lb/in.^{3}

Fig. 1. Finite Element Model of a Uniform Cantilever Beam - Two Substructures

Table I

Substructure Fixed Constraint Principal Mode Frequency Roots

Mode No.	Rad/Sec	Mode No.	Rad/Sec
1	1357.717	1	31.90236
2	3229.496	2	167.2321
3	5129.852	3	409.8979
4	6469.953	4	692.1104
		5	933.1514
		6	1101.468

Table II

Substructure Strain Energy in the Fixed Constraint Normal Modes

Mode No.	Lb-In	Mode No.	Lb-In
1	10942.10	1	9.18108
2	59640.90	2	368.198
3	989095.00	3	3080.94
4	2072210.0	4	36225.20
		5	67337.80
		6	57668.80

Table III

Number of Substructure Normal Modes Retained
Through Substructure Frequency Roots Criterion

Substructure 1 Modes Retained	Substructure 2 Modes Retained	Reduced Problem Size
0	1	3
0	2	4
0	3	5
0	4	6
0	5	7
0	6	8
1	6	9

Table IV

Number of Substructure Normal Modes Retained
Through Substructure Strain Energy Criterion

Substructure 1 Modes Retained	Substructure 2 Modes Retained	Reduced Problem Size
0	1	3
0	2	4
0	3	5
1	3	6
1	4	7
2	4	8
2	5	9

adding the total number of substructure normal modes retained, to the total number of substructure constraint modes. A computer program whose flow chart is presented in Appendix A generates the transformation matrix $[T]_i$ and yields system eigensolutions. Table V gives a comparison of system eigenvalues obtained through the usual direct approach and those obtained by the substructures method with no modal truncation. Table VI presents a similar comparison for the system strain energy in the principal modes. A negligible difference in the numbers must be attributed to different numerical processes used in the two methods to obtain the eigensolutions.

Figures 2 through 5 show percent errors in system frequency roots and strain energy in the principal modes. These errors are plotted for four lower modes against the number of reduced equations of motion solved. The criterion of retaining substructure normal modes in these errors is based on substructure fixed constraint normal mode frequency roots. In this criterion as many modes from each substructure, below a specified frequency level, are used. It should be noted that, while the errors do converge, their convergence is not monotomic. It can also be seen that percent errors in system frequency roots and strain energy in the principal modes follow a similar pattern of convergence. The magnitude of strain energy errors is usually higher than that of frequency root errors, when the number of reduced equations of motion is small and becomes lower than or comes close to the magnitude of frequency root errors, as the number of equations of motion is increased from 3 to 9.

Figures 6 through 9 show the behavior of the above errors obtained

Table V

Comparison of System Eigenvalues

Mode No.	Substructures Approach with no Modal Truncation	Direct Approach
1	293.099433	293.43786
2	9564.70	9574.590
3	62318.095	62371.75
4	185343.50	185491.42
5	423079.14	423150.43
6	785256.81	785511.59
7	1179943.40	1180335.10
8	1238719.00	1238995.60
9	2998270.90	3000077.50
10	11739793.00	11751012.0
11	27270790.00	27274562.0
12	42181632.00	42184530.0

Table VI

Comparison of System Strain Energy in the Principal Modes

Mode No.	Substructures Approach with no Modal Truncation	Direct Approach
1	146.548	146.71893
2	4782.68	4787.295
3	31159.10	31185.875
4	92671.40	92745.71
5	211539.0	211575.215
6	392628.0	392755.795
7	589971.0	590167.55
8	619359.0	619497.80
9	1499130.0	1500038.75
10	5869820.0	5875506.0
11	13635300.0	13637281.0
12	21090700.0	21092265.0

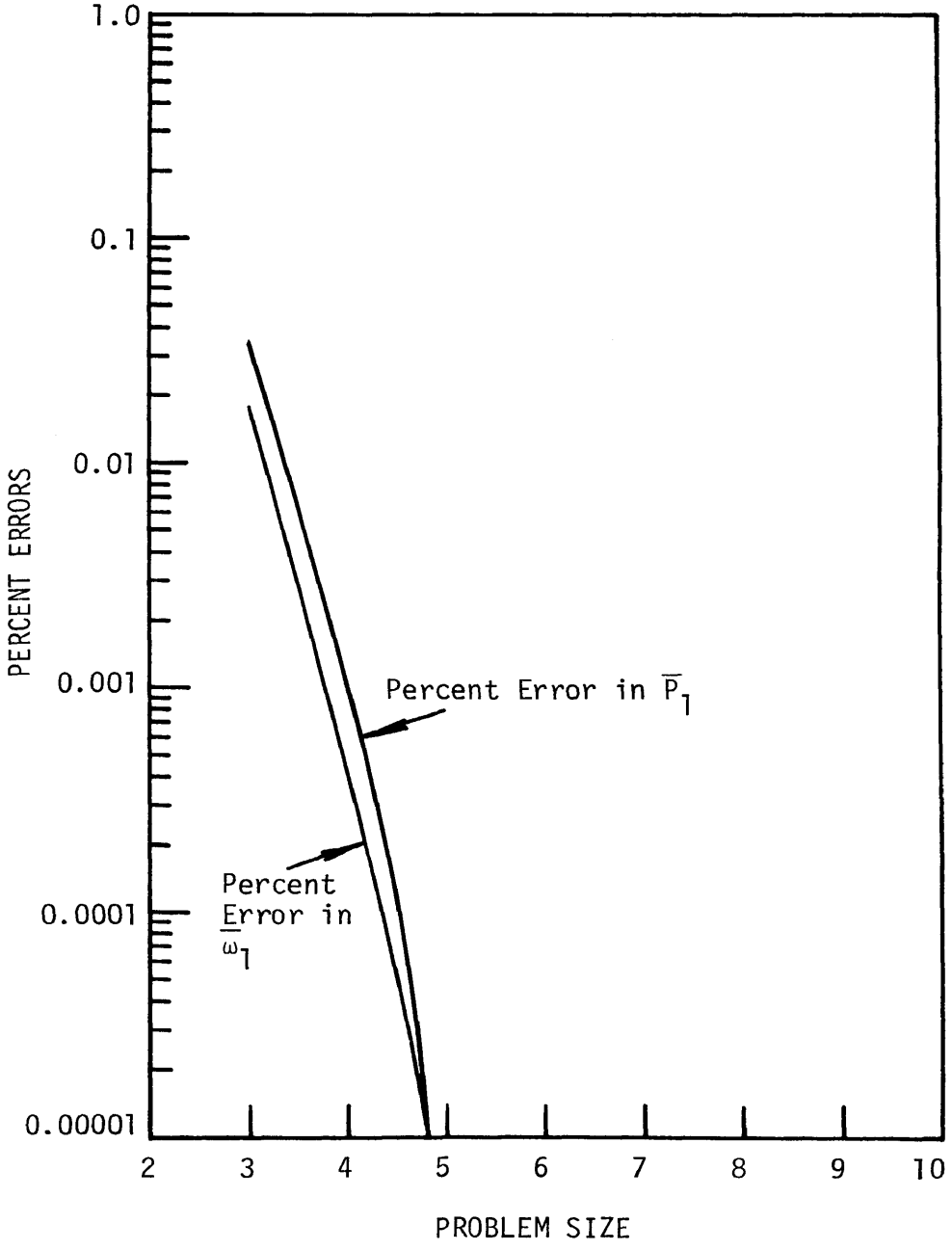

Fig. 2. Error Behavior in the Fundamental Principal Mode Based on Substructure Frequency Root Criterion

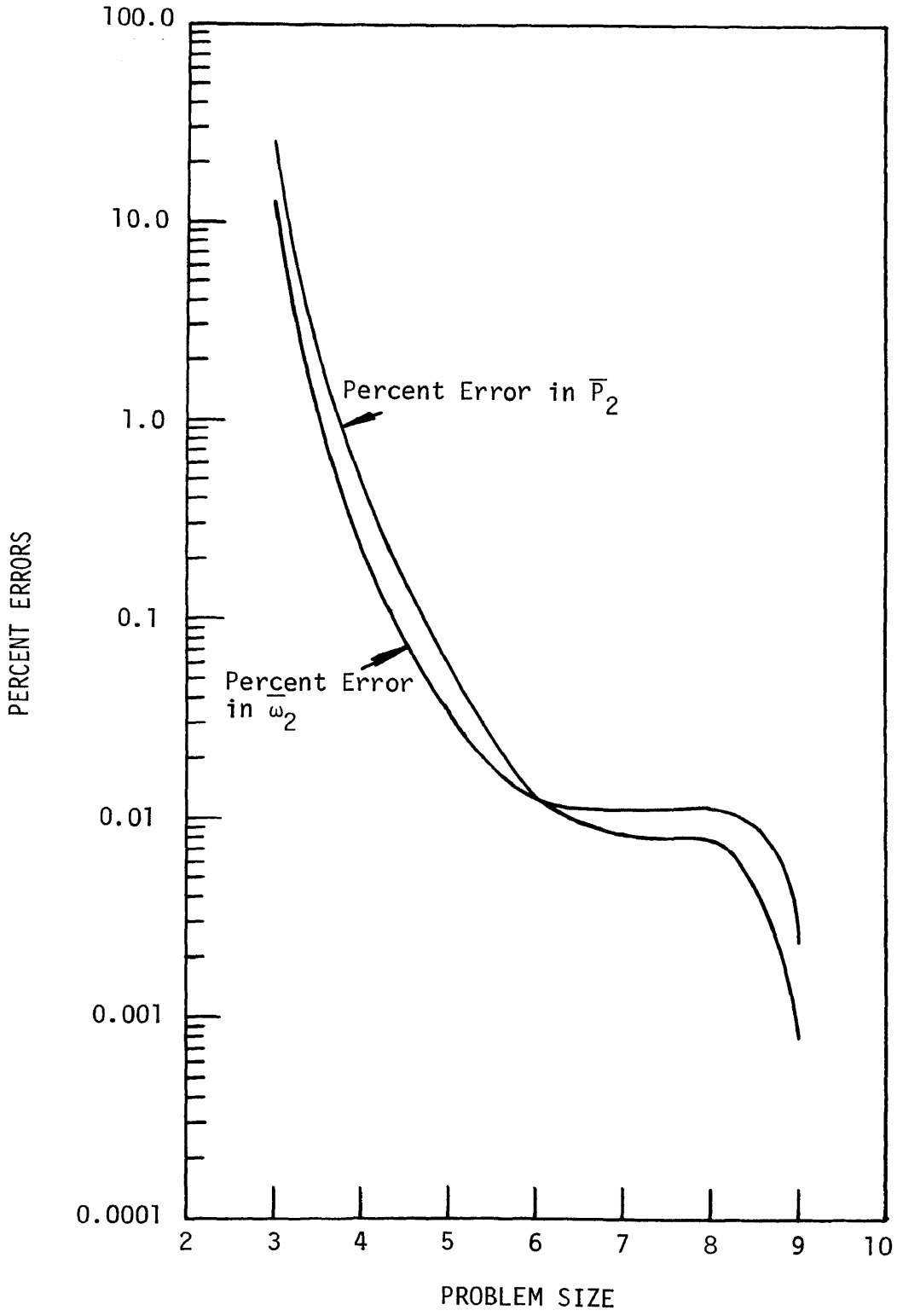

Fig. 3. Error Behavior in the Second Principal Mode Based on Substructure Frequency Root Criterion

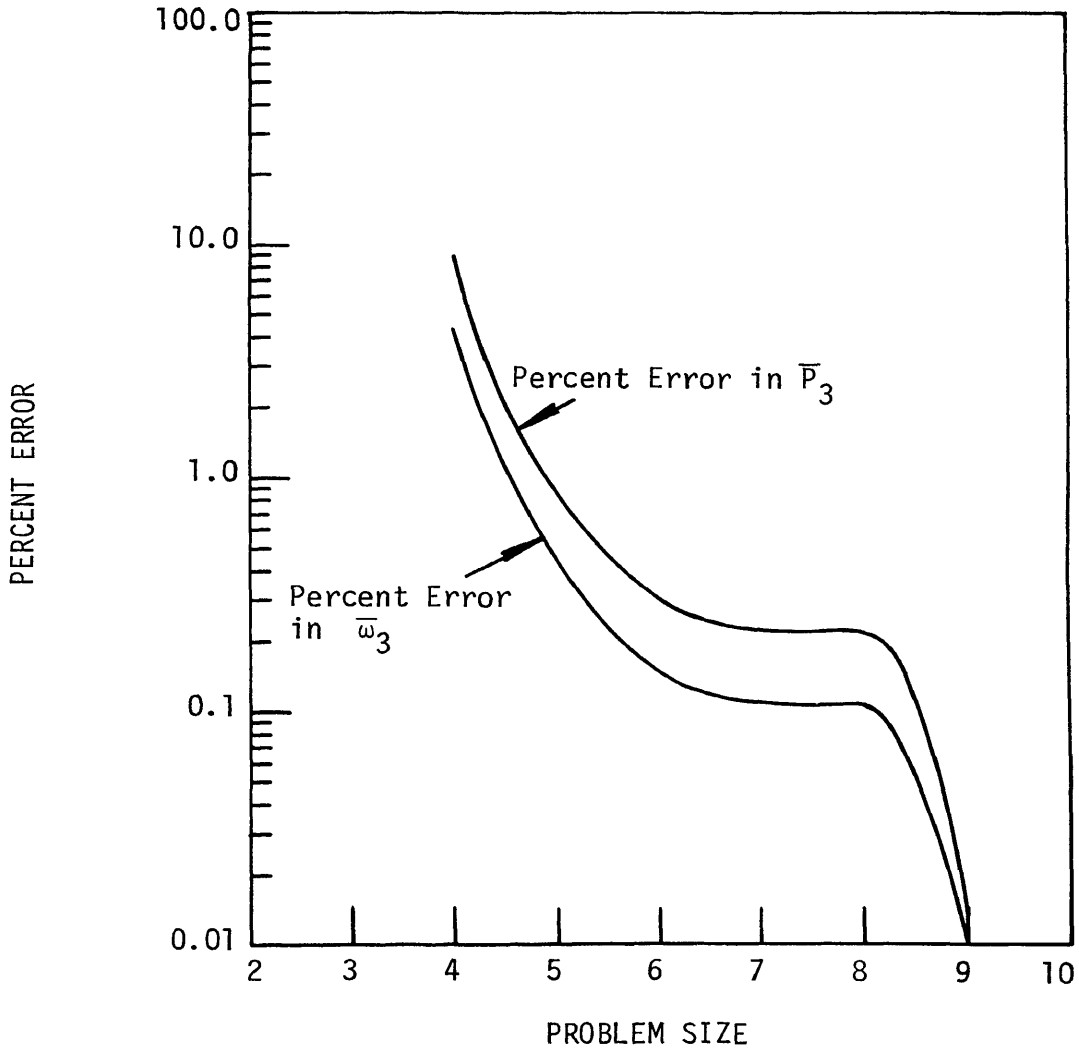

Fig. 4. Error Behavior in the Third Principal Mode Based on Substructure Frequency Root Criterion

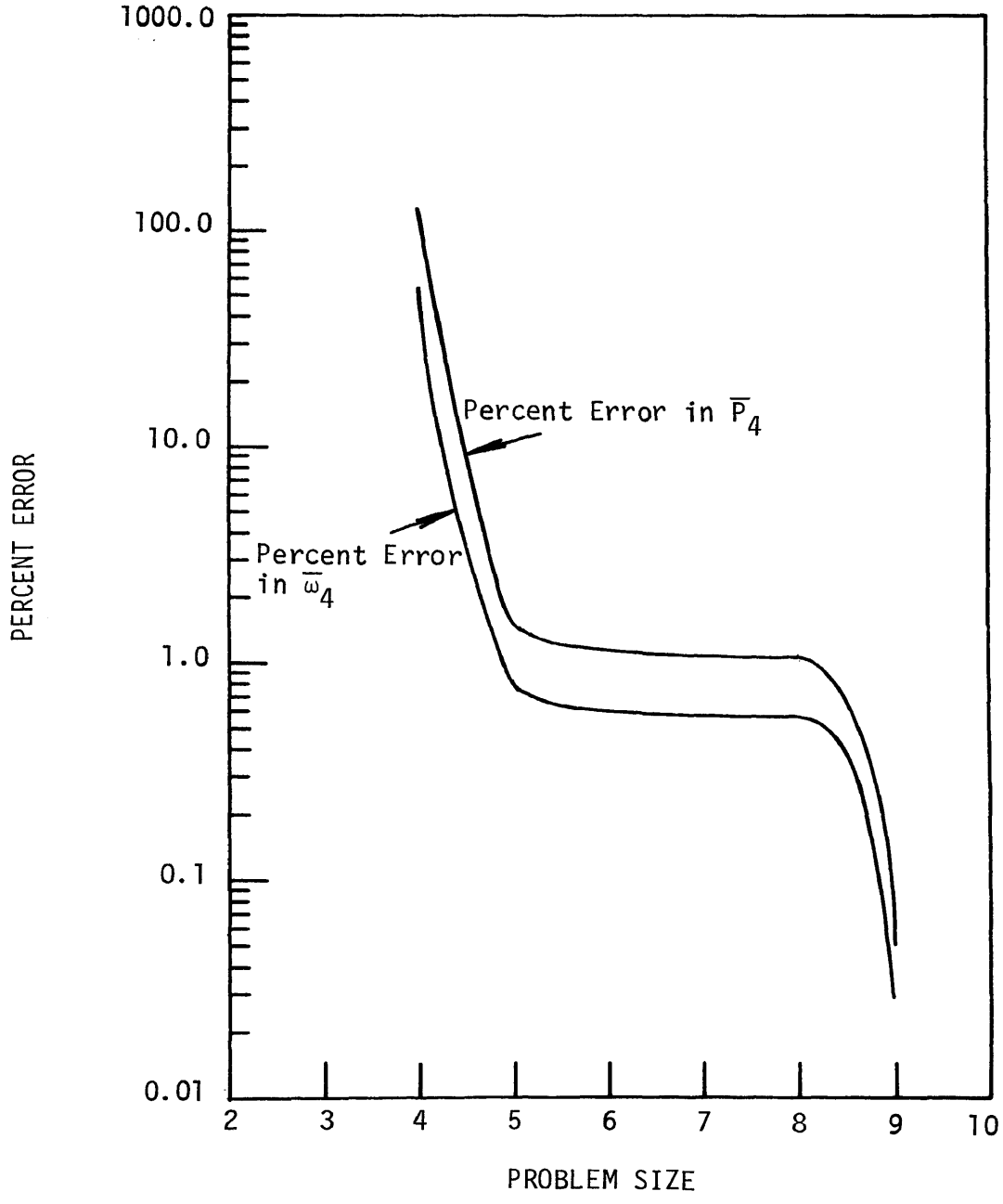

Fig. 5. Error Behavior in the Fourth Principal Mode Based on Substructure Frequency Root Criterion

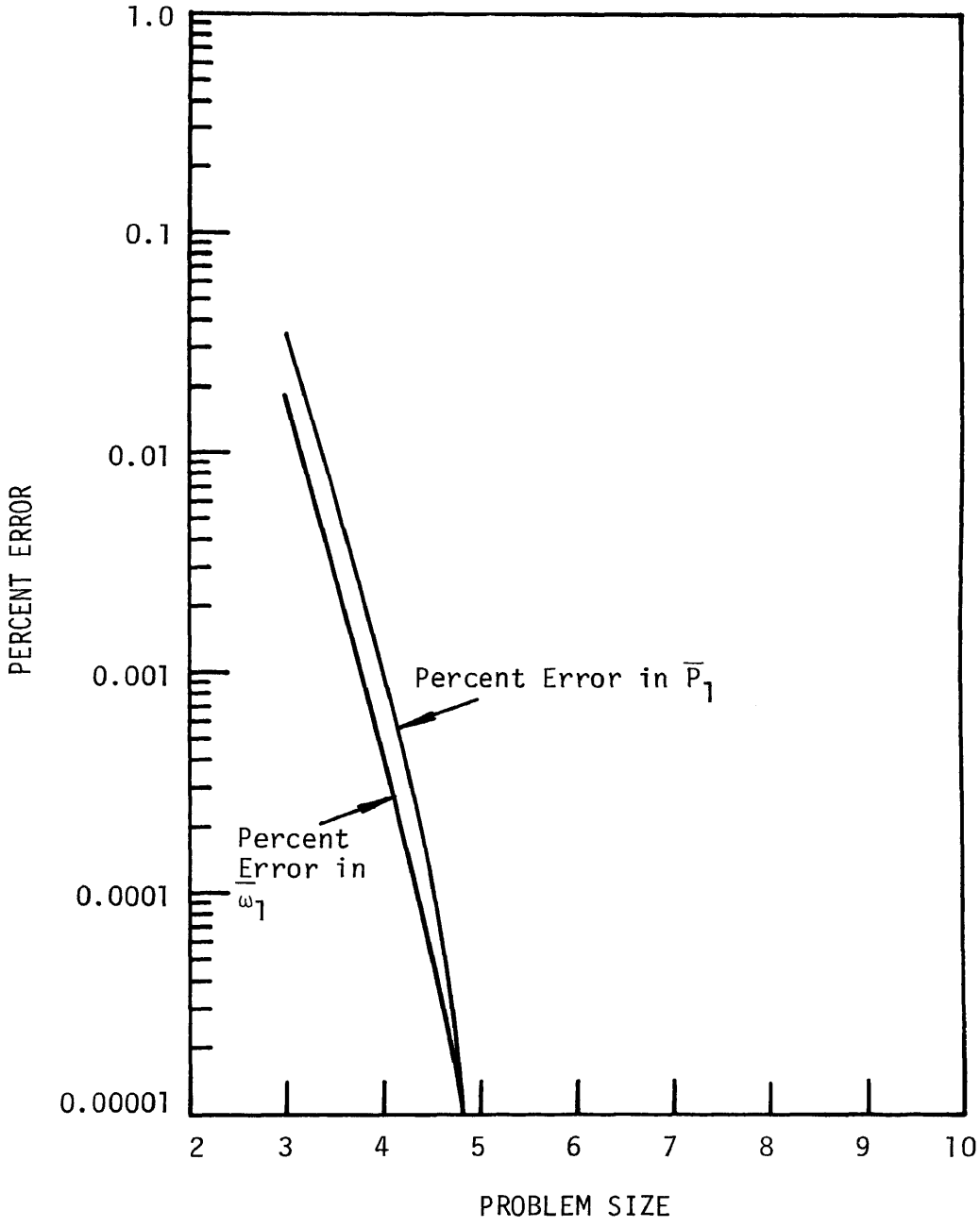

Fig. 6. Error Behavior in the Fundamental Principal Mode Based on Substructure Strain Energy Criterion

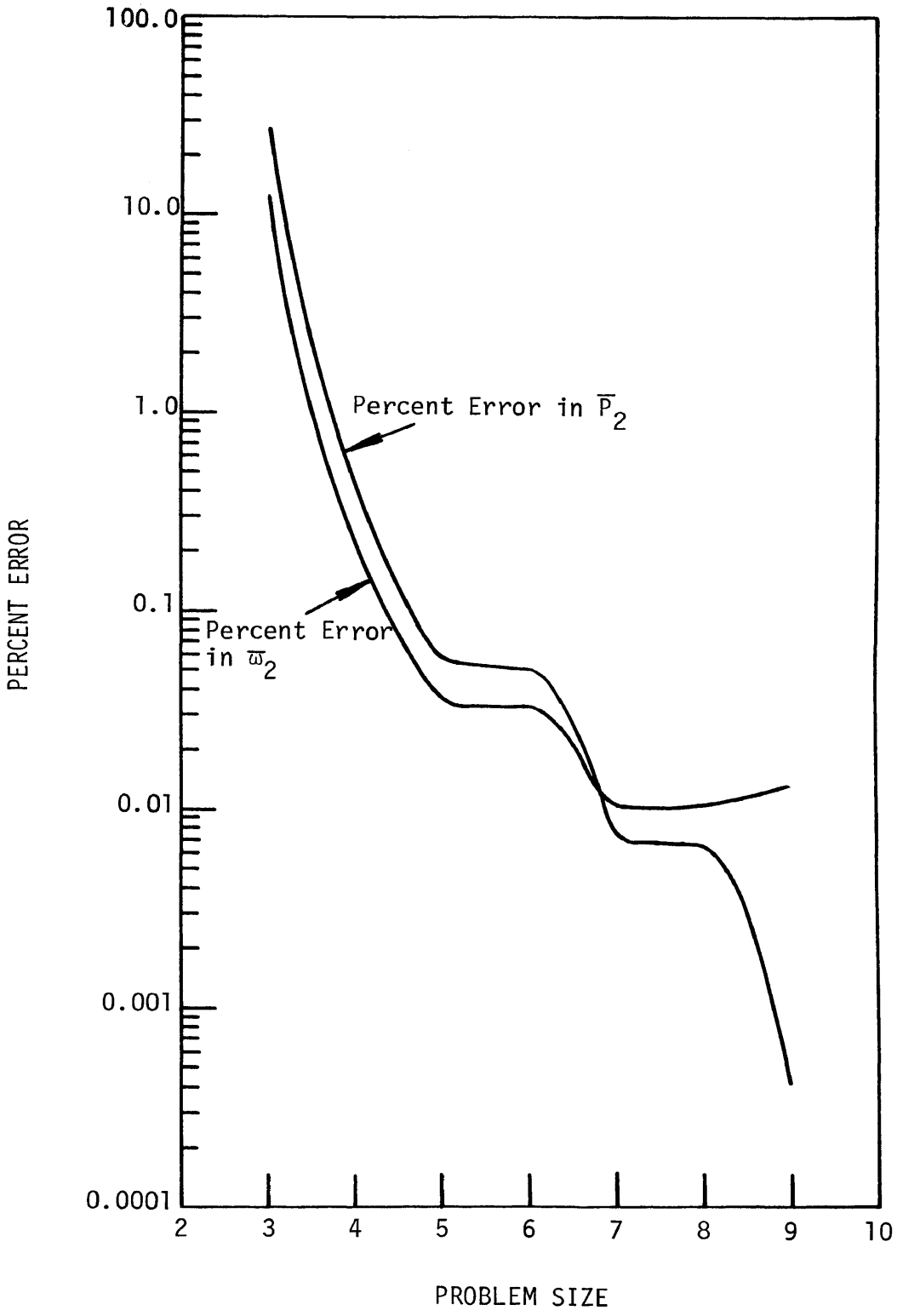

Fig. 7. Error Behavior in the Second Principal Mode Based on Substructure Strain Energy Criterion

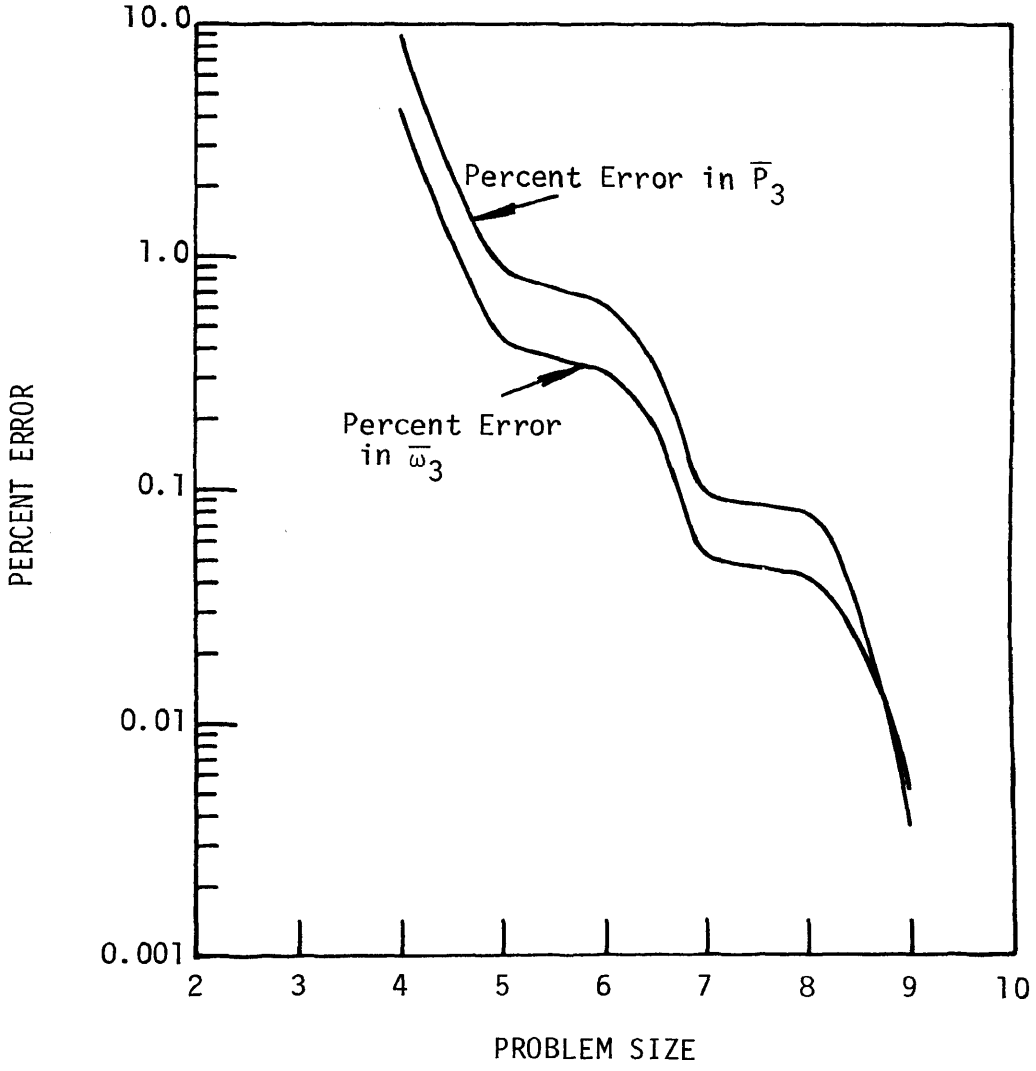

Fig. 8. Error Behavior in the Third Principal Mode Based on Substructure Strain Energy Criterion

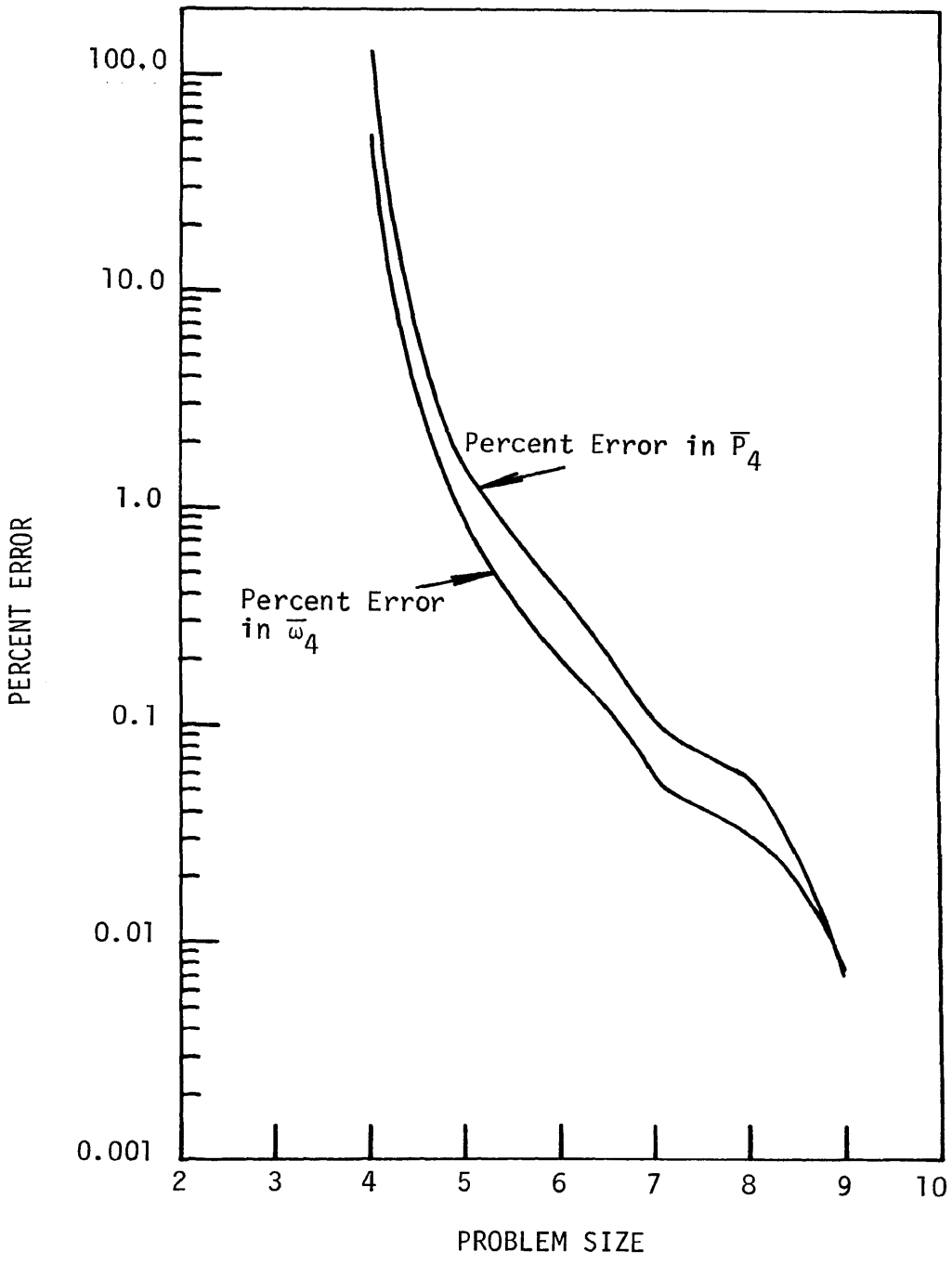

Fig. 9. Error Behavior in the Fourth Principal Mode Based on Substructure Strain Energy Criterion

on the basis of substructure fixed constraint normal mode strain energy. In this case, only those lower order substructure normal modes are retained from all substructures, which have strain energies below a set level of system strain energy. Here again, convergence of the percent errors is not monotonic. The pattern of convergence of the two errors is about the same and is similar to the pattern for the percent errors based on the substructure fixed constraint normal mode frequency roots criterion. The magnitude of the strain energy error is higher than that of the frequency root error, when the number of equations of motion solved is small, but becomes lower than the magnitude of the frequency root error, as the number of equations of motion is increased. The criterion using substructure strain energy for retaining of substructure normal modes usually gives lower frequency root percent errors in the higher system modes as compared to the criterion which uses substructure frequency roots. This situation prevails if the number of equations of motion solved is large. A similar characteristic is noticed for the system strain energy percent errors.

In Figs. 10 through 15, $\delta\lambda$ represents the exact system eigenvalue error between the substructures approach with no modal truncation and the substructures approach yielding approximate eigensolutions; $\overline{\delta\lambda}$ represents approximate system eigenvalue error caused by the omission of certain substructure normal modes and is obtained from Eq. (127). δP indicates exact system strain energy error between the substructures approach with no modal truncation and the one with modal truncation; $\overline{\delta P}$ approximates δP and is obtained from Eq. (135). Error indicators for three lower modes are plotted against the number of equations of

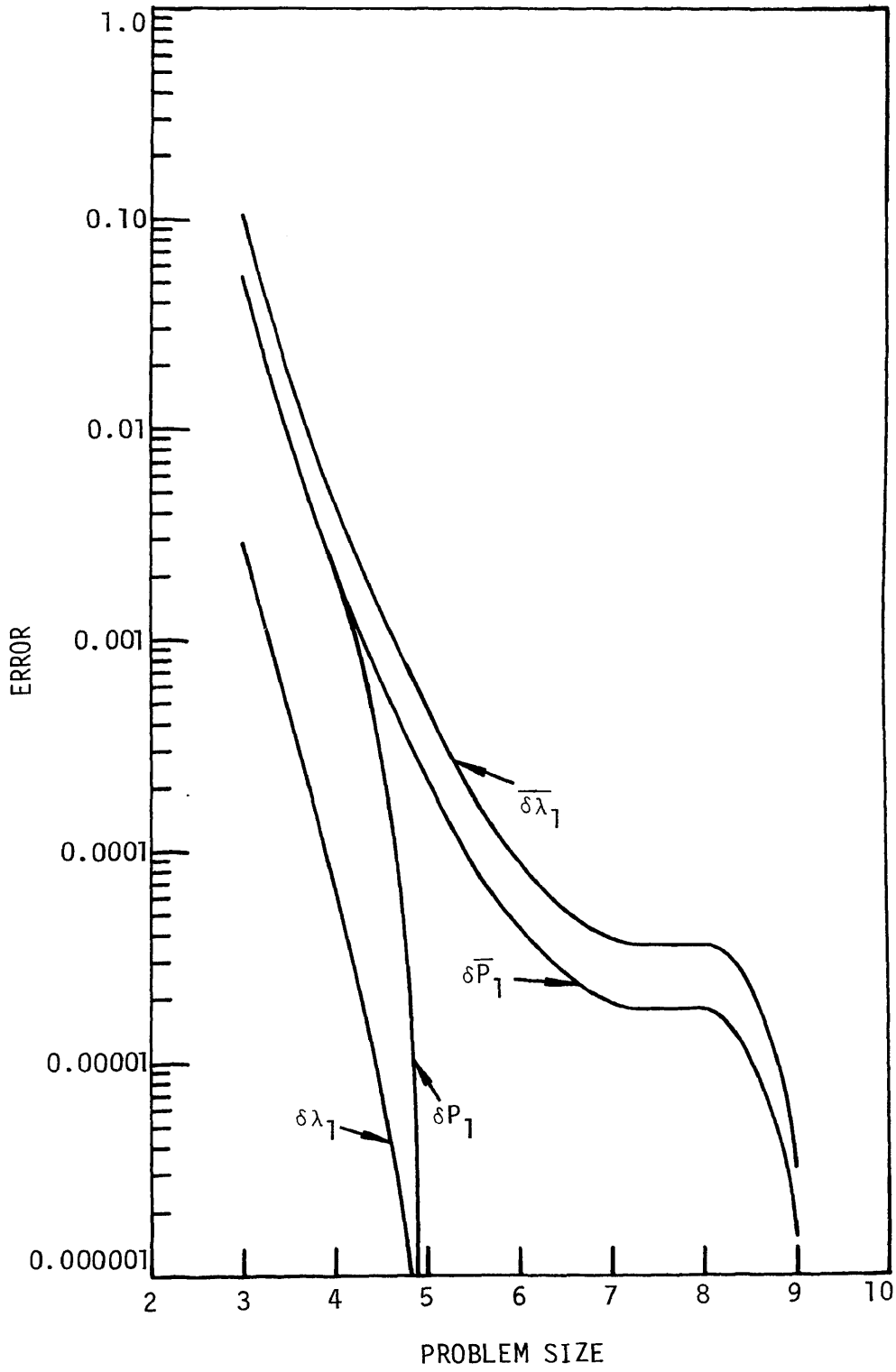

Fig. 10. Comparison of Error Estimate Indicators in the Fundamental Principal Mode Based on Substructure Frequency Root Criteric

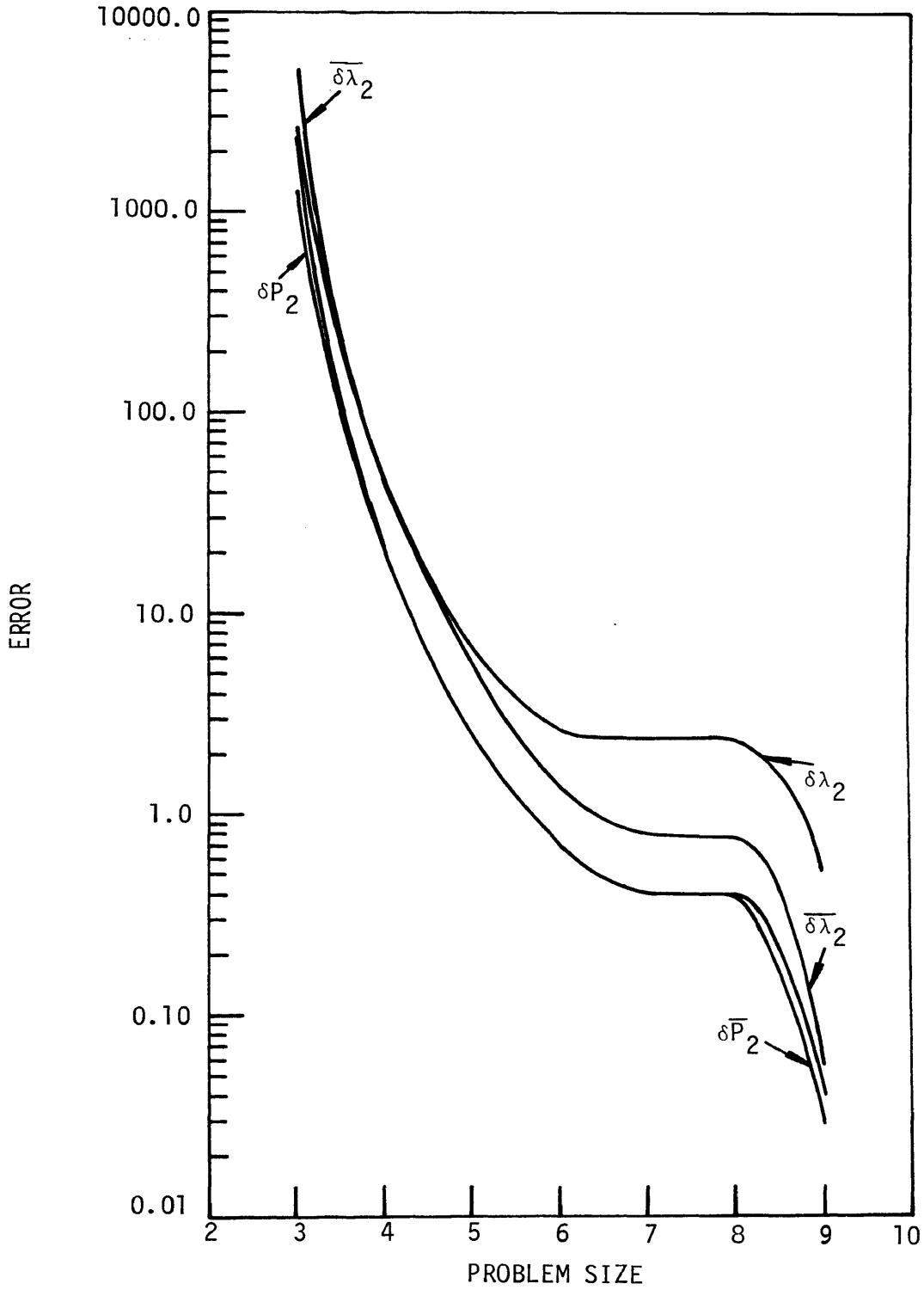

Fig. 11. Comparison of Error Estimate Indicators in the Second Principal Mode Based on Substructure Frequency Root Criterion

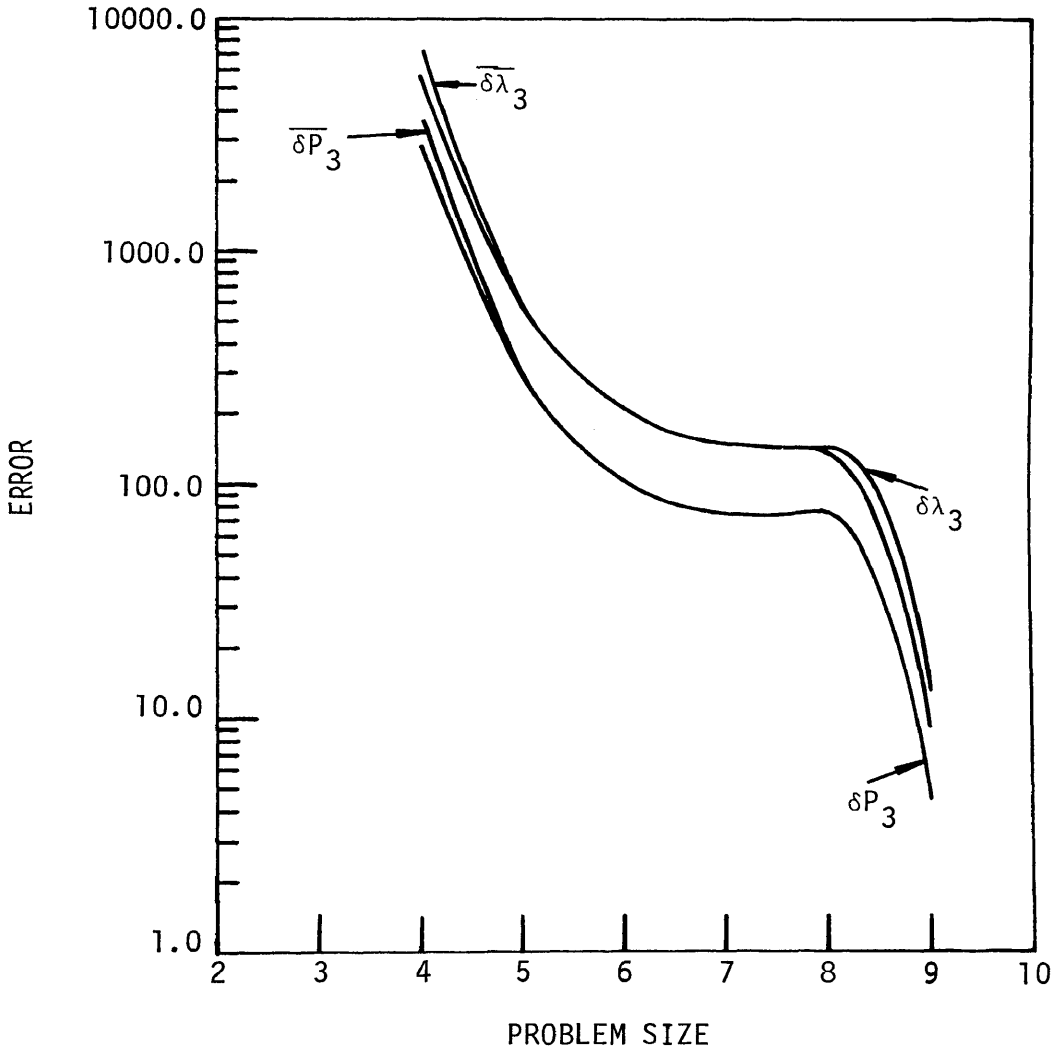

Fig. 12. Comparison of Error Estimate Indicators in the Third Principal Mode Based on Substructure Frequency Root Criterion

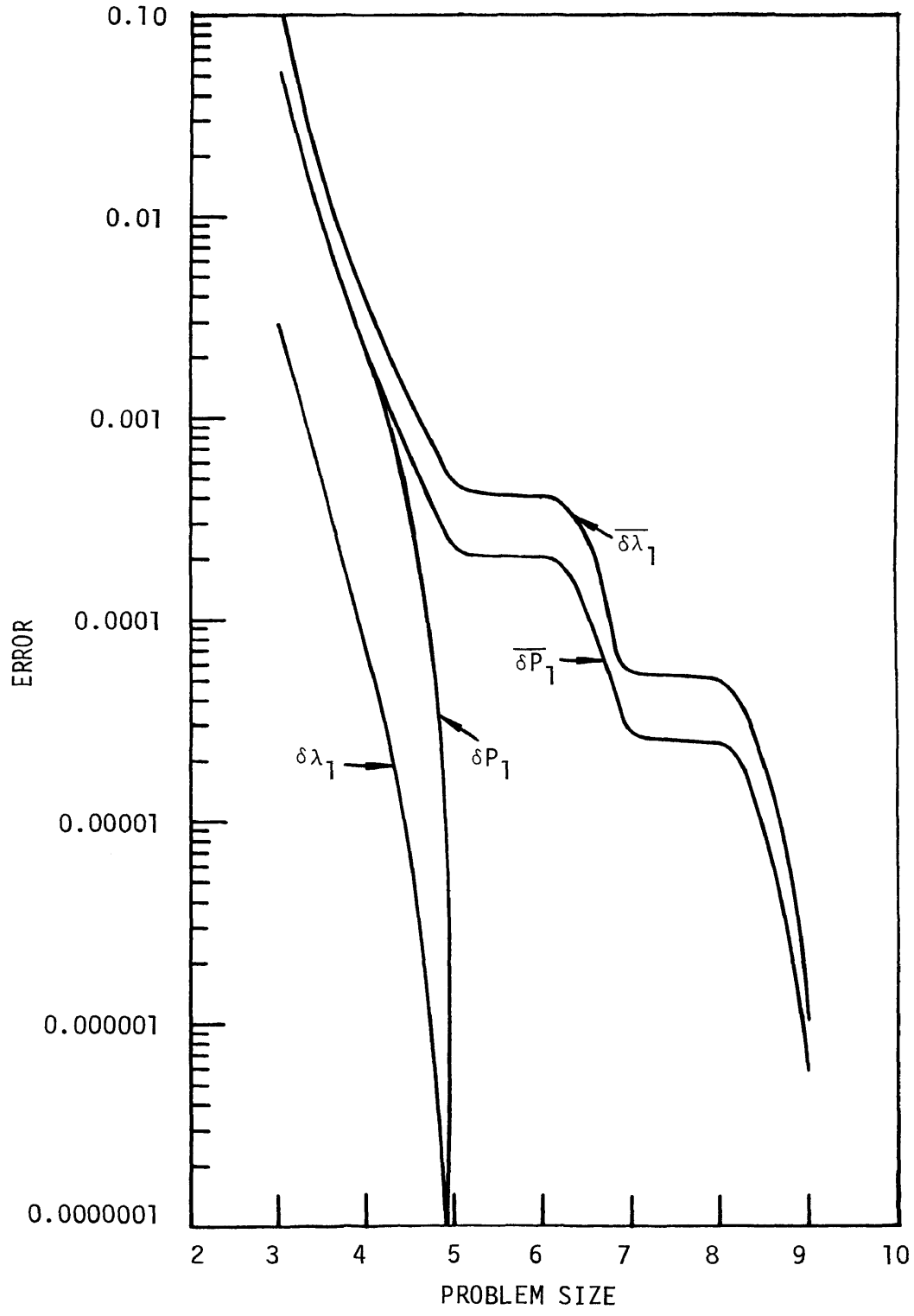

Fig. 13. Comparison of Error Estimate Indicators in the Fundamental Principal Mode Based on Substructure Strain Energy Criterion

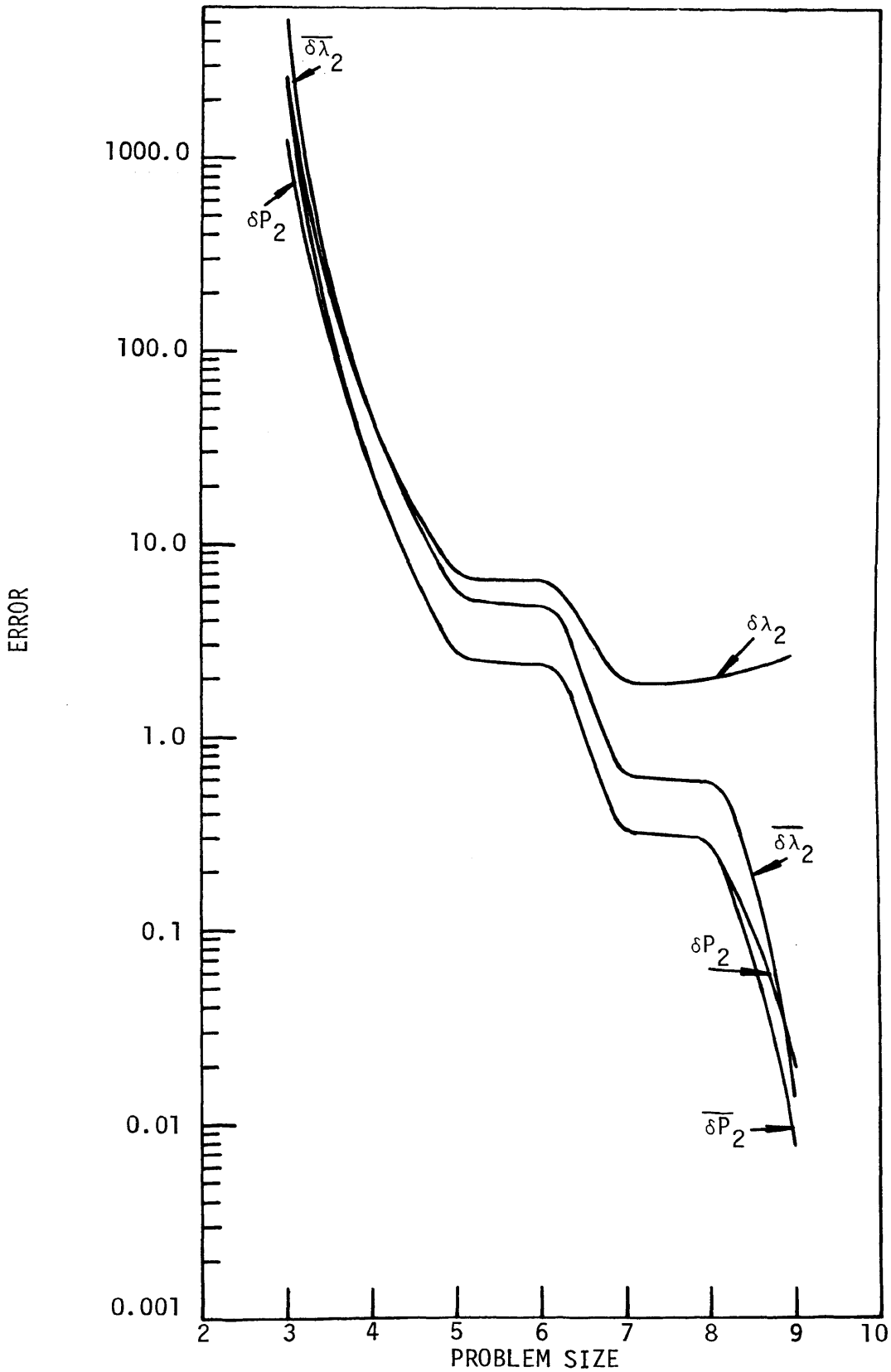

Fig. 14. Comparison of Error Estimate Indicators in the Second Principal Mode Based on Substructure Strain Energy Criterion

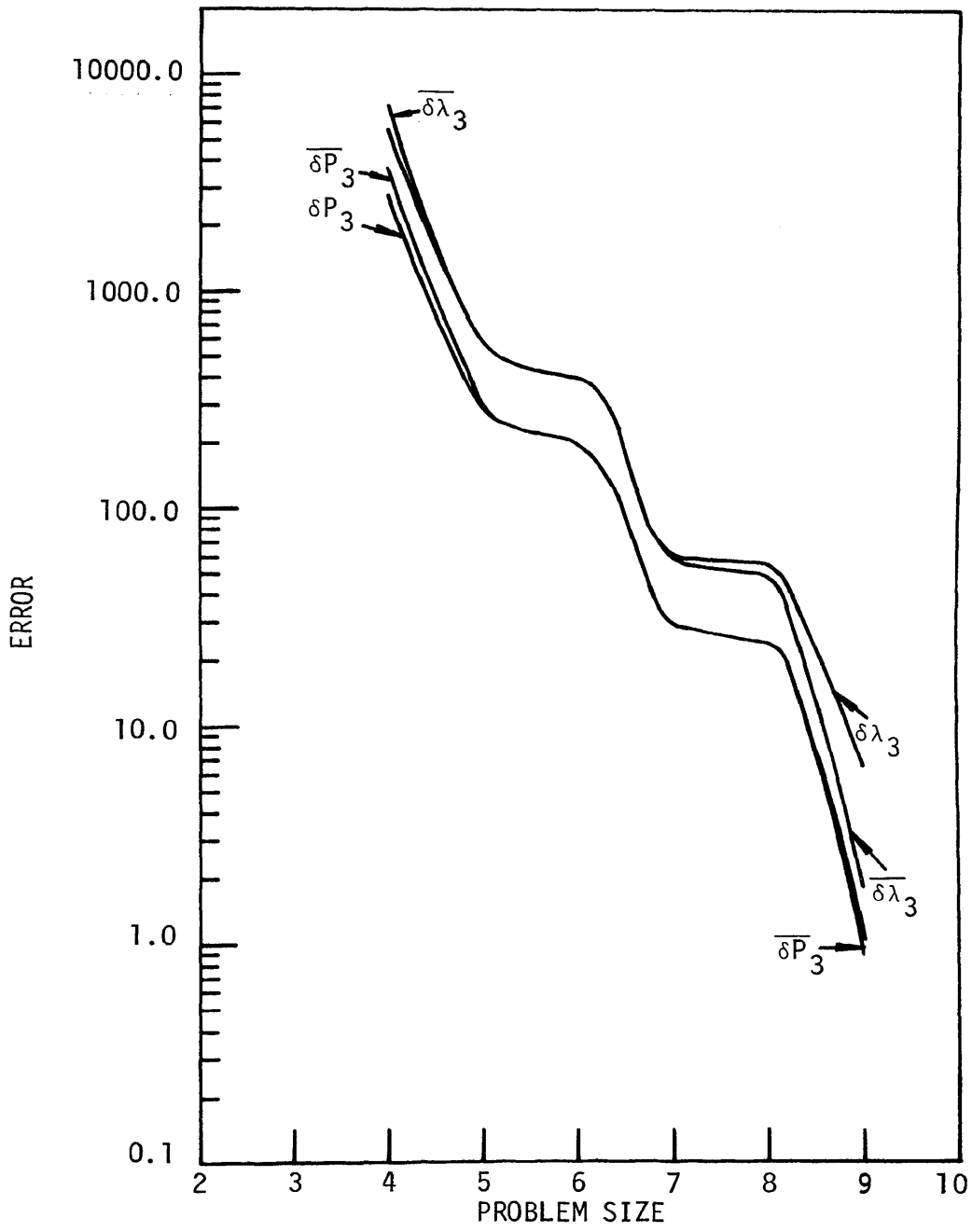

Fig. 15. Comparison of Error Estimate Indicators in the Third Principal Mode Based on Substructure Strain Energy Criterion

motion solved. Errors in Figs. 10 through 12 are based on the substructure frequency roots criterion for retention of substructure normal modes. The error convergence is not monotonic and the estimation of $\delta\lambda$ given by $\overline{\delta\lambda}$ improves considerably in the higher modes. The pattern of convergence in all three modes is about the same for both types of error indicators considered in this report. The estimation of δP by $\overline{\delta P}$ is much better than that of $\delta\lambda$ by $\overline{\delta\lambda}$ in all three modes.

Errors in Figs. 13 through 15 are based on the substructure fixed constraint normal mode strain energy criterion for retention of substructure normal modes. Again, the error convergence is not monotonic. The magnitudes of $\overline{\delta\lambda}$ and $\overline{\delta P}$ are usually higher in comparison to those obtained by the substructure frequency roots criterion, when the number of equations of motion is large.

It is noted from the various data collected, that those system frequency roots which are below the highest substructure frequency root, from that substructure from which the maximum number of normal modes are retained, are well within engineering accuracy. In the case when equal, but largest, number of normal modes are retained from several substructures, the smallest of their highest fixed constraint frequency roots, gives the upper limit for the system frequency roots expected to be within the engineering accuracy.

It is also seen that a particular overall system mode obtained by solving the reduced eigenvalue problem defined in Eq. (78), may be completely omitted due to truncation of substructure normal modes. This may mean that a particular system mode may be dominated by certain substructure normal modes and if these normal modes are deleted from

the analysis, that particular system mode may be deleted too in the final solution. This omission of system modes occurs for system frequency roots greater than those which are expected to be well within the engineering accuracy for a given set of conditions as stated earlier.

B. Initial Conditions Solution

Having presented the results of free undamped vibrations in section A, the initial conditions solution obtained by the substructure method in Chapter III is now verified through numerical examples.

The cantilever beam of section A is divided into six identical elements as shown in Fig. 16. Properties of a typical element are given. Substructure 1 consists of the first three elements while the remaining three elements constitute substructure 2. Again, the number of degrees of freedom at any node is two, transverse displacement and the corresponding rotation. Thus, the total number of degrees of freedom is twelve.

The two substructures are assumed to be given the following initial displacements with zero initial velocities:

$$\{x_0\}_1 = \begin{Bmatrix} x_{0_1} \\ x_{0_2} \\ x_{0_3} \\ x_{0_4} \\ x_{0_5} \\ x_{0_6} \end{Bmatrix} , \text{ or} \qquad (211)$$

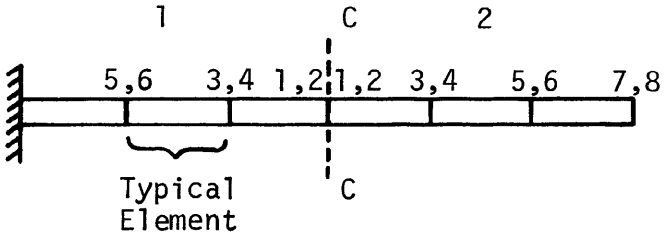

Element Properties

ℓ = 25 in.

$A = \frac{1}{2}$ in. x 2 in.

$E = 30 \times 10^6$ lb/in.^{2}

$\omega = 0.3$ lb/in.^{3}

Fig. 16. Finite Element Model of a Cantilever Beam

$$\{x_0\}_1 = \begin{Bmatrix} 1.950 \\ 0.0446 \\ 0.947 \\ 0.0346 \\ 0.258 \\ 0.0198 \end{Bmatrix}, \text{ and} \tag{212}$$

$$\{x_0\}_2 = \begin{Bmatrix} x_{0_1} \\ x_{0_2} \\ x_{0_3} \\ x_{0_4} \\ x_{0_5} \\ x_{0_6} \\ x_{0_7} \\ x_{0_8} \end{Bmatrix}, \text{ or} \tag{213}$$

$$\{x_0\}_2 = \begin{Bmatrix} 1.950 \\ 0.0446 \\ 3.141 \\ 0.0504 \\ 4.440 \\ 0.0530 \\ 5.770 \\ 0.0534 \end{Bmatrix}. \tag{214}$$

Substructure coordinates are numbered beginning from the constraint coordinates at boundary cc since constraint modes are placed first in the substructure transformation matrix $[T]_i$. Initial displacements of substructures 1 and 2 are given in the same order in Eqs. (212) and (214), respectively. The displacement solution presented in Eq. (105) is numerically evaluated. First, displacement solutions were obtained with no modal truncation so that the substructuring technique solution can be verified against the displacement solution obtained through the ususal direct approach. Direct solutions are derived in Appendix D and Eq. (A.55) gives the direct initial conditions solution. The substructures method with modal truncation gives an approximate displacement solution for the initial conditions described in Eqs. (212) and (214). The reduced problem size is nine for the example considered and is not varied. Three lower normal modes from substructure 1 and four lower normal modes from substructure 2 along with two constraint modes are retained. Two bases of comparisons of the above results are used in this study. Transverse displacements of the free end of the cantilever beam are studied and plotted against time 't'. The other basis is the system strain energy since it is indicative of system behavior as a whole. It also gives a better description of total system distortion.

In Fig. 17, the transverse displacements of the free end of the cantilever beam are plotted. Since these displacements are time dependent, they are plotted against time 't'. To show a direct comparison, free end displacements obtained through the direct method are superimposed on those obtained through the substructure method with, and without modal truncation. It is seen that the direct approach solution

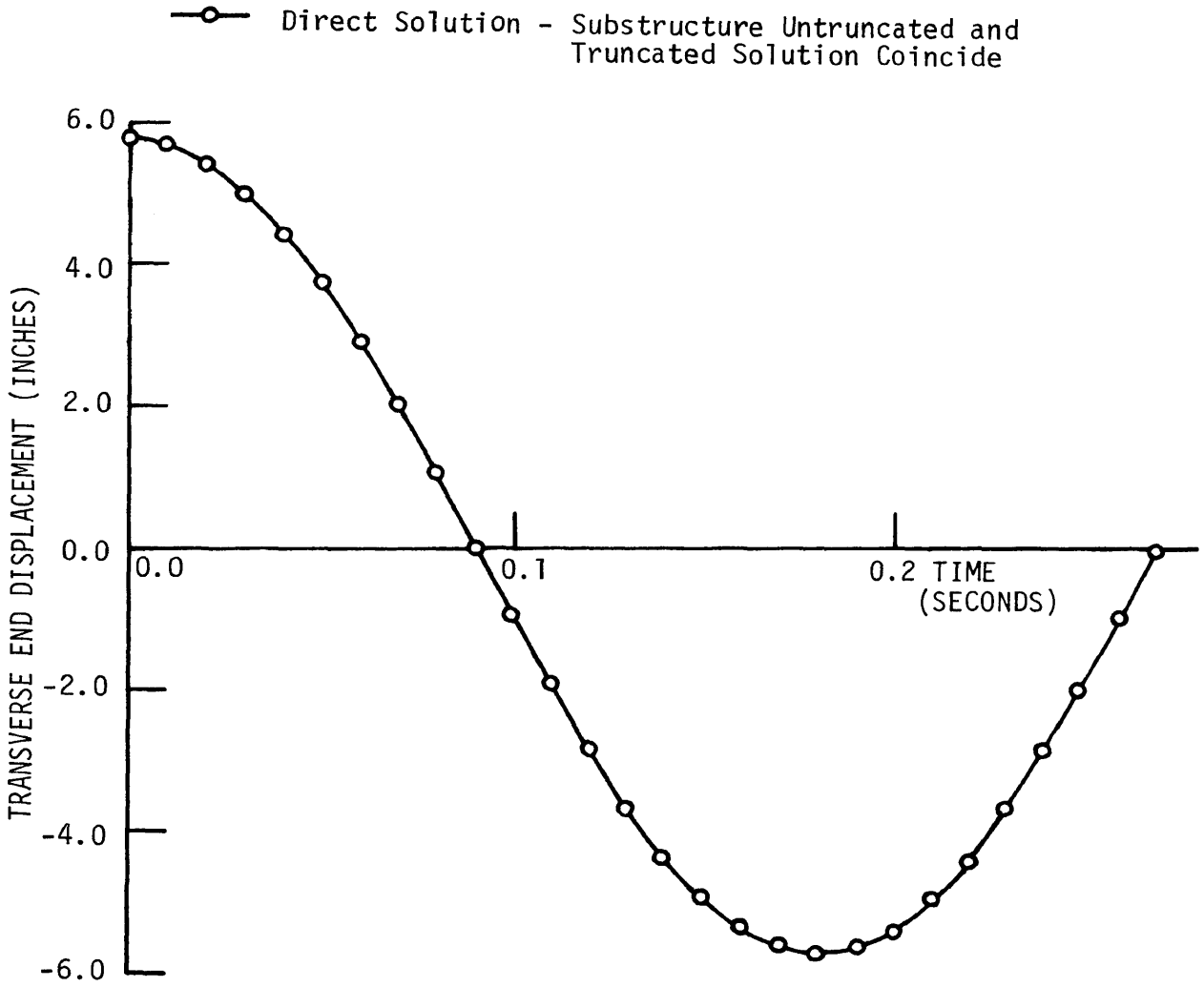

Fig. 17. Comparison of Direct and Substructure Initial Condition Solutions via the Free End Transverse Displacement of a Cantilever Beam

verifies the substructure method solution when all substructure normal modes are retained. The approximate solution solved through modal truncation is very accurate as can be seen in Fig. 17.

From the data of the approximate solution it is noted that representation of system strain energy is accurate, see Fig. 18. Three strain energy solutions; direct, substructures method with no modal truncation, and substructures method with modal truncation are plotted in Fig. 18 to show a direct comparison. Again, the direct solution verifies the substructure solution, when all substructure normal modes are retained and the approximate solution coincides with it.

In the study of a case in which the cantilever beam was given more severe initial conditions, it was found that the modal truncation is sensitive to the type of initial conditions applied. Higher order substructure modes cannot be eliminated if the applied initial conditions excite higher order system modes. This is due to the fact that the higher order system modes are largely dependent on the higher order substructure modes.

1. Comparison of Computer Time for Free Vibration Solutions

In order to complete the comparison between the substructures m method and the direct method, a study of required computer time for the eigenvalue problem is made. It is assumed that the computer time for generating the mass and the stiffness matrices in both the techniques involved is nearly the same. Thus, the computer time taken to solve an eigenvalue problem through both techniques provides a good basis

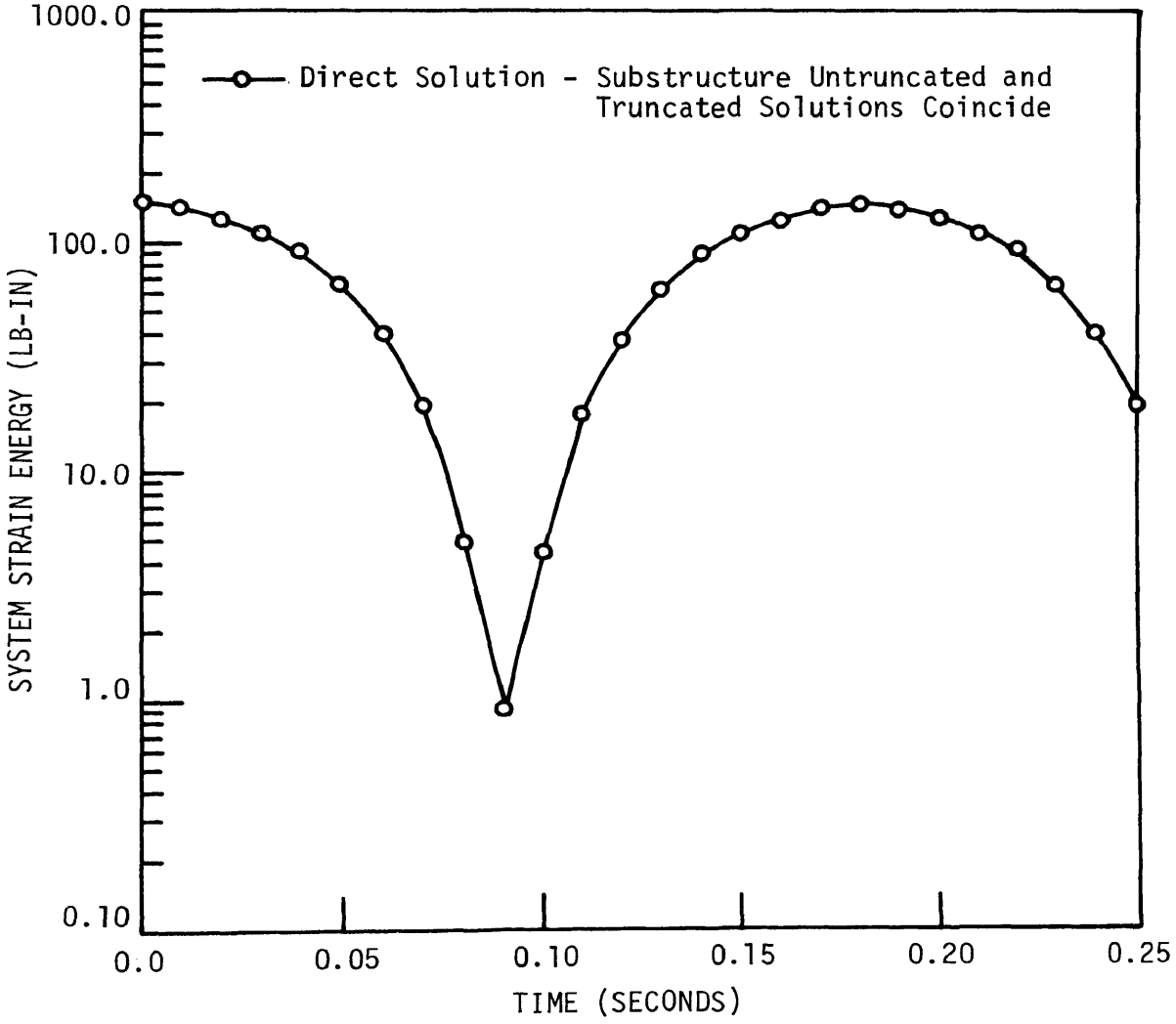

Fig. 18. Comparison of Direct and Substructure Initial Condition Solutions via the System Strain Energy of a Cantilever Beam

to compare the required computer time for the two methods. The number of multiplication and addition operations required to obtain the final initial conditions solution through both the techniques is also presented. Computer times required to obtain eigenvalues are quoted for an IBM 7090 computer system and an eigenvalue routine, BIGMAT, developed at Union Carbide Corp., Nuclear Division, Central Data Processing Facility, Oak Ridge, Tennessee. This routine is basically the Householder tri-diagonalization method (17) and is one of the most efficient eigenvalue routines for real symmetric matrices.

The size of an eigenvalue problem to be solved is assumed to be 102. Computer time required to obtain all eigenvalues and eigenvectors through the usual direct approach is given in Table VII. Computer time for calculating the 20, 32, 52, and 72 lowest eigenvalues and their corresponding eigenvectors is also included, since in many applications, the lower order eigenvalues only are obtained.

Table VII

Computer Times for Solving Directly
An Eigenvalue Problem of Size 102

No. of Lowest Eigenvalues and Eigenvectors	Computer Time In Seconds
102 (All)	167.0
72	134.06
52	112.10
32	90.14
20	76.96

To obtain eigenvalue computer time using the substructures method, it is assumed that the given structure is split into two substructures and that substructure 1 has forty interior coordinates yielding forty normal modes while substructure 2 contains sixty interior coordinates giving sixty normal modes. Using this approach requires basically three eigenvalue problems to be solved. Two of these are at the substructure's level and thus much smaller in size. The final or third solution is of the reduced set of equations for system eigenvalues and eigenvectors. Computer times for the three eigenvalue problems are added and presented in Table VIII, for various sizes of the reduced problem. This, then, gives some comparison of the time required for a classical single large order matrix solution versus the multiple smaller order approach.

Table VIII

Computer Times for Solving an Eigenvalue Problem of Size 102 Using Substructures Method

Substructure 1 Modes Retained	Substructure 2 Modes Retained	Final Problem Size	Computer Time for all System Modes in Sec.	Computer Time for 20 Lower Modes in Sec.
40	60	102	226.8	136.76
35	35	72	115.0	77.86
40	30	72	113.9	76.76
10	60	72	120.5	83.36
40	10	52	65.3	50.22
0	50	52	70.3	55.22
25	25	52	68.6	53.52
30	0	32	23.6	20.6
0	30	32	38.2	35.2
15	15	32	38.7	35.7

It can be seen from Tables VII and VIII that retaining all substructure normal modes in the method of substructures is not profitable. Since this method with modal truncation still yields accurate solutions in the lower modes, its computer time economics are studied when only some substructure normal modes are retained. As for example, when the reduced problem size is 52, with equal number of substructure normal modes retained from each substructure, a saving of approximately 30% of computer time results, in comparison to the direct approach computer time for calculating 20 lower system eigenvalues and eigenvectors. If the substructure frequency roots are known, the accuracy of these 20 modes may be predicted through the trends stated in section A. Since the substructure frequency roots are not known in the present example, the consensus of past experience (10) may be utilized. Indications are that at least 50% of the total number of degrees of freedom in {q} coordinates may be expected to have converged to within the limits of engineering accuracy of the untruncated solution. This means that at least 25 lower modes may be expected to be described accurately.

2. Comparison of Multiplication and Addition Operations

For a comparison of multiplication and addition operations required to calculate the initial condition solution through the substructures and the direct methods, consider two matrices [A] and [B] of sizes m x n and n x ℓ, respectively. If the two matrices are multiplied the total number of multiplication and addition operations are given by:

Total number of multiplication operations required to obtain the product $[A]\cdot[B] = m \times n \times \ell$, and (215)

Total number of addition operations required to obtain the product $[A]\cdot[B] = (n-1) \times m \times \ell$. (216)

Using Eqs. (215) and (216) the total number of multiplication and addition operations involved in obtaining initial conditions solution through direct approach and given by Eq. (A.55), in Appendix D, are now calculated. If all system eigenvectors are available, the size of the modal matrix $[\phi]$ in Eq. (A.55) is given by m x m. In this case total number of multiplication operations required are $7m^2$, and the number of addition operations are given by m(7m-6). If only r lower modes are available in matrix $[\phi]$, its size becomes m x r and the corresponding multiplication and addition operations required to solve for vector $\{x\}$ in Eq. (A.55) are given by:

Total multiplication operations = $3mr + 2(m^2+r^2)$, and

Total addition operations = $2(m-1)(m+r) + (r-1)(2r+m) + r$.

Table IX gives the number of multiplication and addition operations required to solve an initial conditions problem, directly. The value of m is assumed to be equal to 100 and that of r is varied over the range 30 to 100.

Table IX

Multiplication and Addition Operations Required for a Direct Initial Conditions Solution

Value of m	Value of r	Multiplication Operations	Addition Operations
100	100	70000	69400
100	70	50800	50290
100	50	40000	39550
100	30	30800	30410

In Eq. (105) of Chapter III is given the initial conditions solution obtained through the substructures method. Assuming that the size of structure transformation matrix [T] is given by m x r, m > r, the total number of multiplication and addition operations required to solve for displacement vector {x} become:

$$\text{Total multiplication operations} = 2m^2 + 5r^2 + 3mr, \text{ and}$$

$$\text{Total addition operations} = 2m^2 + 5r^2 + 3mr - 6r - 3m.$$

Assuming, for the purpose of comparison, that the number of substructure constraint modes is 2 and that the total number of interior coordinates is 100, the value of m becomes 102. The value of r is varied, for comparisons, from 30 to 100. Table X gives the total number of multiplication and addition operations required for obtaining displacements {x} in Eq. (105) through the method of substructures.

Table X

Multiplication and Addition Operations Required for Initial Conditions Solution Through Substructures Method

Value of m	Value of r	Total Multiplication Operations	Total Addition Operations
102	100	101408	100502
102	70	66728	66002
102	50	48608	48002
102	30	34488	34002

Comparisons between Tables IX and X show that the substructures method does not economize on the multiplication or addition operations

in the solution of an initial conditions problem. Thus, the major advantage of substructuring a given complex structure lies in the solving the eigenvalue problem economically and accurately. In other operations it is comparable to the usual direct approach.

Having established the behavior of various error indicators for the substructures method in section A, and its usage in the initial conditions problem in section B, an investigation of systems under forced excitations is made. Forced excitation solutions obtained through the substructures approach are derived in chapter IV. For the types of excitations considered in this study, displacement solutions of systems through the usual direct approach are included in Appendix D.

The cantilever beam of Fig. 16 is used for the numerical evaluation of equations. For each excitation case considered, displacement solutions are obtained through a direct matrix method, the substructures method with no modal truncation and the substructures method with modal truncation. The direct matrix solution is obtained via the usual superposition of principal modes and uses complete system matrices at one time. In all cases, when all substructure principal modes are retained, in using the substructures approach, the displacement solution is 'exact' in comparison to the solution obtained through the usual direct approach. When using modal truncation with the substructures approach an approximate solution is obtained which is superimposed on solutions obtained through the other two methods to show a direct and meaningful comparison.

C. General Case of Time-Varying Forced Displacement Excitation

The equations of motion for a structure with imposed known time-varying displacements was treated in section A of Chapter IV. A system displacement solution $\{x_s(t)\}$ is given by Eq. (152) in Chapter IV. The numerical example of Fig. 16 with forced displacement applied at two locations, one in each substructure, is used here to show the applicability of the substructures method of systems under forced displacement excitation.

Figure 19 shows the two known displacements forcing the cantilever beam to vibrate. Vectors $\{x_f\}_1$ and $\{x_f\}_2$ for the two substructures are given by:

$$\{x_f\}_1 = h_1, \text{ or}$$

$$= h_{0_1} \sin \omega_e t, \text{ and} \tag{217}$$

$$\{x_f\}_2 = h_2, \text{ or}$$

$$= h_{0_2} \sin \omega_e t, \tag{218}$$

where the values for h_{0_1}, h_{0_2} and ω_e are assumed to be as follows:

$$h_{0_1} = -1 \text{ in.}$$

$$h_{0_2} = 1 \text{ in.}$$

$$\omega_e = 50 \text{ rad./sec.}$$

A solution was obtained through the usual direct method given by Eq.

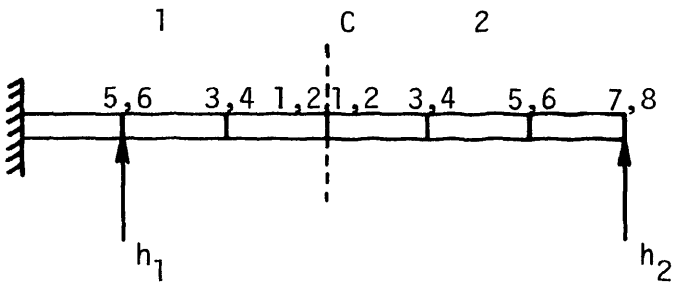

Fig. 19. Cantilever Beam with Two Forced Displacements

(A.82) in Appendix D. This displacement solution is numerically computed for the two forced displacements specified in Eqs. (217) and (218). The substructures method with no modal truncation yields an 'exact' solution which is verified by the direct solution. The approximate solution obtained by substructuring and retaining only a few lower frequency principal modes is compared with the one where all modes are retained. Two lower normal modes are retained from substructure 1 and three lower normal modes are retained from substructure 2. Since the two constraint modes cannot be omitted, a total of seven equations of motion are solved in the reduced set. The transverse displacements of a given point, e.g., mid-point of the cantilever beam, are plotted in Fig. 20 as a function of time 't'. Fig. 20 shows that the approximate solution obtained by modal truncation is very accurate.

The other basis of comparison of results is the system strain energy obtained as a function of time. Figure 21 shows system strain energy behavior as a function of time 't'. Discontinuity of the curve at certain points is due to the fact that system strain energy reduces to zero at these points and cannot be plotted on the log scale. It can be seen that the substructure method with no modal truncation is exact in comparison to the direct solution. However, the approximate system strain energy obtained through modal truncation does not compare too closely with the exact one, although it does follow the same pattern of behavior.

D. Harmonic Force Excitations

A cantilever beam with two harmonic excitations is used for a

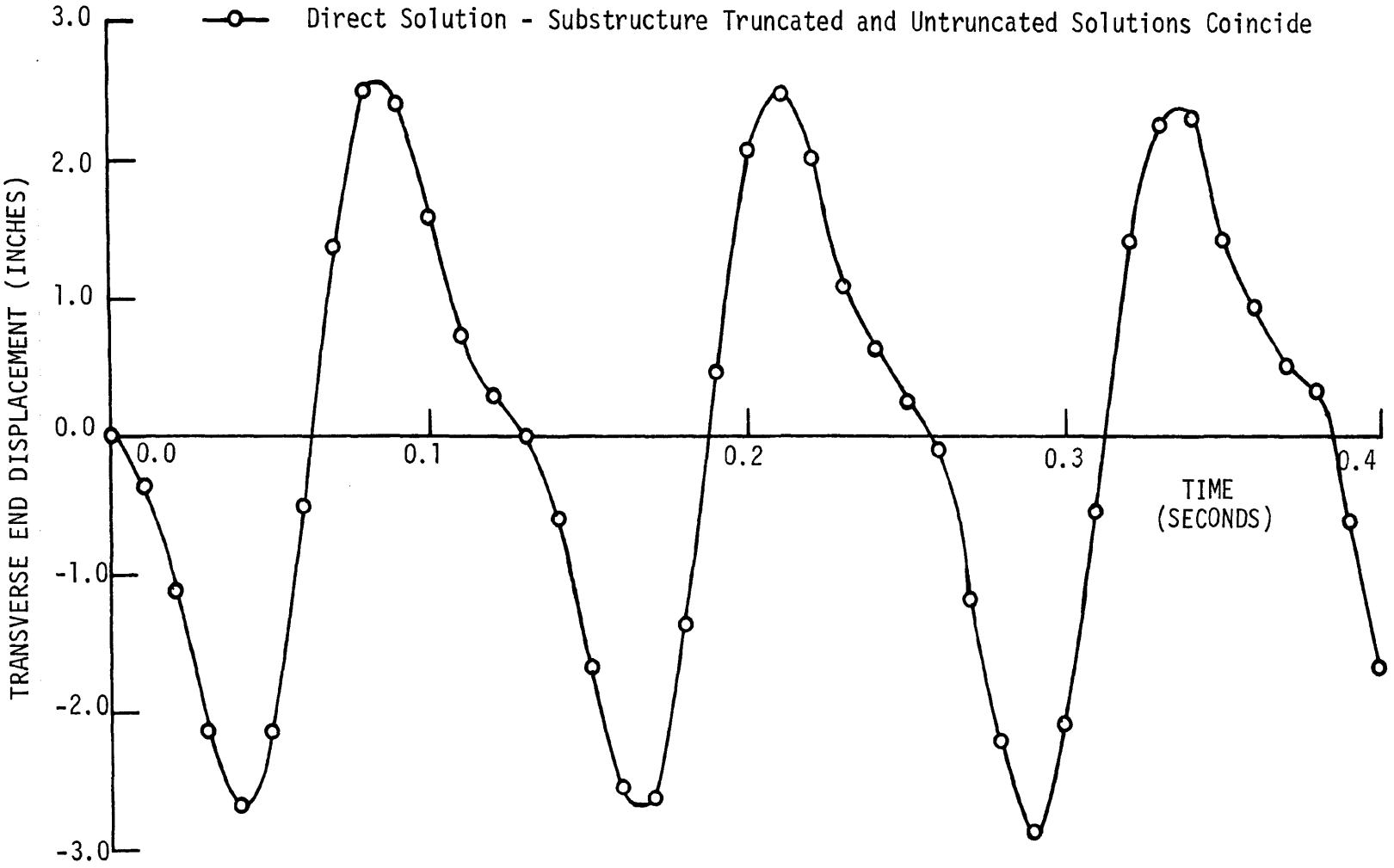

Fig. 20. Comparison of Direct and Substructure Forced Displacement Solutions via the Free End Transverse Displacement of a Cantilever Beam

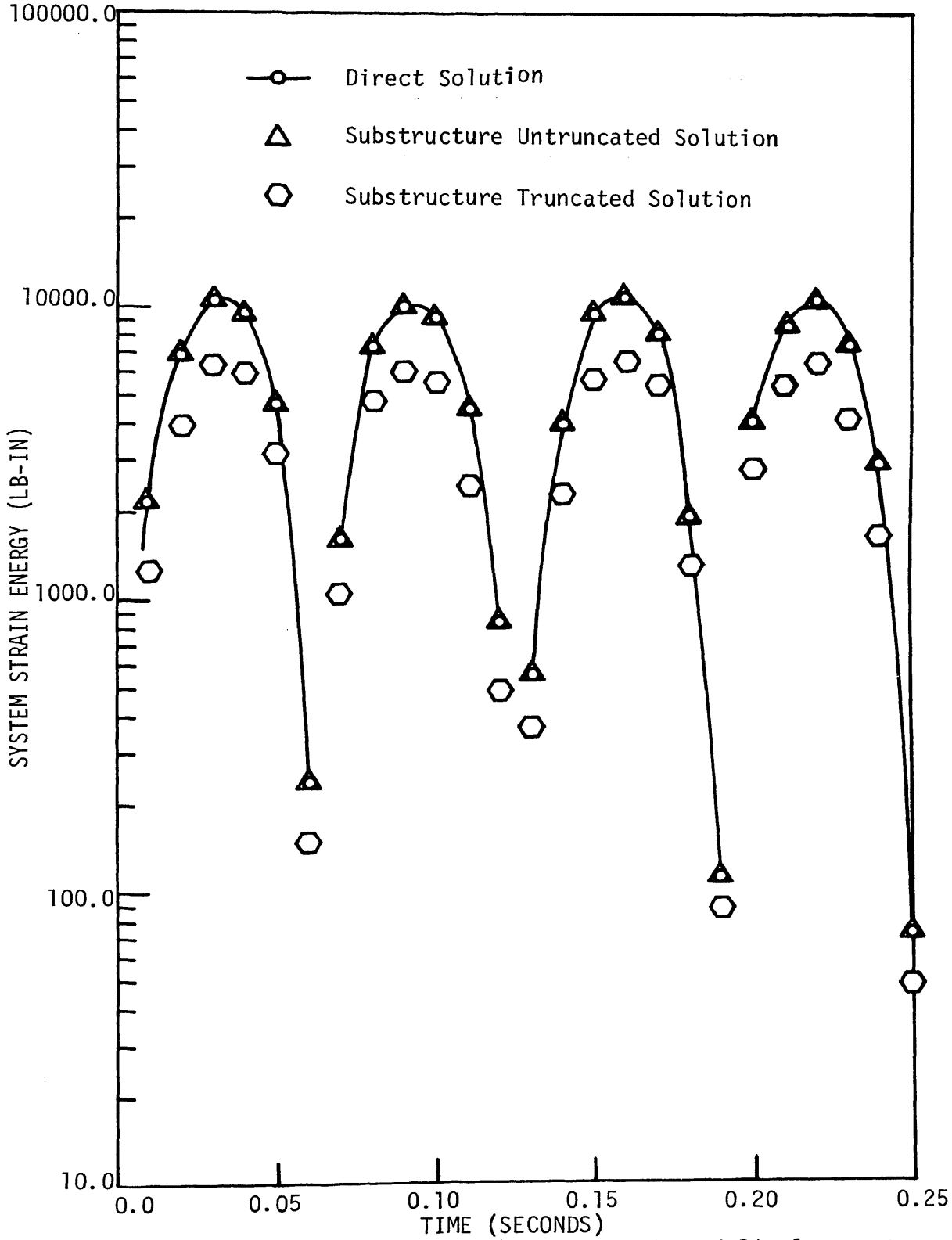

Fig. 21. Comparison of Direct and Substructure Forced Displacement Solutions via the System Strain Energy of a Cantilever Beam

numerical evaluation of Eq. (170) in Chapter IV. These equations give a steady state solution for harmonic excitations through the method of substructures. Figure 22 shows the two excitations acting on the cantilever beam. For convenience, the cantilever beam used in this example is the same used for the numerical example in section C.

The two excitations imposed within the two substructures are assumed to be:

$$\{F(t)\}_1 = \begin{Bmatrix} 0 \\ 0 \\ 0 \\ 0 \\ F_1 \\ 0 \end{Bmatrix} \sin \omega_e t, \text{ and} \tag{219}$$

$$\{F(t)\}_2 = \begin{Bmatrix} 0 \\ 0 \\ 0 \\ 0 \\ 0 \\ 0 \\ F_2 \\ 0 \end{Bmatrix} \sin(\omega_e t + \tfrac{\pi}{4}), \tag{220}$$

in which ω_e is the common forcing frequency and takes the values 10 and 25, the former being less and the latter being greater than the fundamental system frequency root. The values of F_1 and F_2 are assumed to be unity.

The excitation in Eq. (220) is composed of a sine and a cosine function, i.e.,

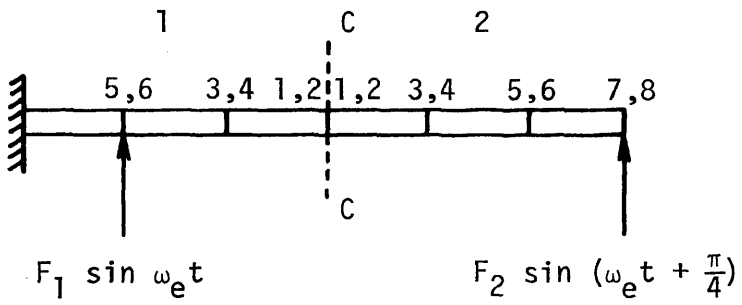

Fig. 22. Cantilever Beam with Two Harmonic Excitations

$$\{F(t)\}_2 = \begin{Bmatrix} 0 \\ 0 \\ 0 \\ 0 \\ 0 \\ 0 \\ F_2/\sqrt{2} \\ 0 \end{Bmatrix} \sin \omega_e t + \begin{Bmatrix} 0 \\ 0 \\ 0 \\ 0 \\ 0 \\ 0 \\ F_2/\sqrt{2} \\ 0 \end{Bmatrix} \cos \omega_e t. \qquad (221)$$

The total system solution for displacements is obtained in two parts. In the first case the applied excitations are given by:

$$\{F(t)\}_1 = \begin{Bmatrix} 0 \\ 0 \\ 0 \\ 0 \\ F_1 \\ 0 \end{Bmatrix} \sin \omega_e t, \text{ and} \qquad (219)$$

$$\{F(t)\}_2 = \begin{Bmatrix} 0 \\ 0 \\ 0 \\ 0 \\ 0 \\ 0 \\ F_2/\sqrt{2} \\ 0 \end{Bmatrix} \sin \omega_e t. \qquad (222)$$

Solution due to the above excitations is superimposed on the one obtained for the following substructure excitations:

$$\{F(t)\}_1 = \{0\}, \text{ and} \qquad (223)$$

$$\{F(t)\}_2 = \begin{Bmatrix} 0 \\ 0 \\ 0 \\ 0 \\ 0 \\ 0 \\ F_2/\sqrt{2} \\ 0 \end{Bmatrix} \cos \omega_e t. \qquad (224)$$

Since it is assumed that the types of structures under investigation are linear, the above superposition yields a total system displacement solution through the method of substructures. In obtaining a solution to substructure excitations defined in Eqs. (214), (222), (223), and (224) two lower normal modes from substructure 1, and four lower normal modes from substructure 2 are retained. Including the two constraint modes, the size of the reduced problem becomes eight.

A displacement solution to the above excitations was first obtained through the method of substructures with no modal truncation. This establishes the numerical accuracy of solutions obtained through substructuring with no modal truncation, in comparison with the solutions obtained through the usual direct method. Direct solutions to harmonic excitations are presented in Eqs. (A.62) and (A.64) in Appendix D. The forcing function, $\{F(t)\}$, in this case is given by:

$$\{F(t)\}= \begin{Bmatrix} F_1 \sin \omega_e t \\ 0 \\ 0 \\ 0 \\ 0 \\ 0 \\ 0 \\ 0 \\ 0 \\ F_2 \sin(\omega_e t + \frac{\pi}{4}) \\ 0 \end{Bmatrix} , \text{ or} \qquad (225)$$

$$\{F(t)\} = \begin{Bmatrix} F_1 \\ 0 \\ 0 \\ 0 \\ 0 \\ 0 \\ 0 \\ 0 \\ 0 \\ F_2/\sqrt{2} \\ 0 \end{Bmatrix} \sin \omega_e t + \begin{Bmatrix} 0 \\ 0 \\ 0 \\ 0 \\ 0 \\ 0 \\ 0 \\ 0 \\ 0 \\ F_2/\sqrt{2} \\ 0 \end{Bmatrix} \cos \omega_e t, \quad (226)$$

in which, $F_1 = F_2 = 1$.

Solution of system equations of motion, due to the excitation described by the first term of Eq. (226), is superimposed on the one due to the excitation defined in the second term. Since this study is limited to linear structures only, the result of the above superposition

yields a direct displacement solution for the given system.

System displacements are obtained for two values of ω_e: 1. ω_e less than the system fundamental frequency root and 2. ω_e greater than the system fundamental frequency root. The two values of ω_e were taken to be 10 and 25, since the system fundamental frequency root is 17·4179.

Transverse displacements of the mid-point of the cantilever beam are plotted as a function of time 't'. For a direct comparison, transverse displacements, obtained directly and through the substructures method, with and without modal truncation, are plotted on the same graph. Direct solution verifies the substructures method when all substructure normal modes are retained. This verification is obtained for the two cases of ω_e. The approximate solutions for both values of ω_e are very accurate, as can be noticed in Figs. 23 and 24. Except for a few points, the approximate displacement solution turns out to be the same as the exact solution.

System strain energy in the steady-state is plotted as a function of time 't' in Figs. 25 and 26. Discontinuities in these curves are due to strain energy being small at these locations and cannot be included in the chosen log scale. Again, the substructures method with no modal truncation is verified by the direct strain energy solutions. However, the approximate system strain energy solution, when modal truncation is used, gives a poor representation of the exact solution, although the general behavior for both the exact and approximate solutions is nearly the same. It can be seen from Figs. 25 and 26 that the approximate system strain energy for ω_e greater

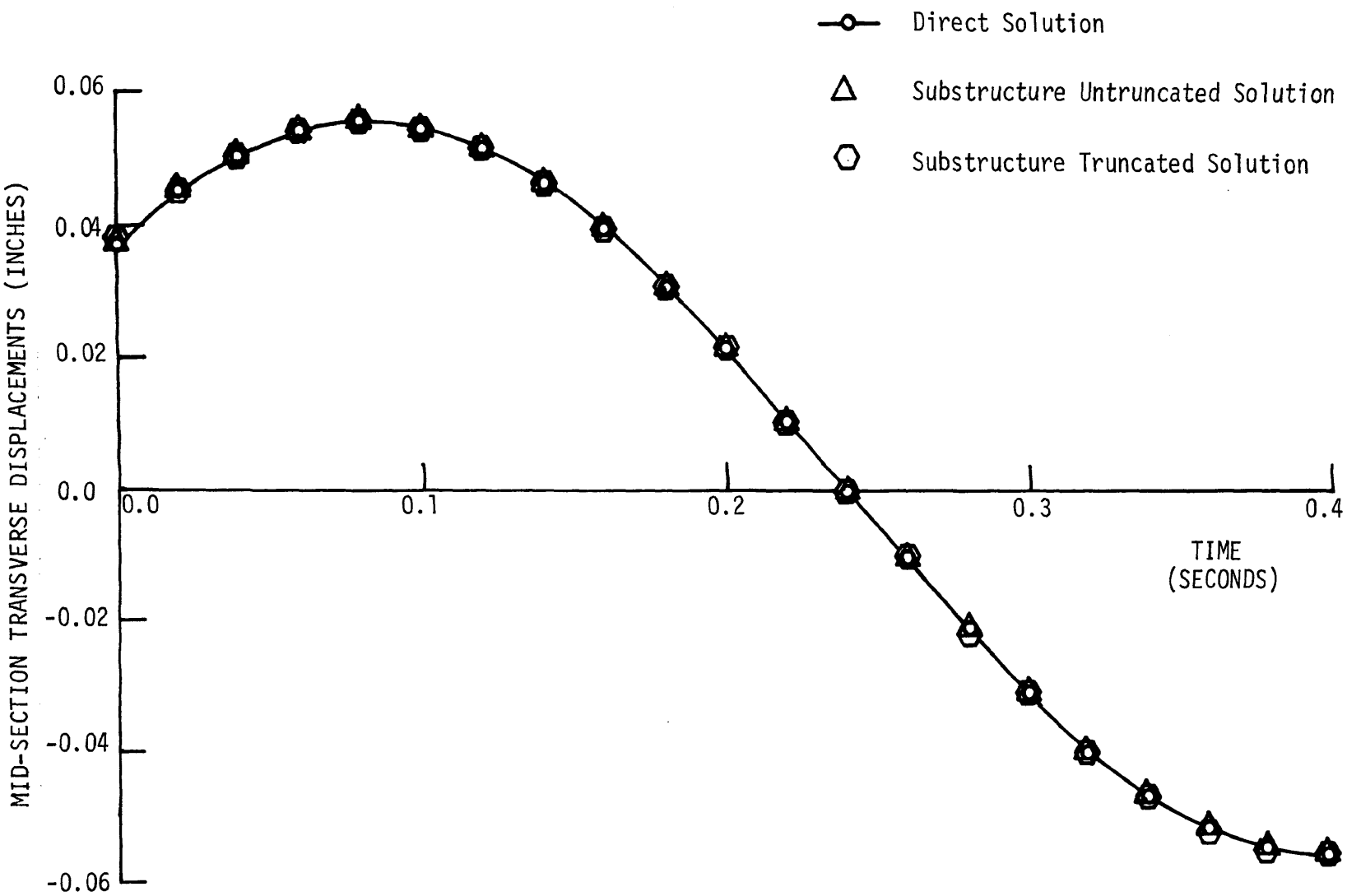

Fig. 23. Comparison of Direct and Substructure Harmonic Excitation Solutions ($\omega_e < \omega_1$) via the Mid-Section Transverse Displacement of a Cantilever Beam.

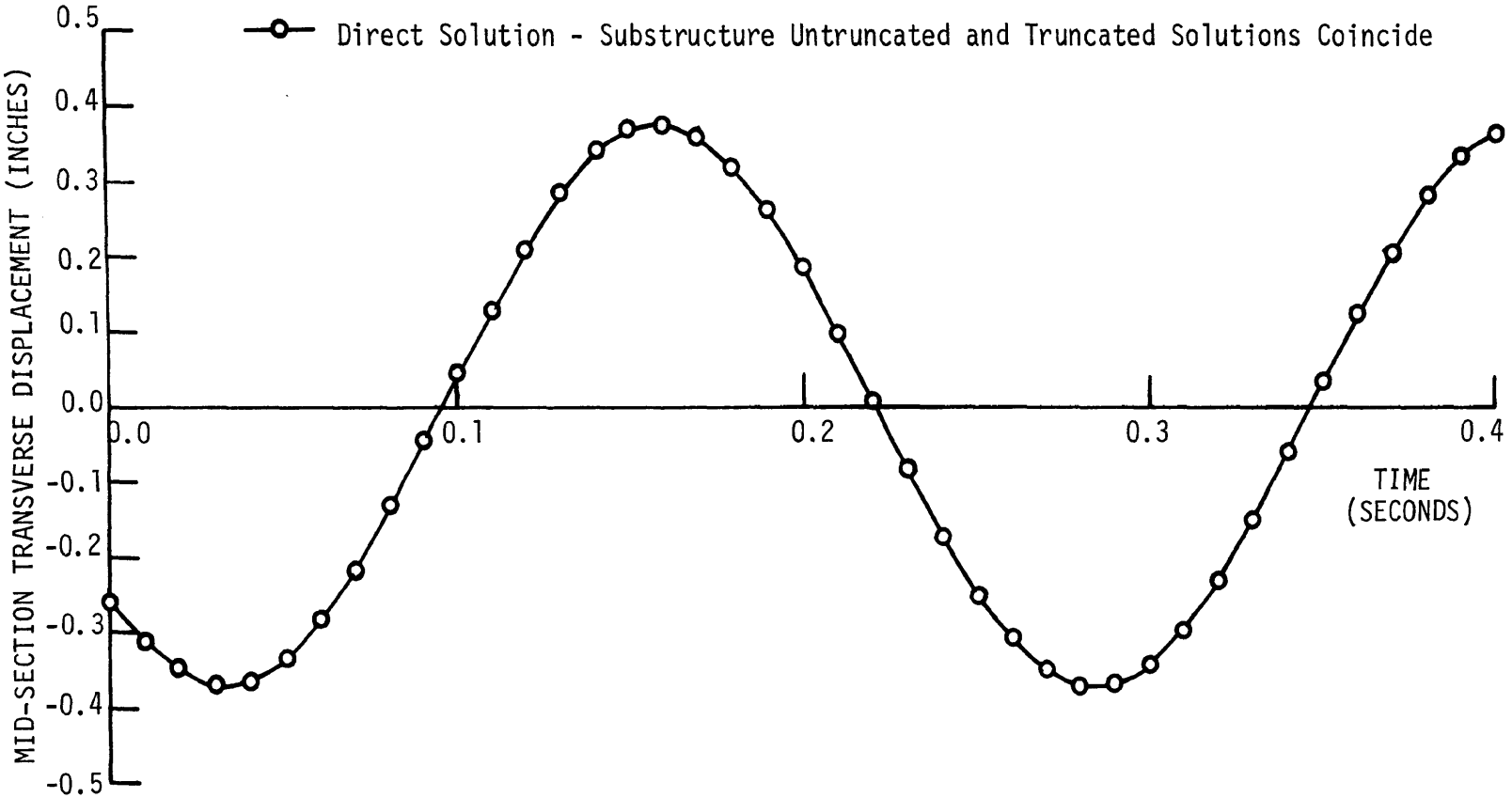

Fig. 24. Comparison of Direct and Substructure Harmonic Excitation Solutions ($\omega_e > \omega_1$) via the Mid-Section Transverse Displacement of a Cantilever Beam

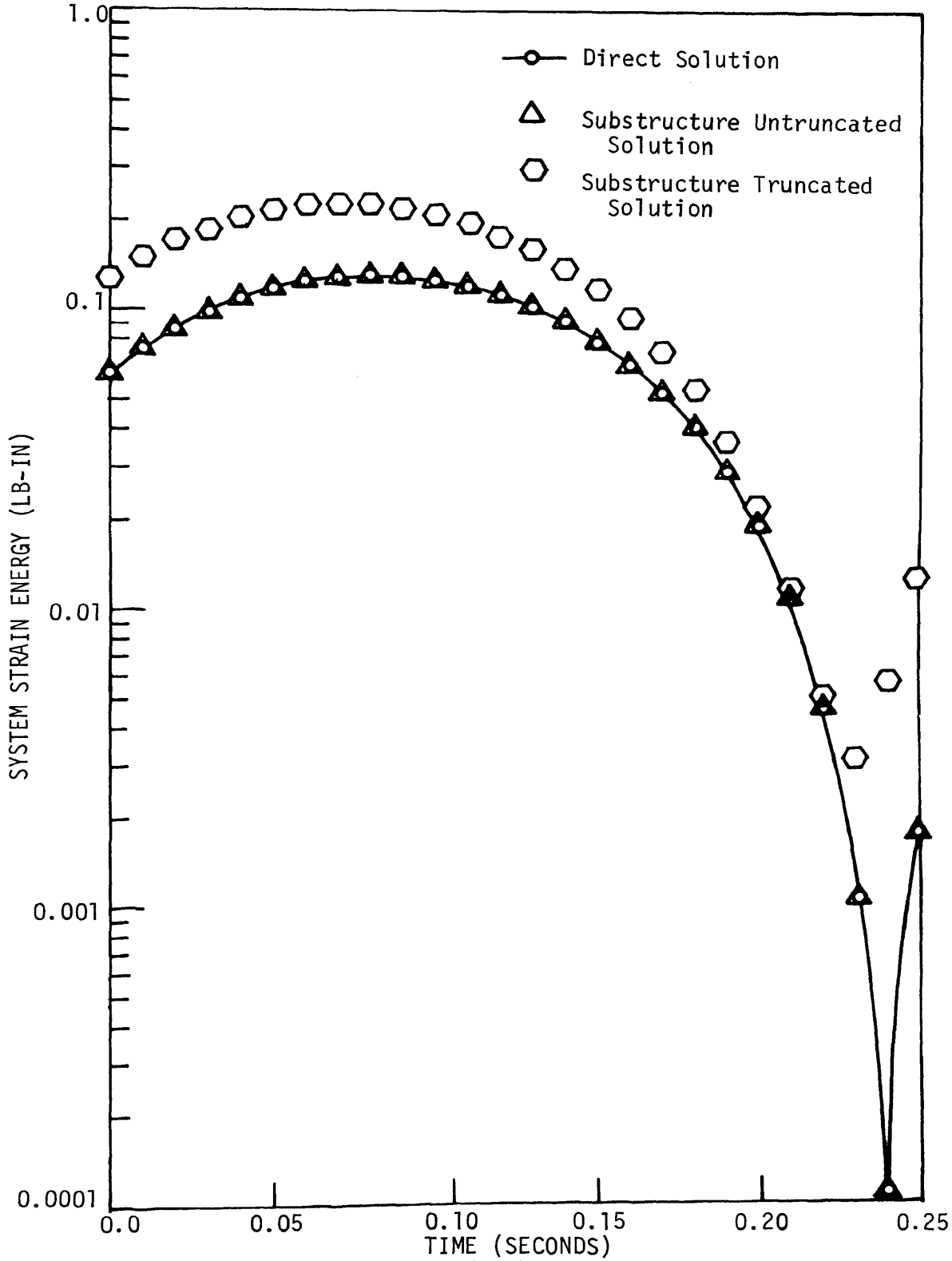

Fig. 25. Comparison of Direct and Substructure Harmonic Excitation Solutions ($\omega_e < \omega_1$) via the System Strain Energy of a Cantilever Beam

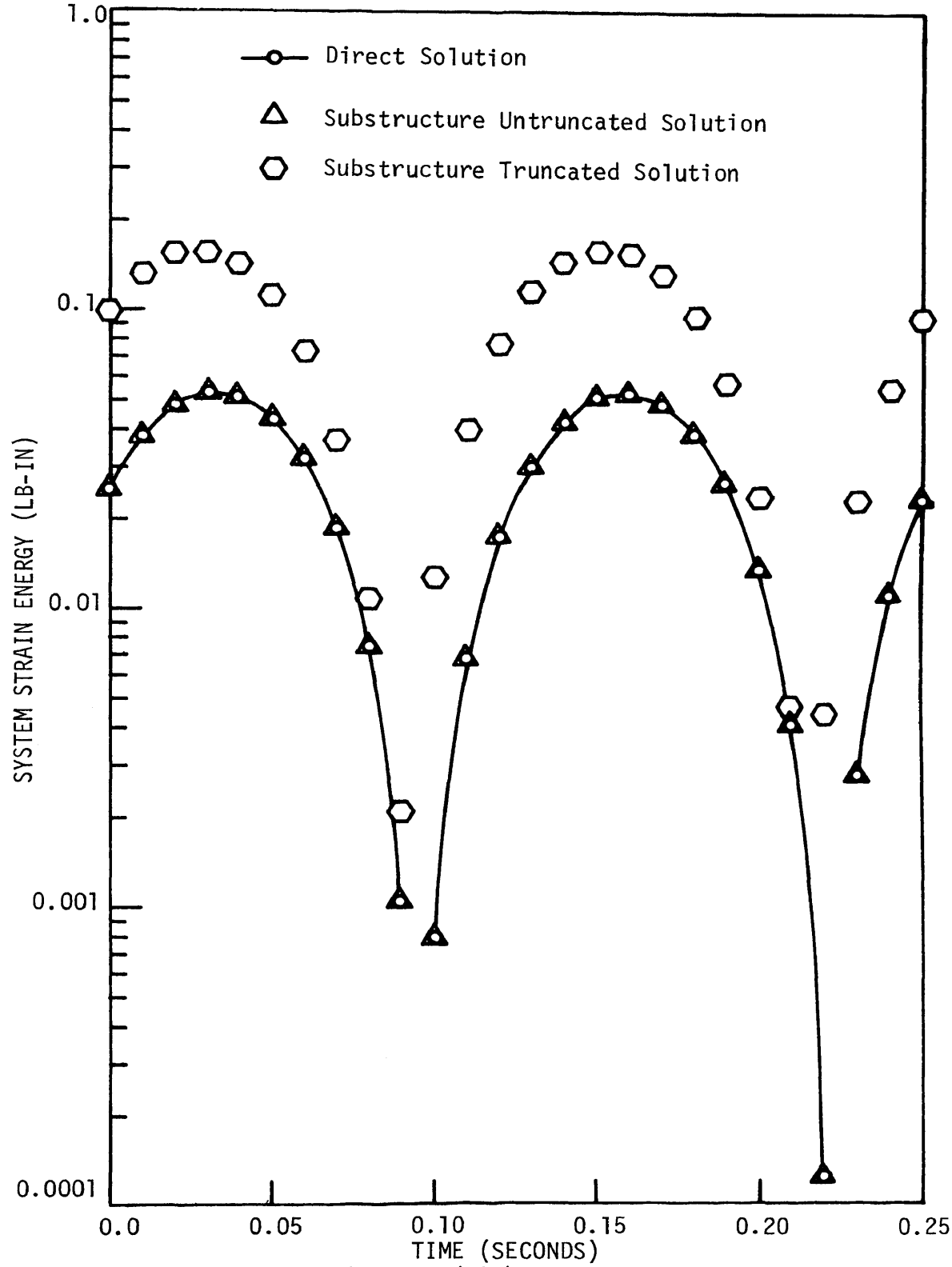

Fig. 26. Comparison of Direct and Substructure Harmonic Excitation Solutions ($\omega_e > \omega_1$) via the System Strain Energy of a Cantilever Beam

than system fundamental frequency, has larger error content in comparison to the case when ω_e is less than system fundamental frequency. Thus a change of forcing frequency may have some effect on the approximate solutions.

E. Base Acceleration Excitation

The fixed end of the cantilever beam in Fig. 16 is given a constant base acceleration as follows:

$$\{\ddot{U}_B(t)\} = \begin{Bmatrix} A_0 \\ \theta_0 \end{Bmatrix}, \tag{227}$$

in which values of A_0 and θ_0 are assumed to be unity.

Assuming zero initial conditions, Eq. (204) in chapter IV gives system displacements relative to the base through the method of substructures.

Matrix [A] in Eq. (204) defines the motion of structure equilibrium position due to the given base motion. If the fixed end of the cantilever beam is given a known transverse and rotational motion, displacement of the rest of the structure is given by:

$$\{\delta_E(t)\} = [A]\{U_B(t)\}. \tag{188}$$

For the two substructures of the cantilever beam under investigation, matrix [A] in its partitioned form becomes:

$$[A] = \left[\begin{array}{c} A_1 \\ \hline A_2 \end{array}\right],$$

where:

$$[A]_1 = \begin{bmatrix} 1 & 3\ell \\ 0 & 1 \\ 1 & 2\ell \\ 0 & 1 \\ 1 & \ell \\ 0 & 1 \end{bmatrix}, \text{ and} \qquad (228)$$

$$[A]_2 = \begin{bmatrix} 1 & 3\ell \\ 0 & 1 \\ 1 & 4\ell \\ 0 & 1 \\ 1 & 5\ell \\ 0 & 1 \\ 1 & 6\ell \\ 0 & 1 \end{bmatrix}, \qquad (229)$$

in which ℓ represents element length and equals 25 inches in this example.

In Eqs. (228) and (229) the boundary constraint coordinates are placed first followed by the substructure interior coordinates. This arrangement of ordering of substructure coordinates is followed throughout the study, since the substructure transformation matrix $[T]_i$ is ordered in the same manner.

The exact solution through the method of substructures, when no modal truncation is used, is verified by the usual direct approach. Equations of motion and their solutions for a base acceleration type of excitation are presented in Appendix D. Equation (A.94) in Appendix D gives system displacement obtained directly, relative to a given base motion. Matrix [A] in this equation is given by:

$$[A] = \begin{bmatrix} 1 & \ell \\ 0 & 1 \\ 1 & 2\ell \\ 0 & 1 \\ 1 & 3\ell \\ 0 & 1 \\ 1 & 4\ell \\ 0 & 1 \\ 1 & 5\ell \\ 0 & 1 \\ 1 & 6\ell \\ 0 & 1 \end{bmatrix}, \qquad (230)$$

in which ℓ equals 25 inches.

Approximate solutions through the substructures method are obtained by retaining two lower modes from substructure 1, four lower modes from substructure 2 and the two constraint modes. Figure 27 shows the transverse displacements of the free end of the cantilever beam obtained through the two exact solutions and the one approximate method when modal truncation is used. It can be seen that the direct displacement solution verifies the solution obtained by the substructures method, when all substructure normal modes are retained. This establishes a check on the numerical evaluations and the computer program. It is evident from Fig. 27 that the approximate solution is fairly accurate in comparison to the exact solutions.

Figure 28 shows the system strain energy as a function of time 't'. Again, system strain energy solutions obtained by three approaches listed above are plotted on the same graph for a direct and meaningful comparison. The direct solution confirms the validity of the substructure

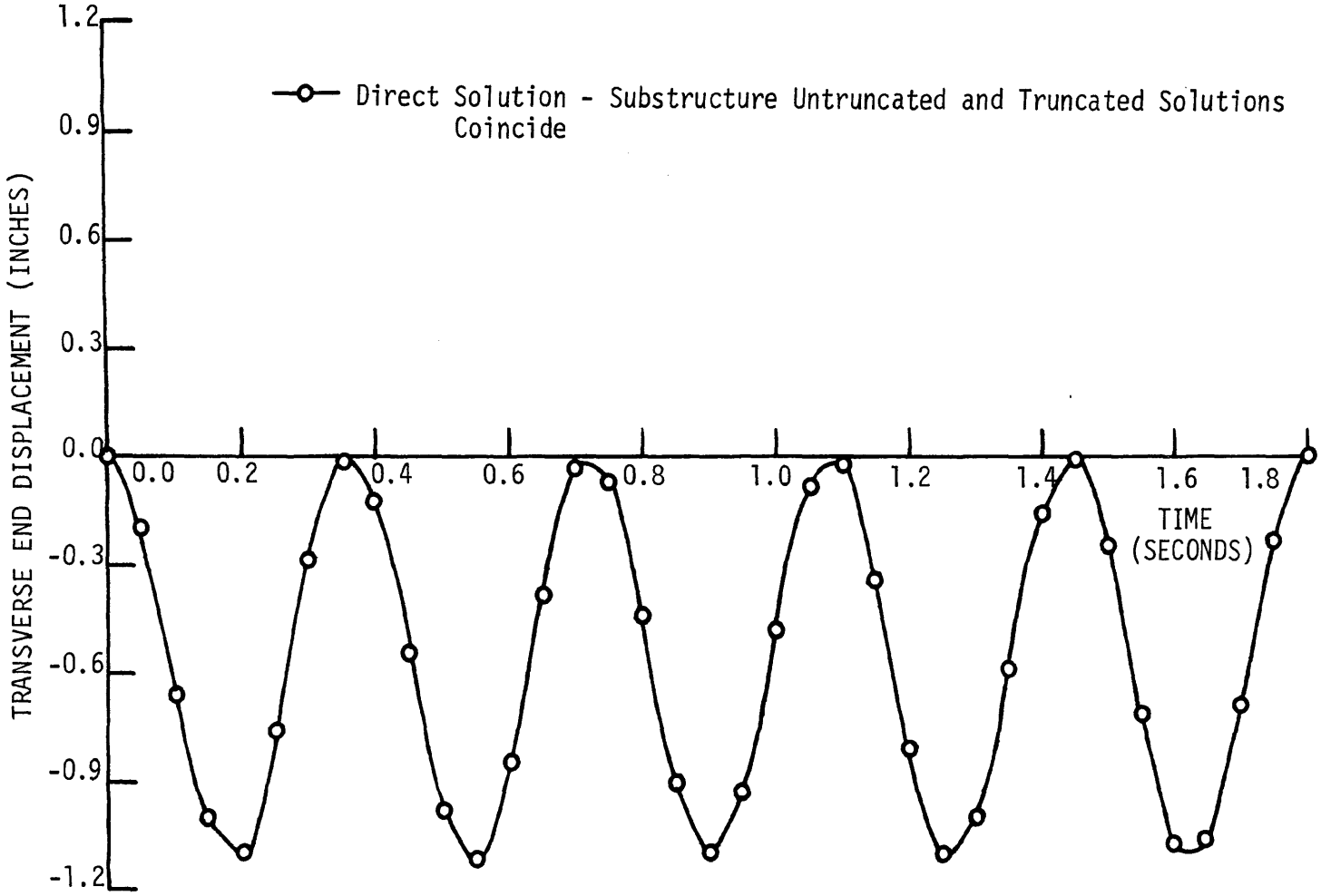

Fig. 27. Comparison of Direct and Substructure Solutions via the Free End Transverse Displacement of a Cantilever Beam with Constant Base Acceleration

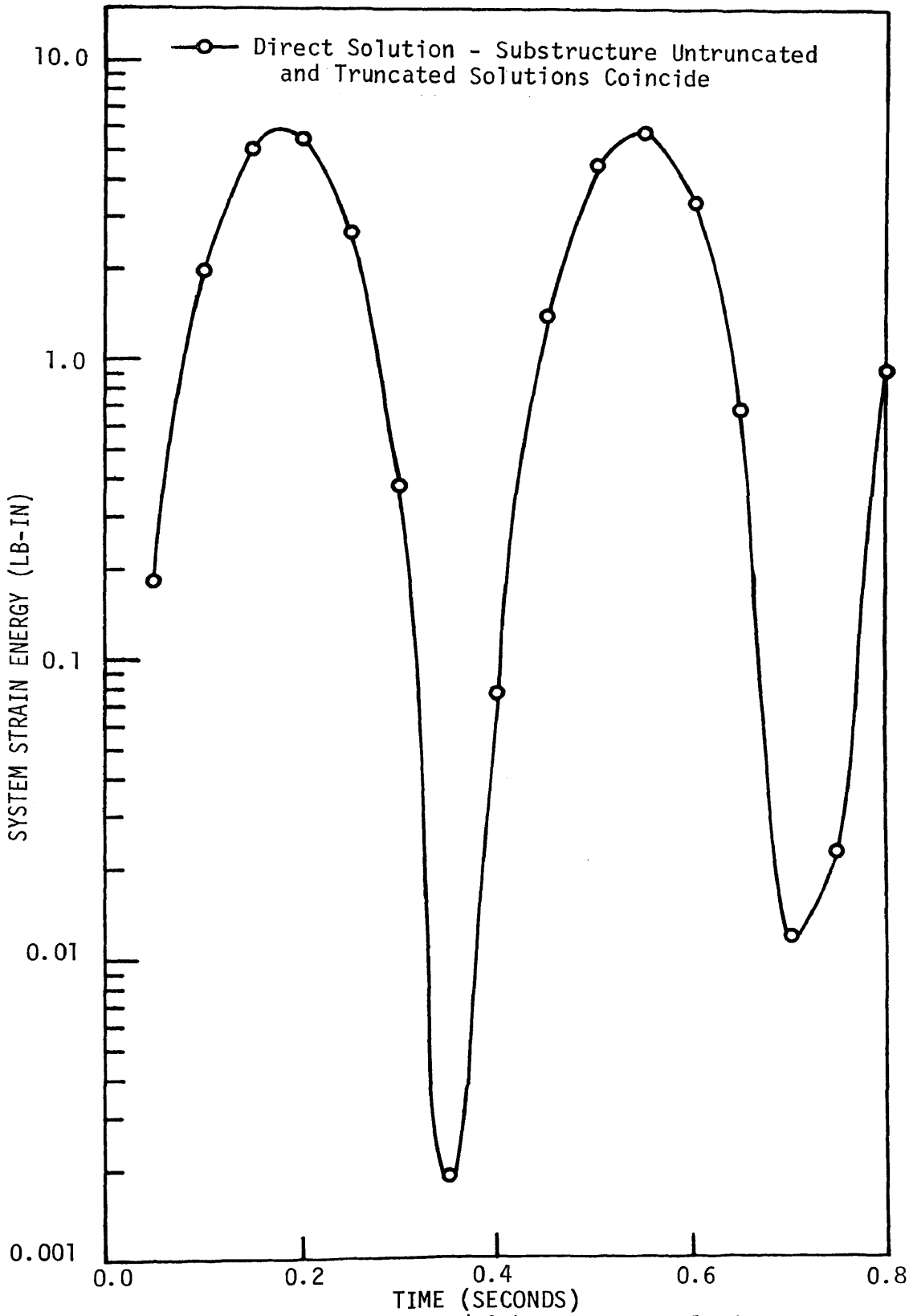

Fig. 28. Comparison of Direct and Substructure Solutions via the System Strain Energy of a Cantilever Beam with Constant Base Acceleration

method, when all substructure normal modes are retained. The approximate system strain energy in this case gives an accurate representation of the exact solution. Based on this simple investigation of a cantilever beam, it is noticed that the substructures method with modal truncation yields satisfactory results for a base acceleration type of excitation. This conclusion can be justified since a step base acceleration, in essence, is equivalent to a uniform acceleration load applied to the entire beam. The displacement solution is nearly a static deflection case under uniform load. The accuracy of the solution, thus, should be good as the first principal mode is probably 90% of total dynamic solution

F. General Time-Varying Force Excitation

A half-sine pulse force, shown in Fig. 29, is applied to the cantilever beam of Fig. 16. This force acts on the central part of the beam as shown in Fig. 30. The applied half-sine pulse at any one node is given by:

$$F(t) = F_0 \sin(t/t_1), \quad 0 \leq t \leq \pi t_1 \qquad (231)$$

$$= 0 \qquad t \geq t_1,$$

in which πt_1 gives the pulse duration time and is assumed to be equal to two seconds for this investigation. The value of F_0 is assumed to be unity.

The one force acting at boundary cc is divided equally between substructure 1 and 2 as shown in Fig. 30. It is assumed that the motion of the cantilever beam starts from rest and, thus, the displacement soluion through the substructures method can be obtained by using the

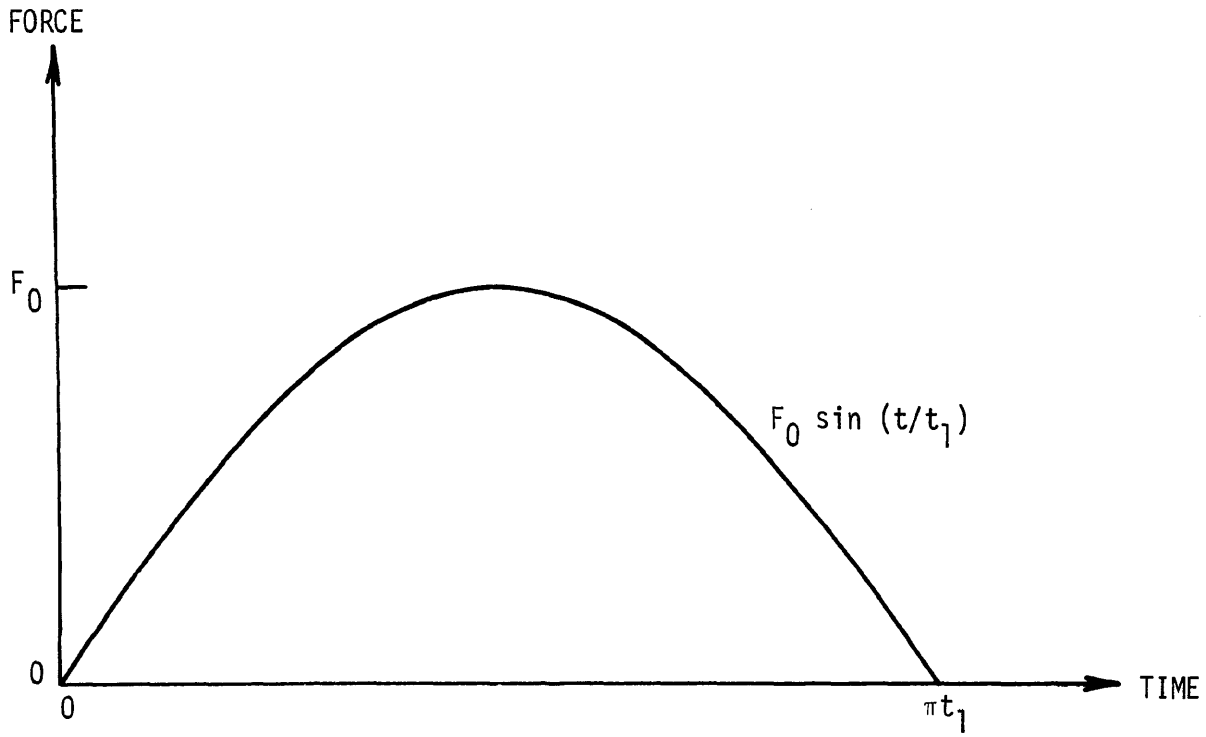

Fig. 29. Half-Sine Force Pulse

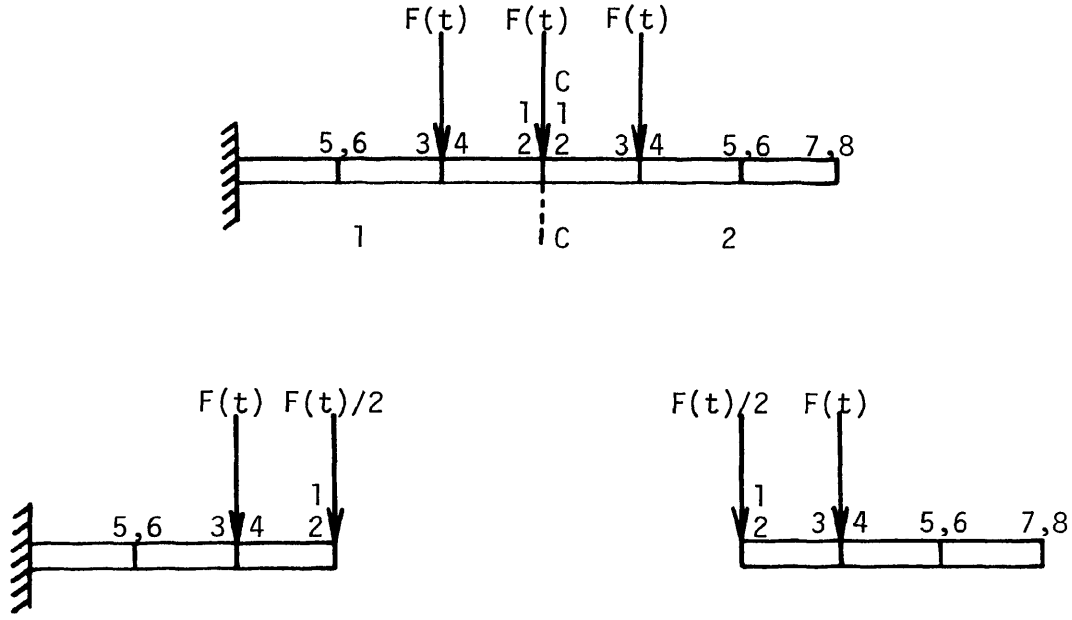

Substructure 1 Substructure 2

$$F(t) = F_0 \sin t/t_1, \quad 0 \leq t \leq \pi t_1$$

$$= 0 \qquad , \quad t \geq \pi t_1$$

Fig. 30. Cantilever Beam - Two Substructures and Applied Half-Sine Pulse

equations derived in section D of Chapter IV. Equation (209) yields displacements for $0 \leq t \leq \pi t_1$ while Eq. (210) gives system displacements for $t \geq \pi t_1$. The forcing function vectors for the two substructures are given by:

$$\{f(t)\}_1 = \begin{Bmatrix} F_0/2 \\ 0 \\ F_0 \\ 0 \\ 0 \\ 0 \end{Bmatrix} \sin(t/t_1), \text{ and} \qquad (232)$$

$$\{f(t)\}_2 = \begin{Bmatrix} F_0/2 \\ 0 \\ F_0 \\ 0 \\ 0 \\ 0 \\ 0 \\ 0 \end{Bmatrix} \sin(t/t_1). \qquad (233)$$

Thus, the product $[T]^T\{f(t)\}$ in Eqs. (209) and (210), for this numerical example, becomes:

$$[T]^T\{f(t)\} = \left([T]_1^T \begin{Bmatrix} F_0/2 \\ 0 \\ F_0 \\ 0 \\ 0 \\ 0 \end{Bmatrix} + [T]_2^T \begin{Bmatrix} F_0/2 \\ 0 \\ F_0 \\ 0 \\ 0 \\ 0 \\ 0 \\ 0 \end{Bmatrix} \right) \cdot \sin(t/t_1), \qquad (234)$$

where F_0 is assumed to be equal to unity and $[T]_1$ and $[T]_2$ are transformation matrices for the two substructures, respectively. Substituting Eq. (234) into Eqs. (209) and (210) and performing the integrations yields:

For $0 \leq t \leq \pi t_1$,

$$\{x(t)\} = F_0[T][\bar{q}][\omega_i]^{-1}\left[\frac{\omega_i \sin(t/t_1) - 1/t_1 \sin(\omega_i t)}{(\omega_i^2 - 1/t_1^2)}\right][\bar{q}]^T$$

$$\times \left([T]_1^T \begin{Bmatrix} F_0/2 \\ 0 \\ F_0 \\ 0 \\ 0 \\ 0 \end{Bmatrix} + [T]_2^T \begin{Bmatrix} F_0/2 \\ 0 \\ F_0 \\ 0 \\ 0 \\ 0 \\ 0 \\ 0 \end{Bmatrix} \right) \quad , \text{ and} \qquad (235)$$

for $t \geq \pi t_1$,

$$\{x(t)\} = F_0[T][\bar{q}][\omega_i]^{-1}\left[\frac{\sin(\omega_i t) + \sin \omega_i(t-\pi t_1)}{t_1(\omega_i^2 - 1/t_1^2)}\right][\bar{q}]^T$$

$$\times \left([T]_1^T \begin{Bmatrix} F_0/2 \\ 0 \\ F_0 \\ 0 \\ 0 \\ 0 \end{Bmatrix} + [T]_2^T \begin{Bmatrix} F_0/2 \\ 0 \\ F_0 \\ 0 \\ 0 \\ 0 \\ 0 \\ 0 \end{Bmatrix} \right) \quad . \qquad (236)$$

A displacement solution obtained through the direct approach for a general time-varying forcing function is derived in Appendix D. In Eq. (A.71) of Appendix D, the forcing vector for this example becomes:

$$\{f(t)\} = \begin{Bmatrix} 0 \\ 0 \\ F_0 \\ 0 \\ F_0 \\ 0 \\ F_0 \\ 0 \\ 0 \\ 0 \\ 0 \\ 0 \end{Bmatrix} \sin(t/t_1),\ 0 \le t \le \pi t_1 \qquad (237)$$

$$= 0 \qquad\qquad ,\ t \ge \pi t_1,$$

in which F_0 equals 1 and πt_1 is the half sine pulse duration time, which is assumed to be two seconds.

Performing the integration in Eq. (A.71) in Appendix D yields cantilever displacement solution, i.e., for $0 \le t \le \pi t_1$,

$$\{x(t)\} = F_0[\phi][\omega_i]^{-1} \left[\frac{\omega_i \sin(t/t_1) - 1/t_1 \sin(\omega_i t)}{(\omega_i^2 - 1/t_1^2)} \right] [\phi]^T$$

$$x\ [0\ 0\ 1\ 0\ 1\ 0\ 1\ 0\ 0\ 0\ 0\ 0]^T, \qquad (238)$$

and for $t \ge \pi t_1$,

$$\{x(t)\} = -F_0[\phi][\omega_i]^{-1} \left[\frac{\sin(\omega_i t) + \sin \omega_i(t-\pi t_1)}{t_1(\omega_i^2 - 1/t_1^2)} \right] [\phi]^T$$

$$\times [0\ 0\ 1\ 0\ 1\ 0\ 1\ 0\ 0\ 0\ 0\ 0]^T. \qquad (239)$$

A displacement solution, obtained by numerically computing Eqs. (235) and (236) with all substructure normal modes retained, is verified against the direct solution given by Eqs. (238) and (239). Transverse displacements of the free end of the cantilever beam are plotted as a function of time 't' for three different cases, the direct approach solution, the substructures method with no modal truncation and the substructures method with modal truncation. The size of the reduced problem, when modal truncation is used, is eight. The substructures method, with all substructure normal modes retained, and the direct method yield theoretically exact solutions for the assumed lumped parameter model of the cantilever beam. Figure 31 shows the transverse displacements of the free end of the cantilever beam when $0 \leq t \leq \pi t_1$. The two exact displacements are the same in the range of time 't' shown, and the approximate solution represents these displacements very accurately. Figure 32 shows the transverse displacements of the free end in the range $t \geq \pi t_1$. The two exact solutions in this range differ slightly. The total solution in this range of time may be regarded as an initial conditions solution with certain initial conditions imposed on the system at time $t = \pi t_1$. Since the initial conditions solution was not described too accurately through the substructures method as seen in section B, the slight difference in the

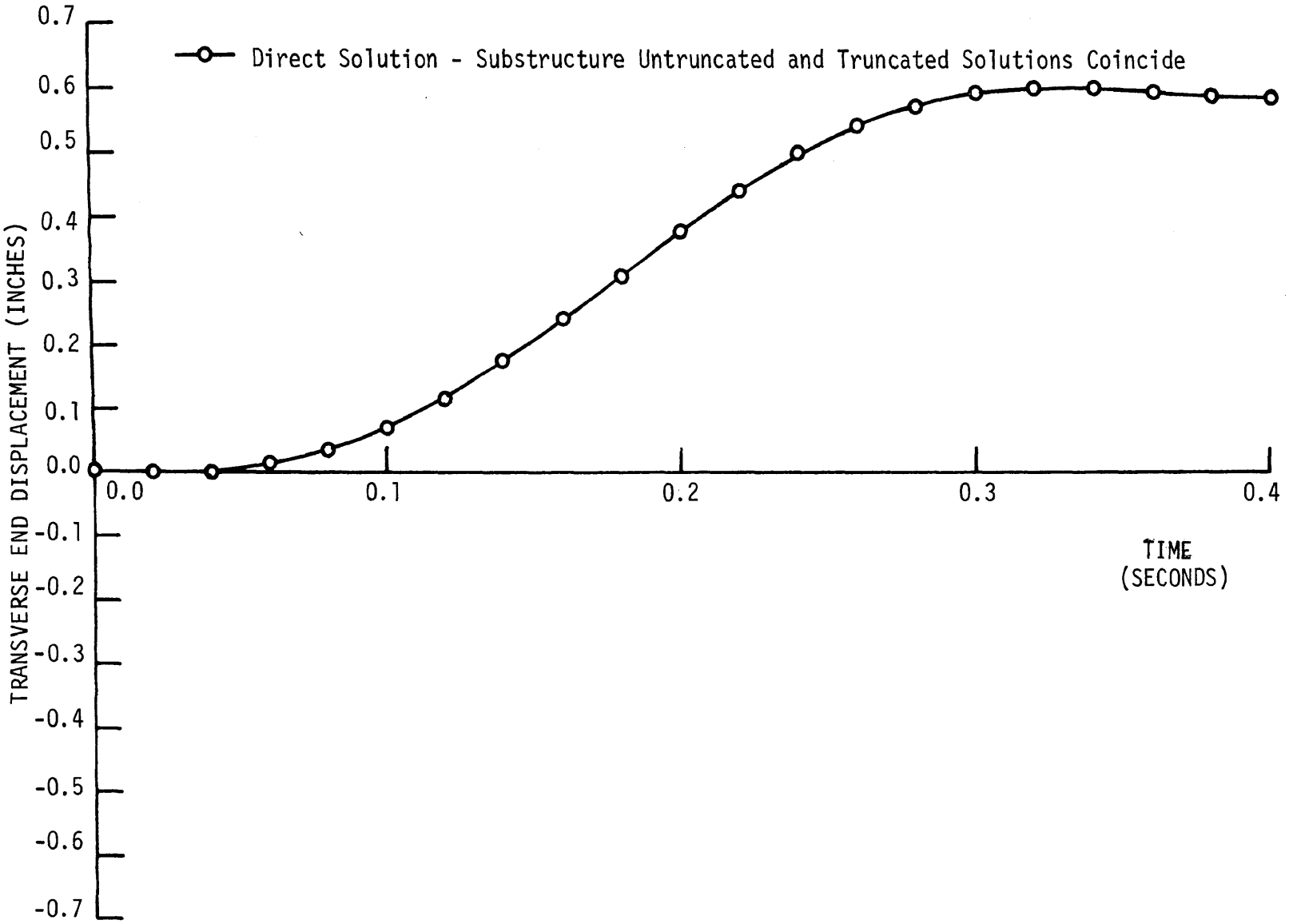

Fig. 31. Comparison of Direct and Substructure Solutions ($0 \leq t \leq \pi t_1$) via the Free End Transverse Displacement of a Cantilever Beam with Half-Sine Pulse Excitation

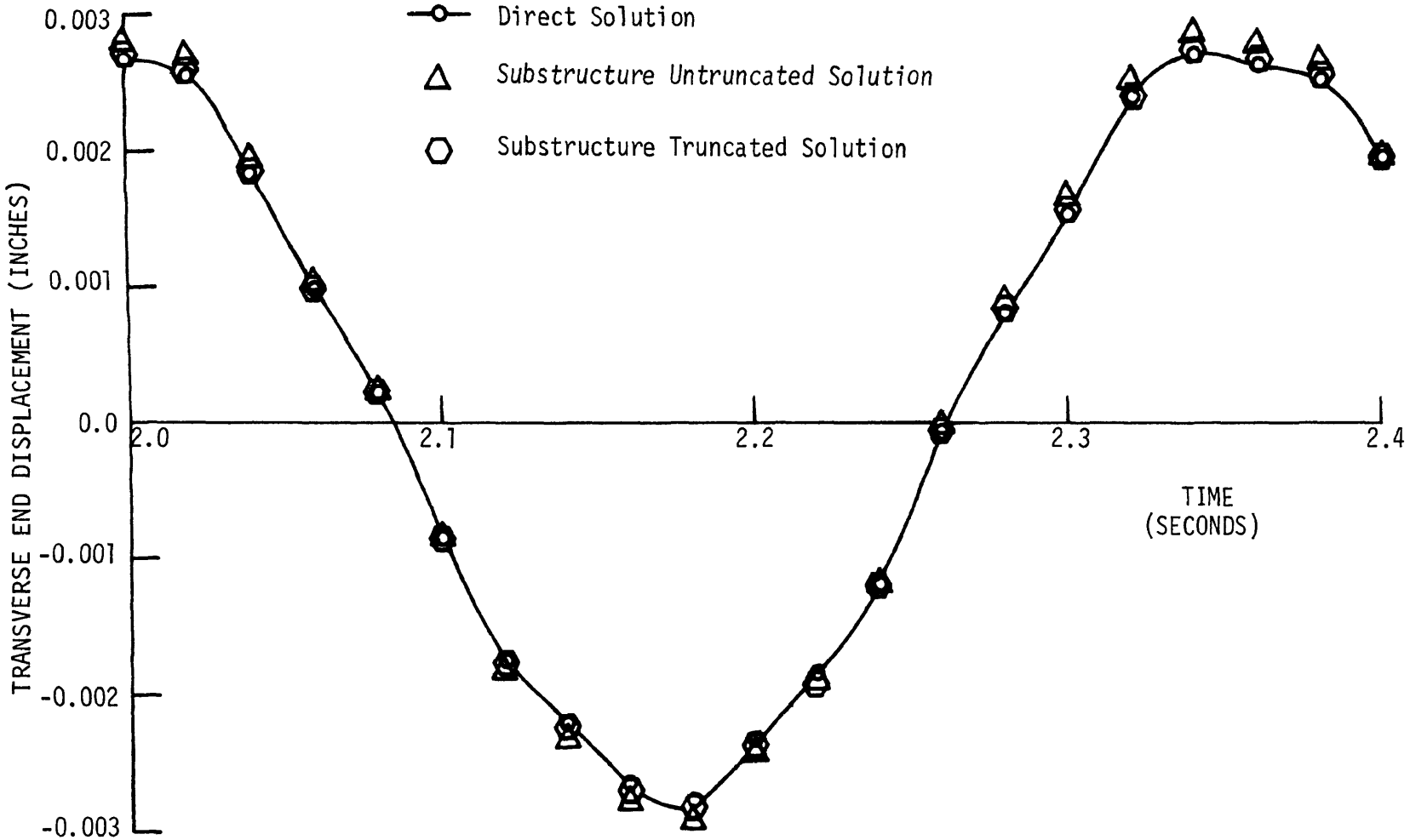

Fig. 32. Comparison of Direct and Substructure Solutions ($t \geq \pi t_1$) via the Free End Transverse Displacement of a Cantilever Beam with Half-Sine Pulse Excitation

two exact solutions of the half sine pulse excitation may be attributed to that. Again, the representation of these displacements by the approximate solution is accurate in the range $t \geq \pi t_1$.

Comparisons are also made on the basis of system strain energy. Three strain energy solutions as obtained by the direct approach, the substructures approach with no modal truncation and the substructures approach with modal truncation are plotted as a function of time 't' for both cases viz. $0 \leq t \leq \pi t_1$ and $t \geq \pi t_1$ in Figs. 33 and 34, respectively. The direct approach solution verifies the substructures approach solution with no modal truncation in the range $0 \leq t \leq \pi t_1$. In the same range of time, the approximate system strain energy solution gives a very accurate representation of the exact solution. However, the two exact solutions differ slightly in the range of time $t \geq \pi t_1$ and this, as explained earlier, may be due to the discrepancies noticed in the initial conditions solution. Approximate system strain energy obtained through modal truncation of substructure normal modes is fairly accurate in comparison to the exact solutions.

Having established the system behavior in Figs. 31 through 34 resulting from a half sine pulse type of excitation force, it can be seen that modal truncation through the substructures method yields satisfactory results.

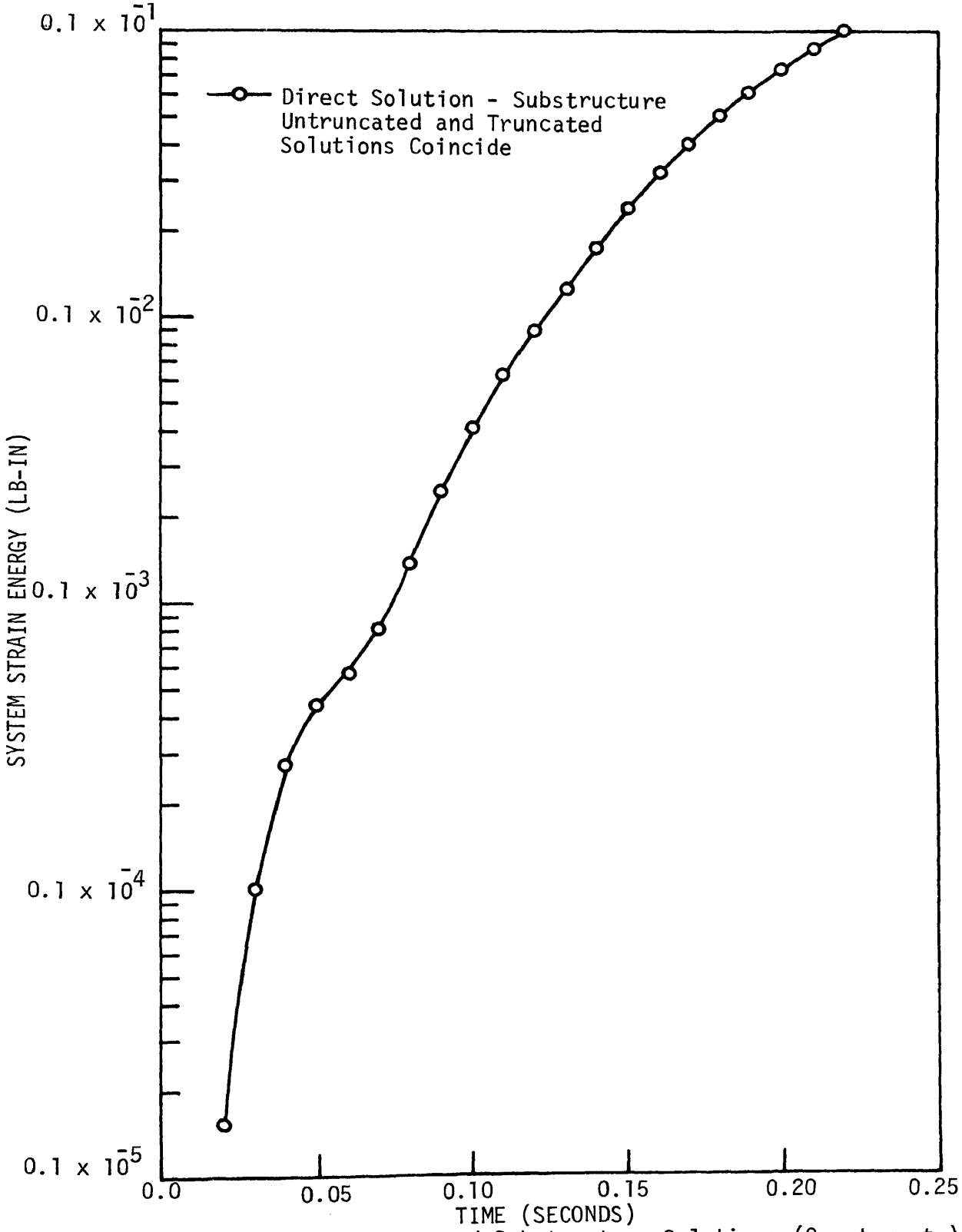

Fig. 33. Comparison of Direct and Substructure Solutions ($0 \leq t \leq \pi t_1$) via the System Strain Energy of a Cantilever Beam with Half-Sine Pulse Excitation

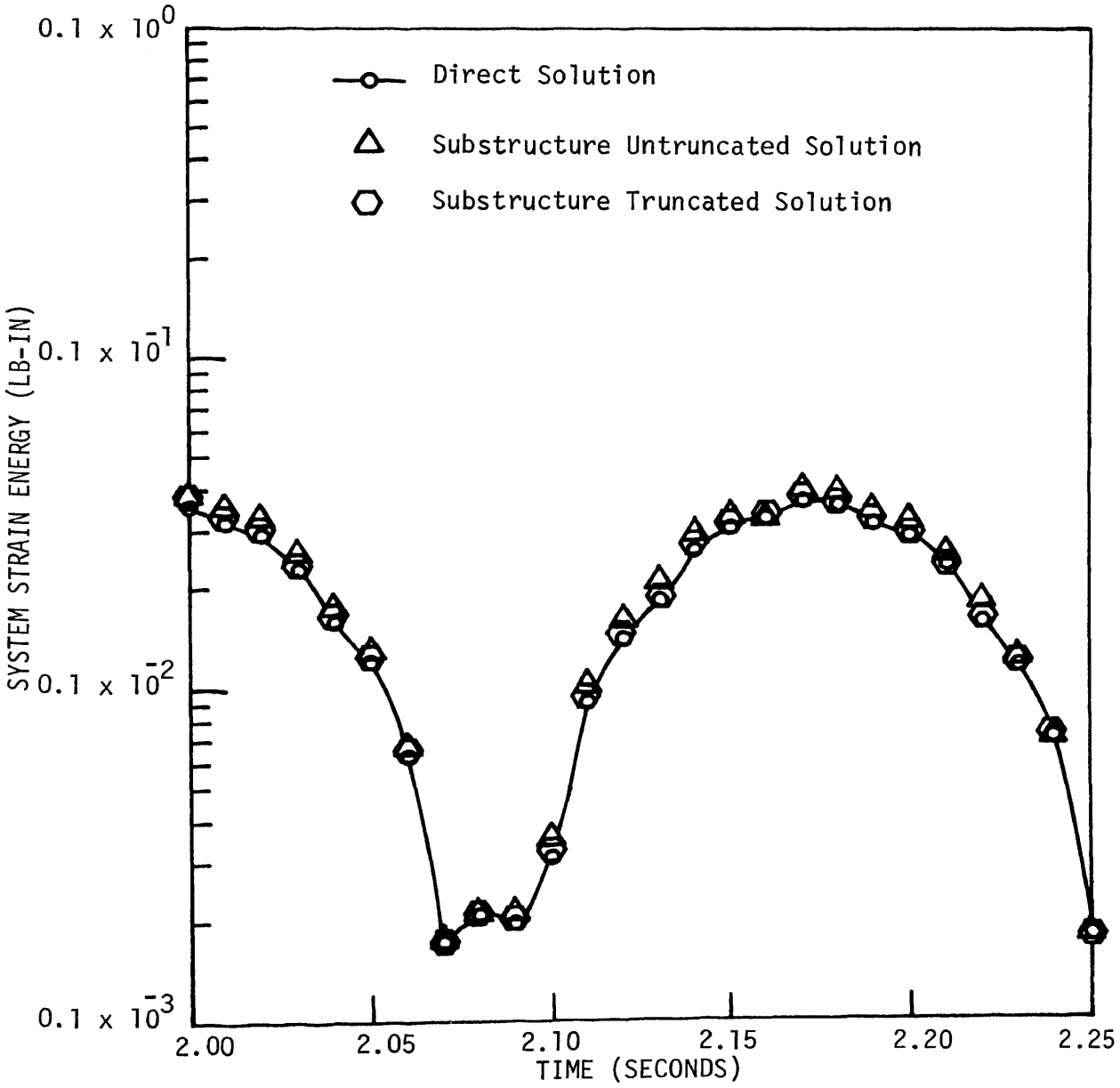

Fig. 34. Comparison of Direct and Substructure Solutions ($t \geq \pi t_1$) via the System Strain Energy of a Cantilever Beam with Half-Sine Pulse Excitation

CHAPTER VI

SUMMARY AND CONCLUSIONS

The objective of this study has been to clarify and give some unified treatment to the use of a substructures method for solving complex structural dynamics problems which include the common types of excitations encountered in practice. The approach has been applied to obtain system eigenvalues and eigenvectors and response solutions via the classical superposition of principal modes approach.

In Chapters II and III a systematic approach for the derivation of substructure modes was presented. A compatability matrix to ensure compatible displacements at substructure boundary connections was derived. Two criteria, based on substructure principal mode frequency roots and substructure normal mode strain energies, are presented for a judicious selection of which substructure principal modes or the approximate number to use, when truncation of normal modes is utilized to obtain a reduced size problem. A long thin cantilever beam divided into two substructures is used throughout for the numerical verification of solutions obtained. The size of the transformation matrix, [T], is varied when studying the two criteria of selection of substructure principal modes. A standard use of partitioned matrices and vectors is made throughout the work. System frequency roots and system strain energy in the principal modes and their error estimates from modal truncation are obtained for each size of matrix [T] considered. On the basis of this investigation several conclusions are drawn concerning free vibration solutions:

1. A systematic approach for a free undamped vibration solution of complex structures has been developed using partitioning of matrices to its fullest extent. This economizes on computer time and storage. A comparison of eigenvalue computer timings and multiplication and addition operations, required for initial conditions solutions, between the usual direct approach and the substructures method with modal truncation shows that the latter method is economical if too many substructure normal modes are not retained. Maximum economization of computer time is a result of the reduction of the size of the eigenvalue problem.

2. While the percent errors in system frequency roots, and in strain energy in the principal modes in the four lower system modes do converge, yet the mode of convergence is non-monotonic. The pattern of convergence for both types of erros, as the reduced number of equations was varied from 3 to 9, is similar. However, the errors based on substructure normal mode strain energy converge in a slightly different manner (Figs. 2-9) than those based on substructure frequency roots criterion. The former has two almost flat steps while the latter has only one in the range of the number of equations considered.

3. The magnitude of errors in system strain energy in the four lower modes is usually higher than that of errors in system frequency roots, when the number of equations solved is small. However, the two errors close in as the number of

equations solved is increased from 3 to 9. This behavior is observed in the two errors obtained through both types of substructure modes selection criteria.

4. In the higher system modes when the number of equations solved is large, substructure normal mode strain energy criterion for modal truncation yields lower errors in system frequency roots, compared to the criterion which uses substructure frequency roots. A similar characteristic is noticed for errors in system strain energy.

5. In the lower three modes plotted for each criteria of retaining substructure normal modes, convergence of error indicators $\overline{\delta\lambda}$ and $\overline{\delta P}$ is non-monotonic. The patterns of convergence are found to be similar to those of percent errors in system frequency roots and system strain energy in the principal modes, respectively.

6. Estimation of $\delta\lambda$ by $\overline{\delta\lambda}$ and that of δP by $\overline{\delta P}$ improves considerably in the higher system modes. Estimation of δP by $\overline{\delta P}$ is much better in comparison to that of $\delta\lambda$ by $\overline{\delta\lambda}$ in all three modes considered. This suggests that system strain energy may provide a better measure of system response, since errors in system strain energy due to the omission of certain substructure normal modes are better approximated in comparison to estimates of errors in system eigenvalues.

7. It is found from the data collected with the cantilever

beam example that system frequency roots, below the largest substructure normal mode frequency root of the substructure from which the maximum number of modes are retained, are well within the engineering accuracy. If there are two or more substructures with an equal but maximum number of modes retained, the smallest of the largest frequency roots from these substructures appears to provide an upper limit for system frequency roots to be within engineering accuracy

8. It is noted that a particular system mode may be completely omitted in the final solution when modal truncation is allowed. This may be caused by omission of certain substructure normal modes which dominate the missing system mode. This omission of system modes occurs for system frequency roots greater than the largest system frequency root, expected to be well within engineering accuracy through paragraph 7.

9. In the initial conditions solution, the free end transverse displacement of the cantilever beam and the total system strain energy are described accurately by the approximate solution obtained through modal truncation. However, modal truncation in the case of severe initial conditions, has been found to be sensitive to the type of initial conditions applied. Thus further study of the method proposed for retaining substructure modes is warranted.

In Chapter IV results for displacement response of systems under forced excitation are obtained. These solutions depend directly upon the results of the homogeneous solution in the work developed herein

as the method of superposition of principal modes has been used to uncouple the governing differential equations.

Examples which feature a cantilever beam as the structure and divided into two substructures are presented in Chapter V for the verification and evaluation of solutions discussed in Chapter IV. Comparisons of systems displacements and system strain energy are shown for general time-varying displacement excitation, harmonic force excitation, base acceleration excitation and general time varying force excitation. Based on these investigations the following conclusions are drawn:

1. Displacement and system strain energy solutions obtained through the substructures method with no modal truncation are verified by the corresponding solutions obtained through the classical direct approach in which superposition of principal modes yields the uncoupled equations of motion and complete structure matrices are used directly. Both analyses are thus inherently theoretically exact for the assumed lumped mass model of the cantilever beam.

2. Transverse displacements at the mid-section of the cantilever beam for the forced displacement solution and harmonic excitations treated are very accurately described by the approximate solution obtained through modal truncation. In the case of constant base acceleration and half sine pulse type of excitations, free end transverse displacements plotted for comparisons are represented almost exactly by the approximate

solution. In all cases treated, the final size of the reduced problem was about two thirds that of the original.

3. System strain energy solutions in the case of constant base acceleration and half sine pulse type of excitations are well approximated, within the engineering accuracy limit, by solutions using modal truncation. However, the approximate representations for strain energy, in the case of forced displacements and harmonic excitations, are poor. Again, the final size of the reduced problem was about two thirds that of the original.

4. From the comparison of results it is seen that the dynamic substructures method provides a rational procedure for reducing the number of equations to diminish the size of matrices treated in the computer analysis of structures, since some of the higher order substructure normal modes, which contribute little to the final solution for low frequency excitations and step excitations considered in this study, are eliminated.

The work presented herein has by no means completed the study on using a substructures method for complex structural dynamics analyses. The size of problems which have been investigated numerically for solution verification and comparisons has been kept small to allow for treatment of all the cases considered with reasonable scope and computer time cost.

The criteria presented for selection of substructure principal

modes need checking under larger analyses and need extension for generalization into some rule or guide line. The solutions have been verified, but modal truncation will also need further investigation.

CHAPTER VII
BIBLIOGRAPHY

1. Hunn, B. A., "A Method of Calculating the Space Free Resonant Modes of an Aircraft," Journal of Royal Aeronautical Society, Vol. 57, June, 1953, pp. 420-422.

2. Hunn, B. A., "A Method of Calculating the Normal Modes of an Aircraft," Quart. Journal of Mechanics, Vol. 8, Pt. 1, 1955, pp.38-58.

3. Turner, M. J., Martin, H. C., and Weikel, R. C., "Further Development and Applications of the Stiffness Method," Matrix Methods of Structural Analysis, edited by F. de Veubeke (Perganon Press, London, 1964).

4. Argyris, J. H., and Kelsey, S., "Modern Fuselage Analysis and the Elastic Aircraft," (Butterworths Scientific Publications, Ltd., London, 1963).

5. Gladwell, G. M. L., "Branch-Mode Analysis of Vibrating Systems," Journal of Sound and Vibration, vol. 1, pp. 41-59, 1964.

6. Przemieniecki, J. S., "Matrix Structural Analysis of Substructures," AIAA Journal, vol. 1, No. 1, Jan. 1963, pp. 138-147.

7. Hurty, W. C., " Dynamic Analysis of Structural Systems Using Component Modes," AIAA Journal, vol. 3, No. 4, April 1965, pp. 678-685.

8. Hurty, W. C., "Dynamic Analysis of Structural Systems by Component Mode Synthesis," Technical Report 32-530, 1964, Jet Propulsion Lab., Pasadena, Calif., Jan. 15, 1964.

9. Craig, R. R., and Bampton, M.C.C.," Coupling of Substructures for Dynamic Analyses," AIAA Journal, Vol. 6, No. 7, July 1968, pp. 1313-1319.

10. Hurty, W. C., "A Criterion for Selecting Realistic Natural Modes of a Structure," Technical Memorandum 33-364, Jet Propulsion Lab., Pasadena, Calif., Nov. 1, 1967.

11. Bajan, R. L., and Feng, C. C., "Free Vibration Aanlysis by the Modal Substitution Method," AAS Symposium, Space Projections from the Rocky Mountain Region, Denver, Colorado, July 1968.

12. Bajan, R. L., Feng, C. C., and Jaszlics, I. J., "Vibration Analysis of Complex Structural Systems by Modal Substitution," Shock and Vibration Bulletin, No. 39, pt. 3, Jan. 1969.

13. Collins, J. D., and Thompson, W. T., "The Eigenvalue Problem for Structural Systems with Statistical Properties," AIAA Journal, Vol. 7 No. 4, April, 1969.

14. Hasselman, T. K., and Hart, G. C., "Solution of the Structural Dynamics Eigenproblem by Modal Synthesis: Sensitivity to Coordinate Selection and Parameter Variation," (Ph.D. Dessertation), Mechanics and Structures Dept., University of California, Los Angeles, UCLA-ENG-7239, June 1972.

15. Pakstys, M. Jr., "Dynamic Substructures Method for Shock Analysis," General Dynamics, Electric Boat Division, Groton, Connecticut.

16. Saczalski, K. J., and Huang, T. C., "Elastodynamics of Complex Structural System" Developments in Mechanics, Vol. 6, Proceedings of the 12th Midwestern Mechanics Conference, pp 675-688.

17. Bishop, R. E. D., Gladwell, G. M. L., and Michaelson, S., "The Matrix Analysis of Vibration," (Cambridge University Press, England, 1965).

18. Zienkiewicz, O. C., "The Finite Element Method in Structural and Continuum Mechanics," (McGraw-Hill, London, 1967).

19. Willems, N., and Lucar, W. M. Jr., "Matrix Analysis for Structural Engineers," (Prentice-Hall Inc./Englewood Cliffs, N.J., 1968), pp. 184-196.

20. Gallagher, R. H., "A Correlation Study of Methods of Matrix Structural Analysis," (Pergamon Press, London, 1964).

21. Pestel, E. C., and Leckie, F. A., "Matrix Methods in Elastomechanics," (McGraw Hill Book Company, Inc., New York, 1963).

22. Anderson, R. A., "Fundamentals of Vibration," (The Macmillan Company, New York, 1967).

23. Thompson, W. T., "Vibration Theory and Applications," (Prentice-Hall Inc., N. J., 1965).

24. Chen, Y., "Vibrations: Theoretical Methods," (Addison-Wesley Publishing Company, Inc., Reading, Massachusetts, 1966 .

25. Tolani, S. K. and Rocke, R. D., "A Strain Energy Comparison of Discrete Modeling for Vibrating Continuous Systems," Transactions of the ASME, Journal of Engineering for Industry, Vol. 94, Series B, No. 1, Paper No. 71-Vibr-5, Feb. 1972, pp. 23-30.

26. Turner, M. J., Clough, R. W. Martin, H. C., and Topp, L. J., "Stiffness and Deflection Analysis of Complex Structures," Journal of Aeronautical Sciences, Vol. 23, No. 9, Sept. 1956.

27. Guyan, R. J., "Reduction of Stiffness and Mass Matrices," AIAA Journal, Vol. 3, No. 2, Feb. 1965, pp. 380.

28. Kaufman, S., and Hall, D. B., "Reduction of Mass and Loading Matrices," AIAA Journal, Vol. 6, No. 3, March 1968, pp. 550-551.

29. Fox, R. L., and Stanton, E. L., "Developments in Structural Analysis by Direct Energy Minimization.", AIAA Journal, Vol. 6, No. 6, June 1968, pp. 1036-1042.

30. Zarghamee, M. S., "Optimum Frequency of Structures," AIAA Journal, Vol. 6, No. 4, April 1968, pp. 749-750.

31. Ramsden, J. N., and Stoker, J. R., "Mass Condensation: A Semi-Automatic Method for Reducing the Size of Vibration Problems," International Journal for Numerical Methods in Engineering, Vol. 1, No. 4, October-December 1969, pp. 333-349.

32. Ojalvo, I. U., and Newman, M., "Vibration Modes of Large Structures by an Automatic Matrix-Reduction Method," AIAA Journal, Vol. 8, No. 7 July 1970, pp. 1234-1239.

CHAPTER VIII
VITA

Suresh Kumar Tolani was born on January 15, 1946 in Calcutta, India. He received his primary and secondary education in New Delhi, India. He received a Bachelor of Engineering degree in Mechanical Engineering from Sardar Patel University in Anand, India, and a Master of Science degree in Mechanical Engineering from the University of Missouri-Rolla in Rolla, Missouri, in January 1970.

He has been enrolled in the Graduate School of the University of Missouri-Rolla since September 1968 and has held an N.S.F. Scholarship during the period June 1969 to August 1970 and several teaching assistantships during other periods.

CHAPTER IX
APPENDIX A
STRUCTURES PROGRAM FLOW CHART

A flow chart of the computer program used with the IBM-360-50 computer for generating substructure mass and stiffness matrices, the transformation matrix, $[T]_i$, and system eigenvalues and eigenvectors by the method of substructures as discussed in Chapters II and III is presented in this appendix. In this program, Fortran language was used throughout and no special routines were needed.

Information obtained from this computer program was used to compute estimates to errors in system eigenvalues and system strain energy in the principal modes due to a partial retaining of substructure normal modes. Further, system eigenvalues and eigenvectors and other pertinent information generated were used to obtain solutions to the initial conditions problem and for systems under forced excitations.

Structures Program

Flow Chart

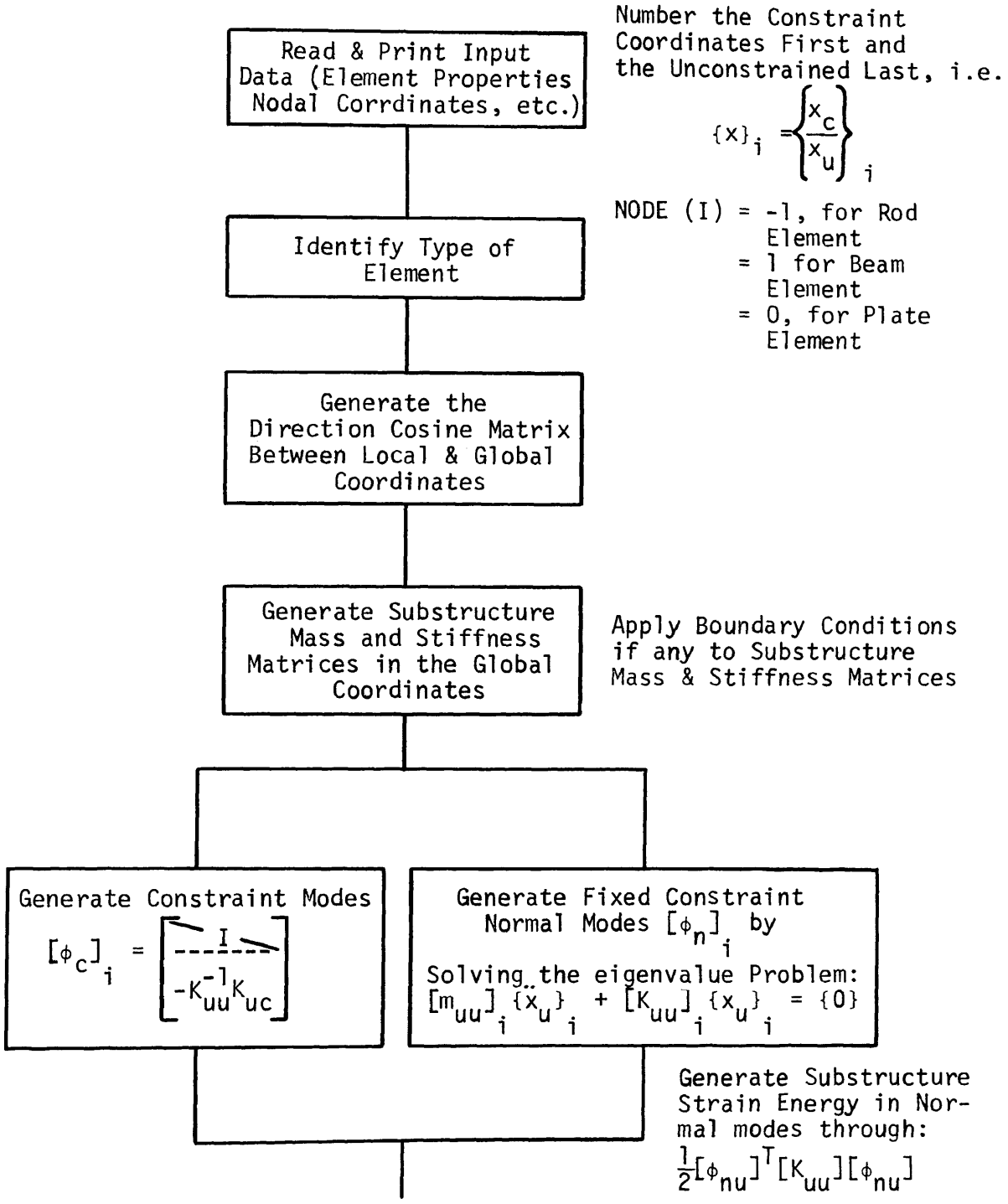

(continued)

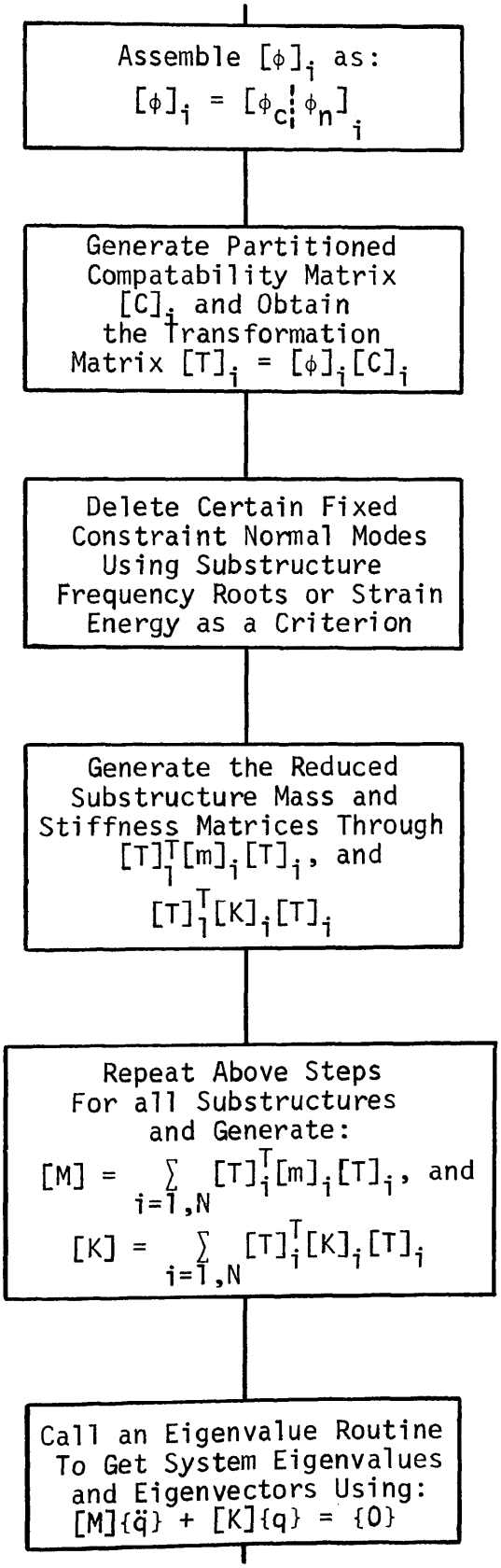
Assemble $[\phi]_i$ as:
$[\phi]_i = [\phi_{c_i} \vdots \phi_n]_i$
Generate Partitioned Compatability Matrix $[C]_i$ and Obtain the Transformation Matrix $[T]_i = [\phi]_i[C]_i$
Delete Certain Fixed Constraint Normal Modes Using Substructure Frequency Roots or Strain Energy as a Criterion
Generate the Reduced Substructure Mass and Stiffness Matrices Through $[T]_1^T[m]_i[T]_i$, and $[T]_1^T[K]_i[T]_i$
Repeat Above Steps For all Substructures and Generate:
$[M] = \sum_{i=1,N} [T]_i^T[m]_i[T]_i$, and
$[K] = \sum_{i=1,N} [T]_i^T[K]_i[T]_i$
Call an Eigenvalue Routine To Get System Eigenvalues and Eigenvectors Using:
$[M]\{\ddot{q}\} + [K]\{q\} = \{0\}$

(continued)

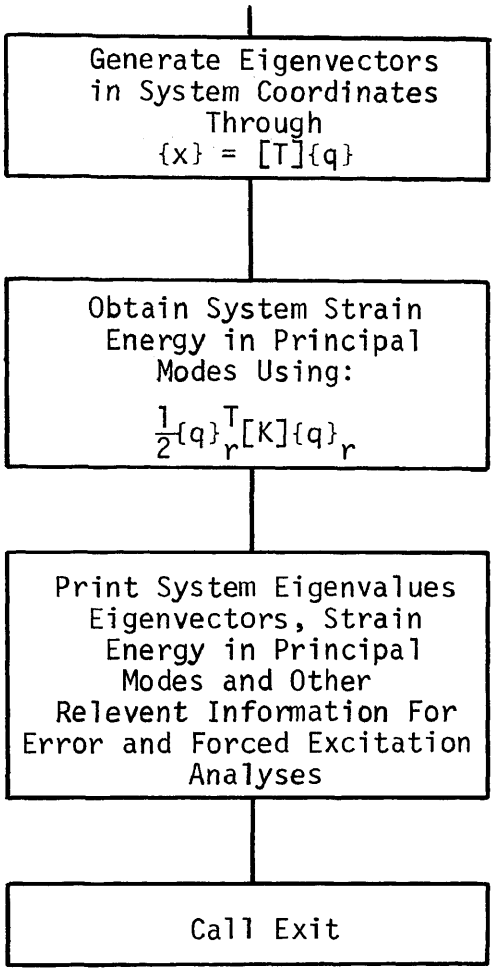
Generate Eigenvectors in System Coordinates Through {x} = [T]{q}
Obtain System Strain Energy in Principal Modes Using: $\frac{1}{2}\{q\}_r^T[K]\{q\}_r$
Print System Eigenvalues Eigenvectors, Strain Energy in Principal Modes and Other Relevent Information For Error and Forced Excitation Analyses
Call Exit

CHAPTER X

APPENDIX B

FINITE ELEMENTS

Three types of finite elements, the most common components of aerospace structures, were used in the computer program developed for this study. These finite elements are discussed briefly in the following paragraphs and their mass and stiffness matrices are given in local element coordinates. The elements used are:

(i) One-Dimensional Rod Element

(ii) Beam Element

(iii) Plate Element.

Before assembling substructure matrices, element matrices are transformed into a common set of substructure global coordinates. For simplicity, modeling of structure inertial forces is done by lumping mass at discrete points resulting in diagonal element mass matrices.

A. One-Dimensional Rod Element

The one-dimensional rod element represents those parts of a structure in which the displacement is unidirectional and along the element's longitudinal axis, e.g., longitudinal vibrations of a rod, a bar element in a stringer, shear panel type structure. Such a finite element is shown with its local coordinates (x'y'z') in Fig. 35. The stiffness matrix for this type of finite element (18) in coordinates x'y'z' is given by:

$$[k'] = \frac{AE}{\ell} \begin{bmatrix} 1 & -1 \\ & \\ 1 & 1 \end{bmatrix} , \qquad (A.1)$$

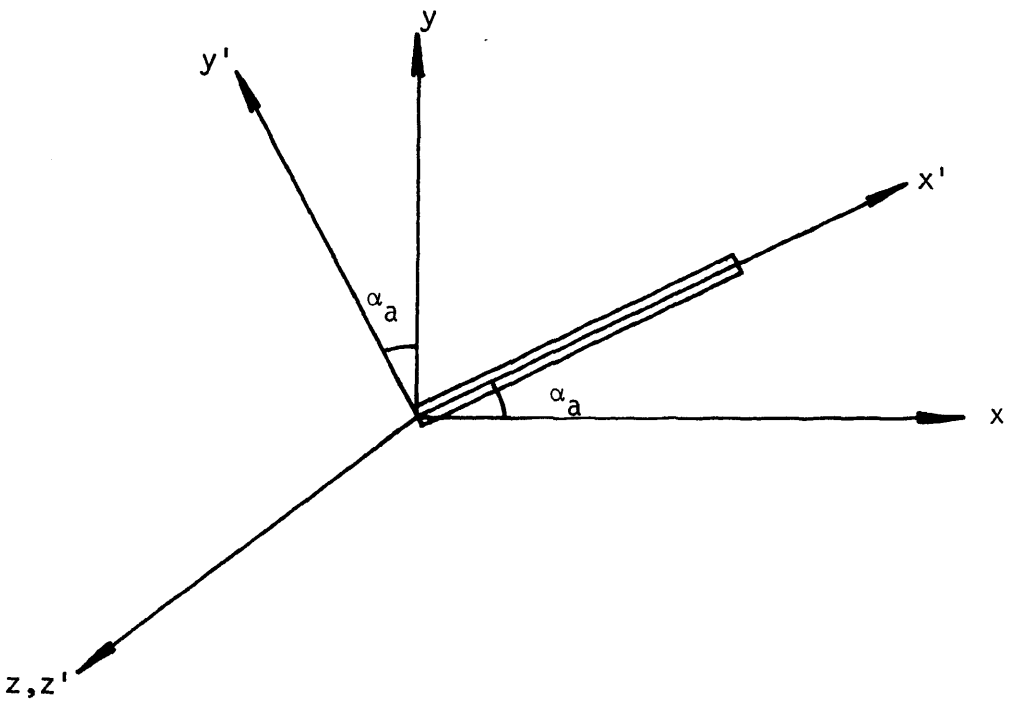

Fig. 35. One-Dimensional Rod Element

in which,

A = Area of cross section of the rod

E = Modulus of elasticity of the material of the rod

ℓ = length of the element.

The lumped mass matrix for the one-dimensional rod element is given by:

$$[\lceil m' \rfloor] = \frac{\rho \ell}{2} \begin{bmatrix} 1 & 0 \\ 0 & 1 \end{bmatrix} , \qquad (A.2)$$

where ρ is the mass density per unit length of the material of the rod.

The transformation of above element matrices into substructure global coordinates can be obtained through the following relations:

$$[k] = [R]^T[k'][R], \text{ and} \qquad (A.3)$$

$$[m] = [R]^T[\lceil m' \rfloor][R], \qquad (A.4)$$

where matrix [R] is the rotation matrix and when considering six degrees of freedom at nodes 1 and 2 of the rod element, it becomes:

$$[R] = \begin{bmatrix} D & 0 & 0 & 0 \\ 0 & D & 0 & 0 \\ 0 & 0 & D & 0 \\ 0 & 0 & 0 & D \end{bmatrix} , \qquad (A.5)$$

in which matrix [D] contains the direction cosines of the element coordinates defined from local axes to global axes.

Since moments are not considered in the one-dimensional rod elements, the transformation matrix [R] reduces to:

$$[R] = \begin{bmatrix} D & 0 \\ 0 & D \end{bmatrix} .$$

The stiffness and mass matrices of Eqs. (A.1) and (A.2) are expanded to the size of matrix [R] by filling them with zeros at coordinates not considered for the element. If the unit vectors in the local coordinates (x'y'z') are represented by e'_x, e'_y and e'_z and those in the global system by e_x, e_y and e_z, the matrix of direction cosines, [D], for the in plane rotation can be formed, see Fig. 35, as follows:

$$\{e'\} = [D]\{e\}, \text{ or}$$

$$\begin{Bmatrix} e'_x \\ e'_y \\ e'_z \end{Bmatrix} = \begin{bmatrix} \cos \alpha_a & \sin \alpha_a & 0 \\ -\sin \alpha_a & \cos \alpha_a & 0 \\ 0 & 0 & 1 \end{bmatrix} \begin{Bmatrix} e_x \\ e_y \\ e_z \end{Bmatrix} , \qquad (A.6)$$

where α_a is the angle of rotation.

B. Beam Element

Figure 36 shows a typical Bernoulii-Euler beam finite element (19) with its local coordinates at nodes 1 and 2. Six degrees of freedom are considered at each node of such elements. The stiffness matrix in local coordinates when the effects of shear are neglected is given by:

$$[k'] = \left[\begin{array}{c|c} k'_{11} & k'_{12} \\ \hline k'_{21} & k'_{22} \end{array}\right] , \qquad (A.7)$$

in which

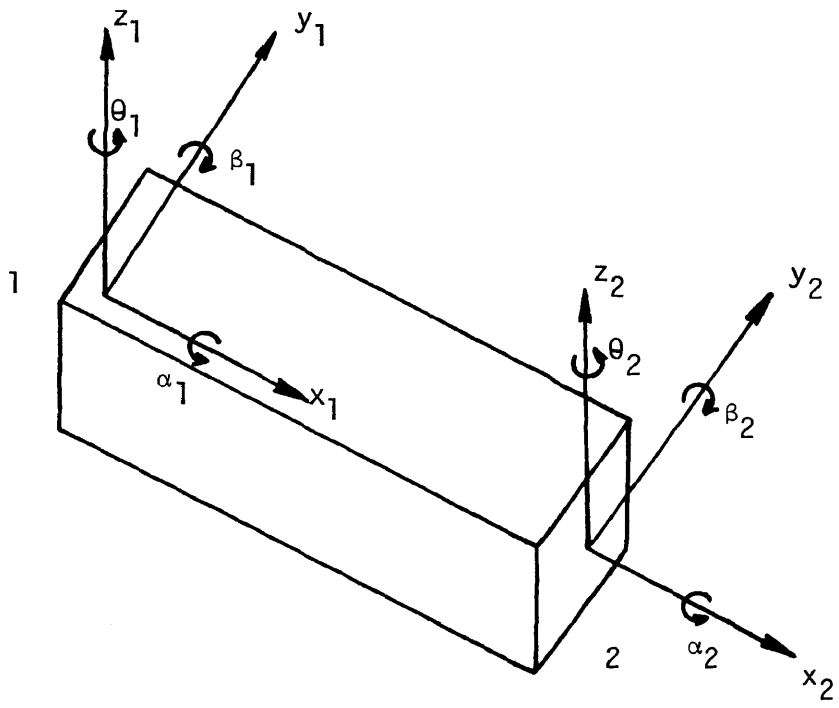

Fig. 36. Finite Beam Element with Local Coordinates

$$[k'_{11}] = \begin{bmatrix} AE/\ell & 0 & 0 & 0 & 0 & 0 \\ & \frac{12EI_{zz}}{\ell^3} & 0 & 0 & 0 & \frac{6EI_{zz}}{\ell^2} \\ & & \frac{12EI_{yy}}{\ell^3} & 0 & \frac{-6EI_{yy}}{\ell^2} & 0 \\ & & & \frac{GI_p}{\ell} & 0 & 0 \\ & \text{Symmetric} & & & \frac{4EI_{yy}}{\ell} & 0 \\ & & & & & \frac{4EI_{zz}}{\ell} \end{bmatrix} \quad (A.8)$$

$$[k'_{12}] = \begin{bmatrix} -AE/\ell & 0 & 0 & 0 & 0 & 0 \\ 0 & \frac{-12EI_{zz}}{\ell^3} & 0 & 0 & 0 & \frac{6EI_{zz}}{\ell^2} \\ 0 & 0 & \frac{-12EI_{yy}}{\ell^3} & 0 & \frac{-6EI_{yy}}{\ell^2} & 0 \\ 0 & 0 & 0 & \frac{-GI_p}{\ell} & 0 & 0 \\ 0 & 0 & \frac{6EI_{yy}}{\ell^2} & 0 & \frac{2EI_{yy}}{\ell} & 0 \\ 0 & \frac{-6EI_{zz}}{\ell^2} & 0 & 0 & 0 & \frac{2EI_{zz}}{\ell} \end{bmatrix} \quad (A.9)$$

$$[k'_{21}] = [k'_{12}]^T, \text{ and} \quad (A.10)$$

$$[k'_{22}]= \begin{bmatrix} AE/\ell & 0 & 0 & 0 & 0 & 0 \\ & \frac{12EI_{zz}}{\ell^3} & 0 & 0 & 0 & \frac{-6EI_{zz}}{\ell^2} \\ & & \frac{12EI_{yy}}{\ell^3} & 0 & \frac{6EI_{yy}}{\ell^2} & 0 \\ & & & \frac{GI_p}{\ell} & 0 & 0 \\ & & \text{Symmetric} & & \frac{4EI_{yy}}{\ell} & 0 \\ & & & & & \frac{4EI_{zz}}{\ell} \end{bmatrix} \quad \text{(A.11)}$$

where:

I_p = second moment of area of the beam cross section about its longitudinal axis

I_{yy} = Second moment of area of the beam cross section about y' axis

I_{zz} = Second moment of area of the beam cross section about its z' axis

A = Area of cross section of the beam

ℓ = Element length

E = Modulus of Elasticity

G = Modulus of Rigidity

The lumped mass matrix is obtained by lumping half of the total element mass and other inertial properties on each end of a massless elastic beam. The element mass matrix in local coordinates becomes:

$$[m'] = \text{Diagonal } \frac{1}{2} [\rho\ell\ J_x\ \rho\ell\ J_y\ \rho\ell\ J_z\ \rho\ell\ J_x\ \rho\ell\ J_y\ \rho\ell\ J_z], \tag{A.12}$$

where:

ρ = Mass density per unit length of the material of the beam

J_x = Mass moment of inertia of the beam element about x' axis

J_y = Mass moment of inertia about y' axis

J_z = Mass moment of inertia about z' axis.

Matrices in Eqs. (A.7) and (A.12) can be transformed into global coordinates through the relations:

$$[k] = [R]^T[k'][R], \text{ and} \tag{A.13}$$

$$[m] = [R]^T[m'][R], \tag{A.14}$$

where rotation matrix [R] is given by Eq. (A.5) for six degrees of freedom.

C. Swept Plate Element (in-plane forces)

Figure 37 shows a plate finite element (20) in plane stress with its local coordinates and corner nodes 1 through 4. Such an element is used to idealize skin members in a structure. Two degrees of freedom in the plane of the plate are considered at each node. The thickness of the element is assumed to be constant. The stiffness matrix in local coordinates for such an element, assuming linear edge displacements, is given by:

$$[k'] = \left[\begin{array}{c|c} k'_{11} & k'_{12} \\ \hline k'_{21} & k'_{22} \end{array}\right] , \tag{A.15}$$

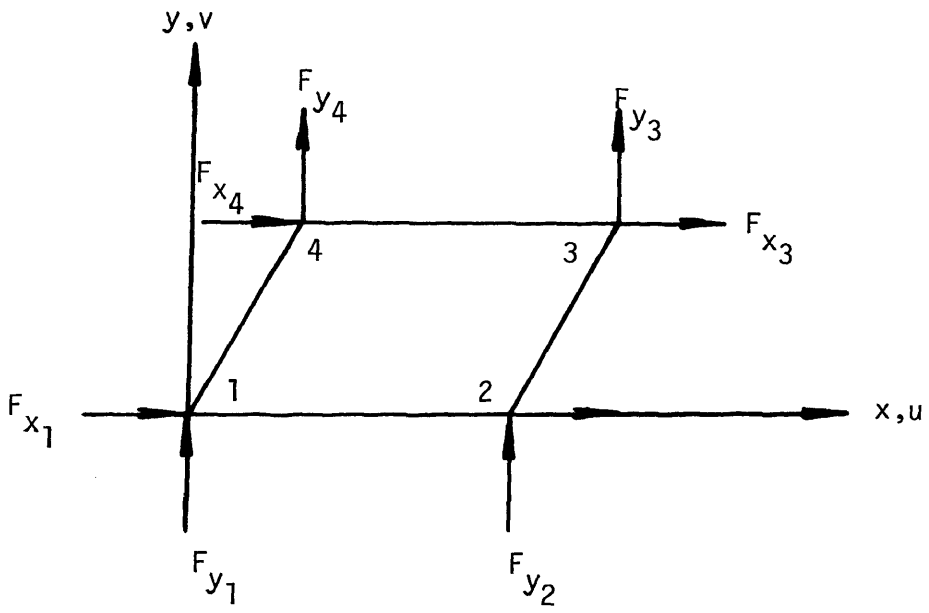

Fig. 37. Swept Plate Finite Element

where:

$$[k'_{11}]=\begin{bmatrix} \left(\frac{E'\psi}{3}+\frac{G'\alpha\beta_1}{3}\right) & (\mu E'+G')\frac{\beta_2}{4} & \left(-\frac{E'\psi}{3}+\frac{G'\alpha\beta_3}{6}\right) & \left(\frac{\mu E'\beta_4}{4}-\frac{G'\beta_2}{4}\right) \\ & \left(\frac{E'\alpha\beta_1}{3}+\frac{G'\psi}{3}\right) & \left(-\frac{\mu E'\beta_2}{4}+\frac{G'\beta_4}{4}\right) & \left(\frac{E'\alpha\beta_3}{6}-\frac{G'\psi}{3}\right) \\ & \text{Symmetric} & \left(\frac{E'\psi}{3}+\frac{G'\alpha\beta_5}{3}\right) & -(\mu E'+G')\frac{\beta_4}{4} \\ & & & \left(\frac{E'\alpha\beta_5}{3}+\frac{G'\psi}{3}\right) \end{bmatrix} \tag{A.16}$$

$$[k'_{21}]=\begin{bmatrix} -\left(\frac{E'\psi}{6}+\frac{E'\alpha\beta_6}{6}\right) & -(\mu E'+G')\frac{\beta_7}{4} & \left(\frac{E'\psi}{6}-\frac{G'\alpha\beta_8}{3}\right) & \left(-\frac{\mu E'\beta_9}{4}+\frac{G'\beta_7}{4}\right) \\ & -\left(\frac{E'\alpha\beta_6}{6}+\frac{G'\psi}{6}\right) & \left(\frac{\mu E'\beta_7}{4}-\frac{G'\beta_9}{4}\right) & \left(-\frac{E'\alpha\beta_8}{3}+\frac{G'\psi}{6}\right) \\ & \text{Symmetric} & -\left(\frac{E'\psi}{6}+\frac{G'\alpha\beta_{10}}{6}\right) & (\mu E'+G')\frac{\beta_9}{4} \\ & & & -\left(\frac{E'\alpha\beta_{10}}{6}+\frac{G'\psi}{6}\right) \end{bmatrix} \tag{A.17}$$

$$[k'_{12}] = [k'_{21}]^T, \text{ and} \tag{A.18}$$

$$[k'_{22}] = [k'_{11}],$$

in which:

$$\alpha = \frac{x_2}{y_3}$$

$$\beta = \frac{x_4}{x_2}$$

$$\psi = \frac{y_3}{x_2}$$

$$E' = \frac{Et}{(1-\mu^2)}$$

$$G' = G.t$$

$$\beta_1 = (1-1.5\beta + \beta^2)$$

$$\beta_2 = (1 - 4\beta/3)$$

$$\beta_3 = (1 - 2\beta^2)$$

$$\beta_4 = (1 + 4\beta/3)$$

$$\beta_5 = (1 + 1.5\beta + \beta^2)$$

$$\beta_6 = (1 - 3\beta + \beta^2)$$

$$\beta_7 = (1 - 2\beta/3)$$

$$\beta_8 = (1 - \beta^2/2)$$

$$\beta_9 = (1 + 2\beta/3)$$

$$\beta_{10} = (1 + 3\beta + \beta^2) \text{ , and}$$

(x_1,y_1), (x_2,y_2), (x_3,y_3) and (x_4,y_4) represent the coordinate locations of the four corner nodes of the element in substructure global coordinates.

A fourth of the total element mass is lumped at the four corner nodes of the massless elastic plate element. The mass matrix of the element in Fig. 36 is given by:

$$[m'] = \text{Diagonal } \frac{W}{4g} [\,1\ 1\ 1\ 1\ 1\ 1\ 1\ 1], \qquad \text{(A.20)}$$

where:

W = weight of the plate element

g = Acceleration due to gravity.

Element stiffness and mass matrices in substructure global coordinates are obtained from:

$$[k] = [R]^T[k'][R], \text{ and} \tag{A.21}$$

$$[m] = [R]^T[m'][R], \tag{A.22}$$

in which,

$$[R] = \begin{bmatrix} D & 0 & 0 & 0 \\ 0 & D & 0 & 0 \\ 0 & 0 & D & 0 \\ 0 & 0 & 0 & D \end{bmatrix}, \text{ and} \tag{A.23}$$

[D] is the matrix of direction cosines from local axes to global axes.

CHAPTER XI

APPENDIX C

RELATIVE COORDINATE FORMULATION FOR BASE EXCITATIONS

Sometimes forced excitations of a structure result from a motion of its base or its supports (21,22). The structure equilibrium position varies with time for such an excitation. The total solution may be obtained by adding the motion of the structure equilibrium position to the structure vibratory motion about this equilibrium position. However, it can be shown that in a dynamic stress analysis of a structure, vibratory motion of the structure relative to its base motion or structure equilibrium position is of prime importance. It is the purpose here to formulate the equations of motion, of a structure with known base excitations, in coordinates expressed relative to the base. Solution of these equations can then be used directly in the structural dynamic stress analysis.

The equations of motion of a structure with known base motion are given by:

$$\begin{bmatrix} m_{BB} & 0 \\ 0 & m \end{bmatrix} \begin{Bmatrix} \ddot{U}_B \\ \ddot{x} \end{Bmatrix} + \begin{bmatrix} K_{BB} & K_{Bs} \\ K_{sB} & K \end{bmatrix} \begin{Bmatrix} U_B \\ x \end{Bmatrix} = \begin{Bmatrix} f_{BB} \\ 0 \end{Bmatrix}, \qquad (A.24)$$

where $[m_{BB}]$ and $[K_{BB}]$ are unknown base mass and stiffness matrices; $\{U_B(t)\}$ and $\{\ddot{U}_B(t)\}$ define the given general time-varying base motion. The vector $\{U_B(t)\}$, for six degrees of freedom, is given by:

$$\{U_B(t)\} = \begin{Bmatrix} x_B(t) \\ y_B(t) \\ z_B(t) \\ \alpha_B(t) \\ \beta_B(t) \\ \theta_B(t) \end{Bmatrix} .$$

Expanding Eq. (A.24) gives:

$$[m_{BB}]\{\ddot{U}_B\} + [K_{BB}]\{U_B\} + [K_{BS}]\{x\} = \{f_{BB}\}, \text{ and} \qquad (A.25)$$

$$[m]\{\ddot{x}\} + [K_{sB}]\{U_B\} + [K]\{x\} = \{0\}, \qquad (A.26)$$

where $\{f_{BB}(t)\}$ represents unknown forces producing a known base motion, $\{U_B(t)\}$; $[m]$ and $[K]$ are structure mass and stiffness matrices with the base fixed.

Rearranging Eq. (A.26) yields:

$$[m]\{\ddot{x}\} + [K]\{x\} = - [K_{sB}]\{U_B\}. \qquad (A.27)$$

The time-varying motion of the structure's equilibrium position caused by a base motion, $\{U_B(t)\}$, where there are no elastic deformations can be defined by:

$$\{\delta_E(t)\} = [A]\{U_B(t)\}, \qquad (A.28)$$

where [A] is a coefficient matrix defining static rigid body displacements of the structure caused by unit base displacements. The structure force-displacement equation for static equilibrium is given by:

$$\{f\} = [K]\{\delta\}, \text{ or} \tag{A.29}$$

in partitioned form,

$$\begin{Bmatrix} f_B \\ \hline 0 \end{Bmatrix} = \left[\begin{array}{c|c} K_{BB} & K_{Bs} \\ \hline K_{sB} & K \end{array}\right] \begin{Bmatrix} U_B \\ \hline \delta_E \end{Bmatrix} . \tag{A.30}$$

where $\{f_B\}$ is the vector of external forces applied to the base resulting in a base displacement, $\{U_B\}$. External forces at structure nodal points other than those at the base are zero. Expanding Eq. (A.30) gives:

$$\{f_B\} = [K_{BB}]\{U_B\} + [K_{Bs}]\{\delta_E\}, \text{ and} \tag{A.31}$$

$$\{0\} = [K_{sB}]\{U_B\} + [K]\{\delta_E\}. \tag{A.32}$$

Defining coordinates, $\{\tilde{x}\}$, relative to the base motion, i.e.,

$$\{\tilde{x}(t)\} = \{x(t)\} - [A]\{U_B(t)\}, \tag{A.33}$$

gives:

$$\{\ddot{\tilde{x}}(t)\} = \{\ddot{x}(t)\} - [A]\{\ddot{U}_B(t)\}. \tag{A.34}$$

Using Eqs. (A.33) and (A.34) into Eq. (A.27) yields:

$$[m]\{\ddot{\tilde{x}}\} + [m][A]\{\ddot{U}_B\} + [K]\{\tilde{x}\} + [K][A]\{U_B\}$$

$$= - [K_{sB}]\{U_B\}, \text{ or} \tag{A.35}$$

$$[m]\{\ddot{\tilde{x}}\} + [K]\{\tilde{x}\} = - [m][A]\{\ddot{U}_B\} - ([K_{sB}]\{U_B\} + [K][A]\{U_B\}). \tag{A.36}$$

Combining Eqs. (A.28) and (A.32) yields:

$$[K_{sB}]\{U_B\} + [K][A]\{U_B\} = \{0\}. \tag{A.37}$$

In view of Eq. (A.37), Eq. (A.36) becomes:

$$\lceil m \rfloor\{\ddot{x}\} + [K]\{\tilde{x}\} = -\lceil m \rfloor[A]\{\ddot{U}_B\}. \tag{A.38}$$

If the structure mass matrix with its base fixed is non-diagonal, Eq. (A.38) modifies to:

$$[m]\{\ddot{\tilde{x}}\} + [K]\{\tilde{x}\} = -[m][A]\{\ddot{U}_B\}, \tag{A.39}$$

where [m] represents the non-diagonal structure mass matrix when the structure base is fixed.

CHAPTER XII

APPENDIX D
DIRECT SOLUTIONS

For the purpose of comparisons, solutions of system equations of motion are derived through the usual direct approach (21-24) in this appendix. The most important step in matrix structural analysis is the formulation of a discrete-element mathematical model which replaces the actual continuous structure. This model is in general necessary in order to have a system with a finite number of degrees of freedom upon which matrix algebra operations can be performed. The formulation of such a model is usually referred to as structural idealization. The most commonly used idealized structural finite elements are described in Appendix C with special emphasis on their elastic and inertia matrix properties.

Consider an idealized elastic system subjected to arbitrary time-varying excitations. Viewing the dynamic problem from the standpoint of D'Alembert's principle, there are inertia forces $-[M]\{\ddot{x}(t)\}$ in addition to the applied forces $\{f(t)\}$ acting on the structure, where $[M]$ denotes the mass matrix. The forces $\{f(t)\}$ and the inertia forces $-[M]\{\ddot{x}(t)\}$ are balanced by the elastic reactions $-[K]\{x(t)\}$ induced by the displacements $\{x(t)\}$, where $[K]$ is the stiffness matrix. Hence the equilibrium equation becomes:

$$-[K]\{x(t)\} - [M]\{\ddot{x}(t)\} + \{f(t)\} = \{0\}, \text{ or} \tag{A.40}$$

$$[M]\{\ddot{x}(t)\} + [K]\{x(t)\} = \{f(t)\}. \tag{A.41}$$

Equation (A.41) gives the equations of motion in matrix notation of the idealized linear, conservative, elastic structure. A homogeneous solution of this equation results in system eigenvalues and system eigenvectors, while a complete solution of Eq. (A.41) gives system response due to the arbitrary excitation $\{f(t)\}$.

A. Free Undamped Vibrations

For free vibrations,

$$\{f(t)\} = \{0\}, \tag{A.42}$$

and Eq. (A.41) becomes:

$$[M]\{\ddot{x}\} + [K]\{x\} = \{0\}. \tag{A.43}$$

The above differential equations in matrix notation are solved by assuming a solution of the form:

$$\{x(t)\} = \{A\}e^{i\omega t}, \tag{A.44}$$

where the column vector $\{A\}$ is referred to as the amplitude matrix.

Using Eq. (A.44) in Eq. (A.43) and rearranging gives:

$$([K] - \omega^2[M])\{A\} = \{0\}, \tag{A.45}$$

where ω^2 represents system eigenvalues. In order for Eq. (A.45) to have a non trivial solution it is necessary that,

$$\det([K] - \omega^2[M]) = 0 . \tag{A.46}$$

Upon expansion Eq. (A.46) gives a polynomial in ω^2, the roots, ω_i, of which are the natural circular frequencies of the system. For each

value of ω_i, it is possible through Eq. (A.45) to compute an amplitude matrix $\{A\}_i$ that is referred to as the normal mode corresponding to ω_i. The normal modes when grouped together in a single square matrix in the ascending order of mode number give the system modal matrix $[\phi]$. The normal modes or columns of matrix $[\phi]$ are so normalized that they satisfy the following orthogonality conditions:

$$[\phi]^T[M][\phi] = [\ulcorner I \urcorner], \text{ and} \tag{A.47}$$

$$[\phi]^T[K][\phi] = [\ulcorner \omega_i^2 \urcorner]. \tag{A.48}$$

1. Initial Conditions Solution

Let the initial displacements, at time $t = t_0$, be represented by $\{x_0\}$ and the initial velocities by $\{\dot{x}_0\}$. Then solution of Eq. (A.43) is found by superposition of all n solutions given by:

$$\{x_i(t)\} = [A_i \sin \omega_i(t-t_0) + B_i \cos \omega_i(t-t_0)]\ \{\phi_i\}, \tag{A.49}$$

where i takes the values from 1 to n and amplitudes A_i and B_i depend on the initial conditions prescribed at time t_0.

Thus the total solution becomes:

$$\{x(t)\} = [\phi](\lceil \sin \omega_i(t-t_0) \rfloor\{A_i\} + \lceil \cos \omega_i(t-t_0) \rfloor\{B_i\}). \tag{A.50}$$

Evaluating Eq. (A.50) at $t = t_0$ gives:

$$\{x_0\} = [\phi]\{B_i\}, \text{ and} \tag{A.51}$$

$$\{\dot{x}_0\} = [\phi][\ulcorner \omega_i \urcorner]\{A_i\}. \tag{A.52}$$

Premultiplying Eq. (A.51) by $[\phi]^T[M]$ on both sides and using Eq. (A.47) yields:

$$\{B_i\} = [\phi]^T[M]\{x_0\}. \tag{A.53}$$

Similarly using Eqs. (A.52) and (A.48) gives:

$$\{A_i\} = [\omega_i]^{-1}[\phi]^T[M]\{\dot{x}_0\}, \tag{A.54}$$

Equation (A.50), which describes the free vibrations with initial conditions $\{x_0\}$ and $\{\dot{x}_0\}$, then becomes:

$$\{x(t)\} = [\phi]([\sin \omega_i(t-t_0)][\omega_i]^{-1}[\phi]^T[M]\{\dot{x}_0\}$$

$$+ [\cos \omega_i(t-t_0)][\phi]^T[M]\{x_0\}). \tag{A.55}$$

B. Forced Undamped Vibrations

The various types of excitations discussed in Chapter IV are now considered in Eq. (A.41) and total system solutions are obtained.

1. Harmonic Force Excitations

Assuming that the applied forces $\{f(t)\}$, are given by:

$$\{f(t)\} = \{F\} \sin \Omega t, \tag{A.56}$$

then the steady-state solution has the form:

$$\{x(t)\} = \{X\} \sin \Omega t, \tag{A.57}$$

where Ω denotes the forcing frequency. Using Eqs. (A.56) and (A.57) in Eq. (A.41) and simplifying gives:

$$-\Omega^2 [M]\{X\} + [K]\{X\} = \{F\}. \tag{A.58}$$

The column vector $\{X\}$ can be expressed as a linear combination of the modal vectors according to the relation:

$$\{X\} = [\phi]\{d\}. \tag{A.59}$$

Substituting Eq. (A.59) into Eq. (A.58) and premultiplying the result by $[\phi]^T$ gives:

$$-\Omega^2[\phi]^T[M][\phi]\{d\}+ [\phi]^T[K][\phi]\{d\} = [\phi]^T\{F\}. \tag{A.60}$$

Using in Eq. (A.60) the orthogonality conditions defined in Eqs. (A.47) and (A.48) and solving for vector $\{d\}$ gives:

$$\{d\} = \left[\omega_i^2-\Omega^2\right]^{-1}[\phi]^T\{F\}. \tag{A.61}$$

Substituting Eq. (A.61) into Eq. (A.59) and in view of Eq. (A.57), the total solution becomes:

$$\{x(t)\} = [\phi]\left[\omega_i^2-\Omega^2\right]^{-1}[\phi]^T\{F\} \sin \Omega t. \tag{A.62}$$

In case of an applied forcing function of the type given by:

$$\{f(t)\} = \{F\} \cos \Omega t,$$

the total solution becomes:

$$\{x(t)\} = [\phi]\left[\omega_i^2-\Omega^2\right]^{-1}[\phi]^T\{F\} \cos \Omega t. \tag{A.64}$$

2. General Case of a Time-Varying Force

To uncouple the equations of motion, a coordinate transformation defined below is used in Eq. (A.41) to give:

$$\{x(t)\} = [\phi]\{p(t)\}, \text{ and} \tag{A.65}$$

$$[M][\phi]\{\ddot{p}\} + [K][\phi]\{p\} = \{f(t)\}. \tag{A.66}$$

Premultiplying Eq. (A.66) by $[\phi]^T$ and simplifying gives:

$$\{\ddot{p}\} + \left[\omega_i^2\right]\{p\} = [\phi]^T\{f(t)\}. \tag{A.67}$$

Equation [A.67) is of the form defined by,

$$\{\ddot{r}(t)\} + \left[\omega_i^2\right]\{r(t)\} = \{Q(t)\}, \tag{A.68}$$

whose solution is given by Duhamel's integral solution, i.e., for zero initial conditions,

$$\{r(t)\} = \left[\omega_i\right]^{-1} \int_0^t \left[\sin \omega_i(t-\tau)\right]\{Q(\tau)\}d\tau. \tag{A.69}$$

Thus solution of Eq. (A.67) becomes:

$$\{p(t)\} = \left[\omega_i\right]^{-1} \int_0^t \left[\sin \omega_i(t-\tau)\right][\phi]^T\{f(\tau)\}d\tau. \tag{A.70}$$

The total solution can now be obtained through Eq. (A.65), i.e.,

$$\{x(t)\} = [\phi]\left[\omega_i\right]^{-1} \int_0^t \left[\sin \omega_i(t-\tau)\right][\phi]^T\{f(\tau)\}d\tau. \tag{A.71}$$

Equation (A.71) gives the system solution starting from rest due to time-varying forces $\{f(t)\}$.

3. General Case of Time-Varying Forced Displacements

Assuming that f of the displacements are forced to vary in a defined manner, Eq. (A.41) can then be partioned so that differential equations of motion for the remaining s displacement (n = s + f) can be determined. Thus,

$$\left[\begin{array}{c|c} M_1 & M_2 \\ \hline M_3 & M_4 \end{array}\right] \left\{\begin{array}{c} \ddot{x}_f \\ \hline \ddot{x}_s \end{array}\right\} + \left[\begin{array}{c|c} K_1 & K_2 \\ \hline K_3 & K_4 \end{array}\right] \left\{\begin{array}{c} x_f \\ \hline x_s \end{array}\right\} = \left\{\begin{array}{c} f_f \\ \hline 0 \end{array}\right\}, \qquad (A.72)$$

where $\{f_f\}$ are the unknown reactions at f points in the directions of $\{x_f\}$.

Expanding Eq. (A.72) leads to:

$$[M_1]\{\ddot{x}_f\} + [M_2]\{\ddot{x}_s\} + [K_1]\{x_f\} + [K_2]\{x_s\} = \{f_f\}, \text{ and} \qquad (A.73)$$

$$[M_3]\{\ddot{x}_f\} + [M_4]\{\ddot{x}_s\} + [K_3]\{x_f\} + [K_4]\{x_s\} = \{0\}. \qquad (A.74)$$

Rearranging Eq. (A.74) gives:

$$[M_4]\{\ddot{x}_s\} + [K_4]\{x_s\} = -[M_3]\{\ddot{x}_f\} - [K_3]\{x_f\}, \qquad (A.75)$$

in which the right hand side is a given function of time.

In Eq. (A.75) $[M_4]$ and $[K_4]$ are symmetric mass and stiffness matrices for the reduced system that is obtained from the original system simply by introducing additional constraints so that $\{x_f\} = \{0\}$. The natural frequencies and the associated normal modes are found from these matrices according to standard practice, and it is assumed that this has been done, i.e., the modal matrix $[\phi_s]$ for the reduced system as well as the frequency matrix $[\omega_s^2]$ are known.

Using the coordinate transformation,

$$\{x_s\} = [\phi_s]\{p_s\}, \tag{A.76}$$

in Eq. (A.75) and premultiplying the result by $[\phi_s]^T$ yields:

$$[\phi_s]^T[M_4][\phi_s]\{\ddot{p}_s\} + [\phi_s]^T[K_4][\phi_s]\{p_s\} = -[\phi_s]^T([M_3]\{\ddot{x}_f\} + [K_3]\{x_f\}). \tag{A.77}$$

The orthogonality relations of the modal matrix $[\phi_s]$ are:

$$[\phi_s]^T[M_4][\phi_s] = [\,I\,], \text{ and} \tag{A.78}$$

$$[\phi_s]^T[K_4][\phi_s] = [\,\omega_s^2\,]. \tag{A.79}$$

In view of Eqs. (A.78) and (A.79), Eq. (A.77) simplifies to:

$$\{\ddot{p}_s\} + [\,\omega_s^2\,]\{p_s\} = -[\phi_s]^T([M_3]\{\ddot{x}_f\} + [K_3]\{x_f\}). \tag{A.80}$$

Assuming zero initial conditions, Eq. (A.80) can be solved by Duhamel's integral solution given by Eq. (A.69), i.e.,

$$\{p_s\} = -[\,\omega_s\,]^{-1}\int_0^t [\,\sin\,\omega_s(t-\tau)\,][\phi_s]^T([M_3]\{\ddot{x}_f(\tau)\} + [K_3]\{x_f(\tau)\})d\tau. \tag{A.81}$$

The total solution for the remaining s displacements thus becomes:

$$\{x_s(t)\} = -[\phi_s][\,\omega_s\,]^{-1}\int_0^t [\,\sin\,\omega_s(t-\tau)\,][\phi_s]^T([M_3]\{\ddot{x}_f(\tau)\} + [K_3]\{x_f(\tau)\})d\tau. \tag{A.82}$$

4. Base Acceleration Excitation

The differential equations of motion in matrix notation for a system, whose base or supports are given a known acceleration type of excitation, are given by:

$$\left[\begin{array}{c|c} M_B & 0 \\ \hline 0 & M \end{array}\right] \left\{\begin{array}{c} \ddot{U}_B \\ \hline \ddot{x} \end{array}\right\} + \left[\begin{array}{c|c} K_B & K_{Bs} \\ \hline K_{sB} & K \end{array}\right] \left\{\begin{array}{c} U_B \\ \hline x \end{array}\right\} = \left\{\begin{array}{c} f_B \\ \hline 0 \end{array}\right\} , \qquad \text{(A.83)}$$

where $[M_B]$ and $[K_B]$ represent the unknown base mass and stiffness matrices. Furthermore, $\{f_B(t)\}$ are unknown forces applied to the base to give it a desired motion, $\{U_B(t)\}$. $[M]$ and $[K]$ are system mass and stiffness matrices obtained by keeping the base fixed. $\{x(t)\}$ represents system discrete coordinates giving absolute system displacements. The second of Eq. (A.83) on expanding is given by:

$$[M]\{\ddot{x}\} + [K_{sB}]\{U_B\} + [K]\{x\} = \{0\}, \text{ or} \qquad \text{(A.84)}$$

$$[M]\{\ddot{x}\} + [K]\{x\} = - [K_{sB}]\{U_B\}. \qquad \text{(A.85)}$$

As shown in appendix C, formulating Eq. (A.85) in terms of coordinates relative to the base yields:

$$\{\tilde{x}(t)\} = \{x(t)\} - [A]\{U_B(t)\}, \text{ and} \qquad \text{(A.86)}$$

$$[M]\{\ddot{\tilde{x}}\} + [K]\{\tilde{x}\} = - [M][A]\{\ddot{U}_B(t)\}, \qquad \text{(A.87)}$$

where $[A]$ is the coefficient matrix defining the time varying structure equilibrium position through the relation:

$$\{\delta_E(t)\} = [A]\{U_B(t)\}. \qquad \text{(A.28)}$$

An eigensolution of the homogeneous part of Eq. (A.87) gives its frequency matrix, $[\omega_i]$, and the normalized modal matrix $[\phi]$ so that,

$$[\phi]^T[M][\phi] = [I], \text{ and} \tag{A.88}$$

$$[\phi]^T[K][\phi] = [\omega_i^2]. \tag{A.89}$$

Defining a coordinate transformation,

$$\{\tilde{x}(t)\} = [\phi]\{\tilde{p}(t)\}, \tag{A.90}$$

and using it in Eq. (A.87) with a premultiplication of results by $[\phi]^T$ yields:

$$[\phi]^T[M][\phi]\{\ddot{\tilde{p}}(t)\} + [\phi]^T[K][\phi]\{\tilde{p}(t)\}$$

$$= - [\phi]^T[M][A]\{\ddot{U}_B(t)\}. \tag{A.91}$$

In view of Eqs. (A.88) and (A.89), Eq. (A.91) simplifies to:

$$\{\ddot{\tilde{p}}(t)\} + [\omega_i^2]\{\tilde{p}(t)\} = -[\phi]^T[M][A]\{\ddot{U}_B(t)\}, \tag{A.92}$$

whose solution through Duhamel's integral solution becomes:

$$\{\tilde{p}(t)\} = - [\omega_i]^{-1} \int_0^t [\sin \omega_i(t-\tau)][\phi]^T[M][A]\{\ddot{U}_B(t)\}d\tau. \tag{A.93}$$

Thus, using Eq. (A.90), the total solution relative to the base motion is given by:

$$\{\tilde{x}(t)\} = -[\phi][\omega_i]^{-1} \int_0^t [\sin \omega_i(t-\tau)][\phi]^T[M][A]\{\ddot{U}_B(t)\}d\tau. \tag{A.94}$$

C. System Strain Energy

Solutions obtained above define the system displacements either in discrete coordinates or in relative coordinates. The system strain energy in the ith principal mode (25) is given by:

$$U_i = \frac{1}{2}\{\phi\}_i^T[K]\{\phi\}_i, \tag{A.95}$$

where $\{\phi\}_i$ are the ith mode system eigenvectors and [K] is the system stiffness matrix.

Under forced excitations, system strain energy may be obtained through the relation

$$U(t) = \frac{1}{2}\{x(t)\}^T[\phi]\{x(t)\}, \tag{A.96}$$

in which $\{x(t)\}$ are time-varying system displacements in discrete coordinates. In case of relative coordinates, $\{x(t)\}$ are replaced by $\{\tilde{x}(t)\}$ in Eq. (A.96).